

1 Combining genotypes and T cell 2 receptor distributions to infer 3 genetic loci determining V(D)J 4 recombination probabilities

5 **Magdalena L Russell**^{1,2}, **Aisha Souquette**^{3,4}, **David M Levine**⁵, **E Kaitlynn Allen**³,
6 **Guillermina Kuan**^{6,7}, **Noah Simon**⁵, **Angel Balmaseda**^{6,7}, **Aubree Gordon**⁸, **Paul G**
7 **Thomas**³, **Frederick A Matsen IV**^{1†*}, **Philip Bradley**^{1,9†*}

*For correspondence:

matsen@fredhutch.org (FAMIV);
pbradley@fredhutch.org (PB)

†Co-senior authors

8 ¹Computational Biology Program, Fred Hutchinson Cancer Research Center, Seattle,
9 United States; ²Molecular and Cellular Biology Program, University of Washington,
10 Seattle, United States; ³Department of Immunology, St. Jude Children's Research Hospital,
11 Memphis, United States; ⁴Department of Microbiology, Immunology, and Biochemistry,
12 University of Tennessee Health Science Center, Memphis, United States; ⁵Department of
13 Biostatistics, University of Washington, Seattle, United States; ⁶Centro Nacional de
14 Diagnóstico y Referencia, Ministry of Health, Managua, Nicaragua; ⁷Sustainable Sciences
15 Institute, Managua, Nicaragua; ⁸Department of Epidemiology, University of Michigan, Ann
16 Arbor, United States; ⁹Institute for Protein Design, Department of Biochemistry,
17 University of Washington, Seattle, United States

18

19 **Abstract** Every T cell receptor (TCR) repertoire is shaped by a complex probabilistic tangle of
20 genetically determined biases and immune exposures. T cells combine a random V(D)J
21 recombination process with a selection process to generate highly diverse and functional TCRs. The
22 extent to which an individual's genetic background is associated with their resulting TCR repertoire
23 diversity has yet to be fully explored. Using a previously published repertoire sequencing dataset
24 paired with high-resolution genome-wide genotyping from a large human cohort, we infer specific
25 genetic loci associated with V(D)J recombination probabilities using genome-wide association
26 inference. We show that V(D)J gene usage profiles are associated with variation in the *TCRB* locus
27 and, specifically for the functional TCR repertoire, variation in the major histocompatibility complex

28 locus. Further, we identify specific variations in the genes encoding the Artemis protein and the TdT
29 protein to be associated with biasing junctional nucleotide deletion and N-insertion, respectively.
30 These results refine our understanding of genetically-determined TCR repertoire biases by
31 confirming and extending previous studies on the genetic determinants of V(D)J gene usage and
32 providing the first examples of *trans* genetic variants which are associated with modifying
33 junctional diversity. Together, these insights lay the groundwork for further explorations into how
34 immune responses vary between individuals.

35

36 Introduction

37 Receptor proteins on the surfaces of T cells are an essential component of the cell-mediated
38 adaptive immune response in humans. Cells throughout the body regularly present protein
39 fragments, known as antigens, on cell-surface molecules called major histocompatibility complex
40 (MHC). Each T cell expresses a randomly-generated T cell receptor (TCR) which can bind the MHC-
41 bound peptide and, if necessary, initiate an immune response. As part of this immune response, a
42 T cell will proliferate and subsequent clones of that T cell will inherit the same antigen-specific TCR.
43 Over time, the collection of all TCRs in an individual (the TCR repertoire) will dynamically summarize
44 their previous immune exposures (*Woodsworth et al., 2013*).

45 To appropriately defend against a wide array of foreign pathogens, each individual has a
46 highly diverse TCR repertoire. To generate diverse and functional TCRs, T cells combine a random
47 generation process called V(D)J recombination with a selection process for proper expression and
48 MHC recognition. Each TCR is composed of an α and a β protein chain which are both generated
49 through V(D)J recombination. In the β chain, the recombination process proceeds by randomly
50 choosing from a pool of V-gene, D-gene, and J-gene segments of the germline T cell receptor beta
51 (*TCRB*) locus over a series of steps. First, the intervening chromosomal DNA between a randomly
52 chosen D- and J-gene is removed to form a hairpin loop at the end of each gene (*Gellert, 1994*;
53 *Fugmann et al., 2000; Schatz and Swanson, 2011*). Next, these hairpin loops are nicked open, often
54 asymmetrically, by the Artemis-DNA-PKcs protein complex to create overhangs at the ends of
55 each gene (*Weigert et al., 1978; Moshous et al., 2001; Ma et al., 2002; Lu et al., 2007; Zhao et al.,*
56 *2020*). Depending on the location of the nick, the single-stranded overhang can contain short
57 inverted repeats of gene terminal sequence known as P-nucleotides (*Nadel and Feeney, 1995*;
58 *Gauss and Lieber, 1996; Nadel and Feeney, 1997; Jackson et al., 2004*). From here, nucleotides
59 may be deleted from the gene ends through an incompletely-understood mechanism suggested
60 to involve Artemis (*Feeney et al., 1994; Nadel and Feeney, 1995, 1997; Jackson et al., 2004; Gu*
61 *et al., 2010; Zhao et al., 2020*). This nucleotide trimming can remove traces of P-nucleotides (*Gauss*
62 *and Lieber, 1996; Srivastava and Robins, 2012*). Next, non-templated nucleotides, known as N-

63 insertions, can be added between the gene segments by the enzyme terminal deoxynucleotidyl
64 transferase (TdT) (*Kallenbach et al., 1992; Gilfillan et al., 1993; Komori et al., 1993*). Once the
65 nucleotide addition and deletion steps are completed, the gene segments are ligated together. The
66 process is then repeated between this D-J junction and a random V-gene segment to generate a
67 complete TCR β protein chain. After the β chain has been generated, a similar α chain recombination
68 proceeds, although without a D-gene, to complete the TCR. Following the generation process, each
69 completed TCR undergoes a selection process in the thymus to limit autoreactivity and ensure
70 its ability to correctly bind peptide antigens presented on a specific MHC molecule (*Goldrath and*
71 *Bevan, 1999; Thomas and Crawford, 2019*).

72 TCR repertoires vary between individuals and are a complicated tangle of genetically determined
73 biases and immune exposures. Disentangling these factors is essential for understanding how our
74 diverse repertoires support a powerful immune response. Previous efforts to unravel the genetic
75 and environmental determinants governing TCR repertoire diversity have been highly impactful
76 despite lacking high-throughput TCR repertoire sequencing data (*Sharon et al., 2016; Gao et al.,*
77 *2019*) and/or high-resolution genotype data (*Rubelt et al., 2016; Emerson et al., 2017; Gao et al.,*
78 *2019; Krishna et al., 2020*). For example, it has been shown that variation in the MHC locus biases
79 TCR V(D)J gene usage (*Sharon et al., 2016; Gao et al., 2019*) and has been associated with clusters
80 of shared receptors in response to Epstein-Barr virus epitope (*DeWitt et al., 2018*). Other studies
81 have reported biases in V(D)J gene usage (*Zvyagin et al., 2014; Qi et al., 2016; Rubelt et al., 2016;*
82 *Pogorelyy et al., 2018; Tanno et al., 2020; Fischer et al., 2021*), N-insertion lengths (*Rubelt et al.,*
83 *2016*), and repertoire similarity in response to acute infection (*Qi et al., 2016; Pogorelyy et al.,*
84 *2018*) for monozygotic twins. While this work clearly illustrates that genetic similarity implies TCR
85 repertoire similarity, the extent to which specific variations are associated with V(D)J recombination
86 probabilities has not been fully explored.

87 In this paper, we directly address the question of how an individual's genetic background
88 influences their V(D)J recombination probabilities using large human discovery and validation
89 cohorts for which both TCR immunosequencing data (*Emerson et al., 2017; DeWitt et al., 2018*) and
90 genotyping data (*Martin et al., 2020*) are available. With the goal of identifying statistically significant
91 associations between single nucleotide polymorphisms (SNPs) and TCR repertoire features of
92 interest using these novel, paired datasets, we treat analysis as a genome-wide association (GWAS)
93 inference with many outcomes. Our results suggest that MHC and *TCRB* loci variations have an
94 important role in determining the V(D)J gene usage profiles of each individual's repertoire. At the
95 junctions, we demonstrate that variations in the genes encoding the Artemis protein and the TdT
96 protein are associated with biasing V- and J-gene nucleotide deletion and V-D and D-J-junction
97 N-insertion, respectively.

98 Results

99 Discovery cohort data description

100 We worked with paired SNP array and TCR β -immunosequencing data representing 398 individuals
101 and over 35 million SNPs and/or indels. TCR sequences can be separated into those that code for a
102 complete, full-length peptide sequence (which we will call “productive” rearrangements) and “non-
103 productive” rearrangements that do not. Non-productive sequences can arise during TCR generation
104 steps if the V- and J-genes are shifted into different reading frames or a premature stop codon is
105 introduced in the junction region. A non-productive rearrangement can be sequenced as part of
106 the repertoire when a recombination event on one of a T cell's two chromosomes fails to create
107 a functional receptor, followed by a successful recombination event on the other chromosome.
108 Because these non-productive sequences do not generate proteins that participate in the T cell
109 selection process within the thymus, they should not be subject to functional selection (*Robins*
110 *et al., 2010*). As such, their recombination statistics should reflect only the V(D)J recombination
111 generation process which occurs before the stage of thymic selection.

112 In the data cohort of 398 individuals, an average of 235,054 unique TCR β -chain nucleotide
113 sequences were sequenced per individual. Within each individual repertoire, roughly 18% of
114 sequences were classified as “non-productive.” Thus, we can analyze the productive and non-
115 productive sequences separately to distinguish between TCR generation and selection effects within
116 each TCR repertoire. Specifically, we inferred the associations between genome-wide variation and
117 V(D)J gene usage of each V-, D-, and J-gene, the extent of TCR nucleotide trimming, the number of
118 TCR N-insertions, and the fraction of non-gene-trimmed TCRs containing P-nucleotides for both
119 productive and non-productive sequences (*Table 1*).

120 *TCRB* and MHC locus variation is associated with V-, D-, and J-gene usage frequency

121 To quantify the effect of SNPs on the expression of various V-, D-, and J-genes during V(D)J recombina-
122 tion, we designed a fixed effects model to assess the relationship between SNP genotype and
123 gene frequency across all individuals. We fit this “simple model” for each different V-, D-, and J-gene
124 in our paired dataset.

125 Because of the potential for population-substructure-related effects to inflate associations
126 between each SNP and gene usage frequency, we incorporated ancestry-informative principal
127 components (*Conomos et al., 2015*) based on the SNP genotypes for a subset of representative
128 subjects as covariates in each model (see Methods for details). Diagnostic statistics show that this
129 bias correction is sufficient (*Figure 1–source data 2*).

130 With these methods, we consider the significance of associations at a Bonferroni-corrected
131 whole-genome P-value significance threshold of 4.72×10^{-11} (see Methods). Using this conservative
132 threshold, we identified 9,957 significant associations between the frequency of various V-, D-,

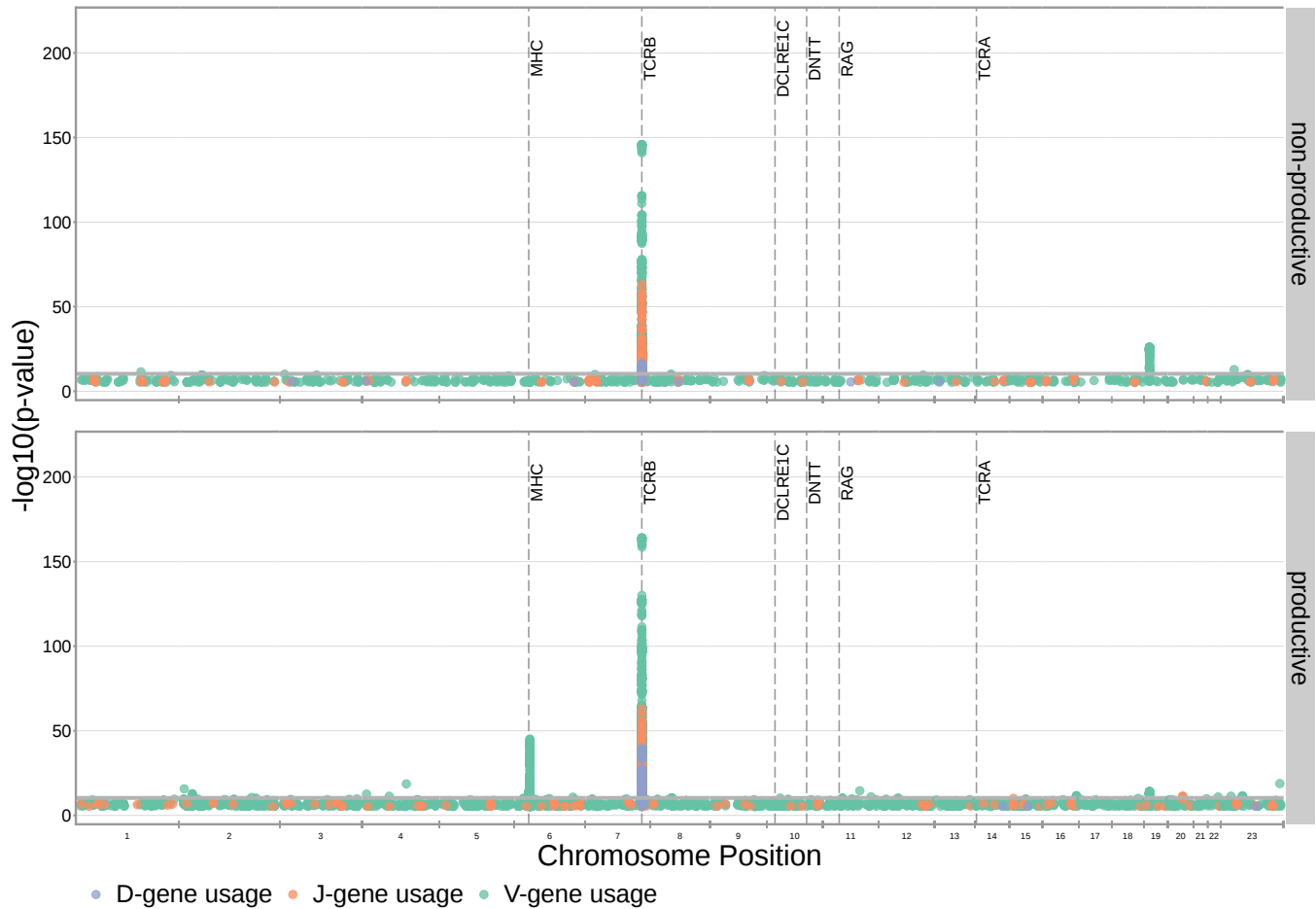


Figure 1. Many strong associations are present between V-, D-, and J-gene usage frequency and various SNPs genome-wide for both productive and non-productive TCRs. The most significant SNP associations for the frequency of each of the 66 V-genes, 2 D-genes, and 14 J-genes are located within the *TCRB* and *MHC* loci. Associations are colored by gene-type instead of by gene identity for simplicity. Only SNP associations whose $P < 5 \times 10^{-6}$ are shown here. The gray horizontal line corresponds to a Bonferroni-corrected P-value significance threshold of 4.72×10^{-11} .

Figure 1-source data 1. There are 9,957 significant associations between the frequency of various V-, D-, and J-genes and the genotype of SNPs genome-wide. The model type and Bonferroni-corrected P-value significance threshold used to identify these significant associations are described in [Table 1](#).

Figure 1-source data 2. Genomic inflation factor values are less than 1.03 for all paired gene-frequency, productivity GWAS analyses. This suggests that we have properly controlled for population-substructure-related biases in all of the gene usage analyses. Genomic inflation factor values were calculated as described in Methods.

Table 1. We inferred the associations between genome-wide variation and many different TCR repertoire features for productive and non-productive TCR sequences, separately. For each TCR repertoire feature, we considered the significance of associations using a Bonferroni-corrected threshold established to correct for each TCR feature subtype, the two TCR productivity types, and the total number of SNPs tested (described in detail in Methods).

Repertoire feature (significance threshold)	Model type	Feature subtype	Productivity	Significant association
V(D)J gene usage (4.72×10^{-11})	simple	Each of 66 V-genes	Productive	Yes
			Non-productive	Yes
		Each of 2 D-genes	Productive	Yes
			Non-productive	Yes
		Each of 14 J-genes	Productive	Yes
			Non-productive	Yes
Amount of nucleotide trimming (9.68×10^{-10})	gene-conditioned	V-gene trimming	Productive	Yes
			Non-productive	Yes
		5' end D-gene trimming	Productive	No
			Non-productive	No
		3' end D-gene trimming	Productive	No
			Non-productive	No
		J-gene trimming	Productive	Yes
			Non-productive	Yes
Number of N-insertions (1.94×10^{-9})	simple	V-D-gene N-insertions	Productive	No
			Non-productive	Yes
		D-J-gene N-insertions	Productive	No
			Non-productive	Yes

133 and J-genes and the genotype of SNPs genome-wide (**Figure 1** and **Figure 1-source data 1**). Of
134 these significant associations, 7,678 were located within the *TCRB* locus for both productive and
135 non-productive TCRs. The *TCRB* gene locus encodes the variable V-, D-, and J-gene segments which
136 are recombined during V(D)J recombination. In our dataset, there are 66 V-genes, 2 D-genes,
137 and 14 J-genes uniquely expressed. As we would expect, we find that the expression of many of
138 these genes is associated with variation in the *TCRB* locus (**Figure 2**). Variation in the *TCRB* locus
139 is most significantly associated with expression of the gene *TRBV28* within both productive and
140 non-productive TCR β chains.

141 Beyond the *TCRB* locus, we also identified 1,242 significant SNP associations within the major
142 histocompatibility complex (MHC) locus. MHC proteins act by presenting self and foreign peptides
143 to TCRs for inspection. Because of this important role in the functionality of T cells, the TCR-MHC
144 interaction is important for thymic selection. We observe the expression of 12.1% of V-genes for
145 productive TCRs to be associated with variation in the MHC locus. This associated MHC locus
146 variation is located within sequences which code for canonical, peptide-presenting MHC proteins.
147 For example, the eight most significantly associated SNPs were located within the *HLA-DRB1* gene
148 within the MHC locus. These top SNPs were all associated with the expression of the gene *TRBV10-3*
149 within productive TCRs. As expected, the expression of V-genes for non-productive TCRs is not
150 associated with variation in the MHC locus. Likewise, the expression of D- and J-genes for both
151 productive and non-productive TCRs is not associated with variation in the MHC locus. These results
152 refine and extend associations found in previous work (*Sharon et al., 2016; Gao et al., 2019*).

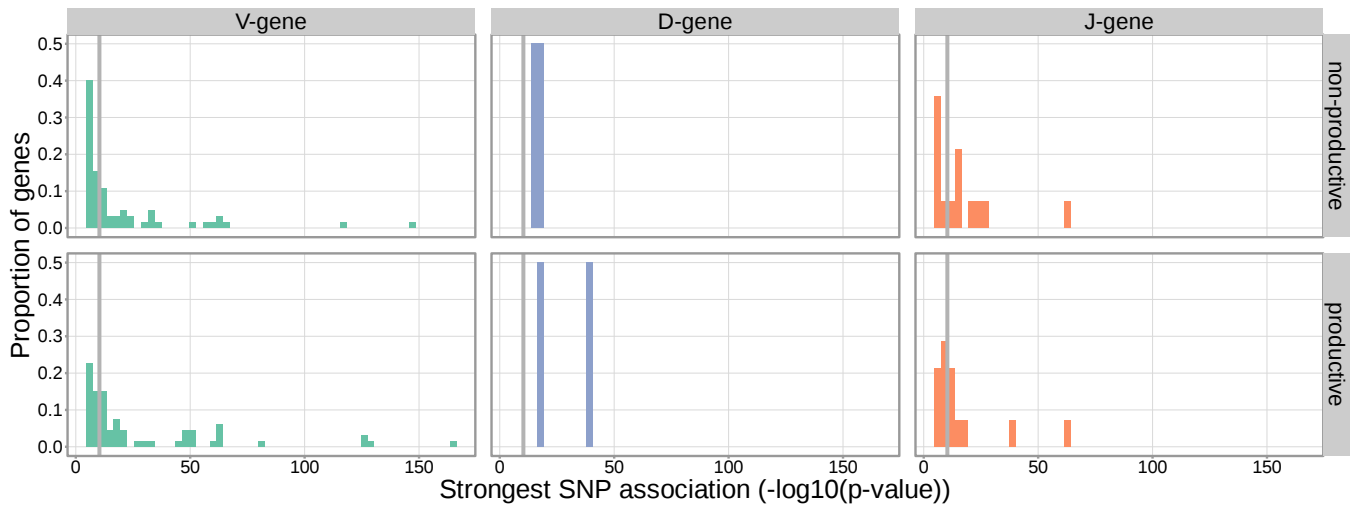


Figure 2. Gene-usage frequency of many V-gene, D-gene, and J-gene segments is significantly associated with variation in the *TCRB* locus. The P-value of the strongest *TCRB* SNP, gene-usage association for each different V-gene, D-gene, and J-gene segment is given on the X-axis. The proportion of gene segments within each gene type is given on the Y-axis. The gray vertical lines correspond to a whole-genome-level Bonferroni-corrected P-value significance threshold of 4.72×10^{-11} .

Figure 2-source data 1. Top *TCRB* SNP, gene-usage association P-value for each different V-gene, D-gene, and J-gene.

153 We observed just one other long-range association region, in addition to the MHC locus, located
154 in proximity to the *ZNF443* and *ZNF709* loci on chromosome 19. Both of these zinc finger proteins
155 contain KRAB-domains and, thus, likely act as transcriptional repressors (*Witzgall et al., 1994*). In
156 this region, we observe 1,004 significant SNP associations for the expression of the V-genes *TRBV24-1*
157 and *TRBV24/OR9-2*. Of these 1,004 SNP associations, 604 were associations for V-gene expression in
158 non-productive TCRs and 400 were associations for V-gene expression in productive TCRs. Because
159 these associations are strongest for non-productive TCRs, this chromosome 19 variation likely
160 influences gene usage during TCR generation steps, as opposed to selection. Variation in proximity
161 to the *ZNF443* and *ZNF709* loci may alter the resulting zinc finger proteins and lead to differential
162 transcriptional repression of a site near *TRBV24*. Because the transcription of unrearranged gene
163 segments influences their recombination potential (*Oltz, 2001*), this difference in repression could
164 subsequently change the usage frequency of the *TRBV24* gene.

165 ***DCLRE1C* locus variation is associated with the extent of V-, D-, and J-gene trimming**

166 We hypothesized that SNPs across the genome, particularly those within V(D)J-recombination-
167 associated genes, may influence the extent of TCR nucleotide trimming at V(D)J *TCRB* gene junctions.
168 It has been previously observed that the extent of trimming varies by V(D)J *TCRB* gene choice
169 (*Figure 3-Figure Supplement 4*) (*Nadel and Feeney, 1995, 1997; Jackson et al., 2004; Murugan*
170 *et al., 2012*). In other words, two different V-genes (*TRBV19* and *TRBV20-1*, for example) will on
171 average be trimmed to different extents due, in part, to differences in their terminal nucleotide
172 sequences (and the same is true for D- and J-genes). Thus, to quantify the effect of SNPs on
173 the extent of V-, D-, and J-gene trimming during V(D)J recombination, without confounding the

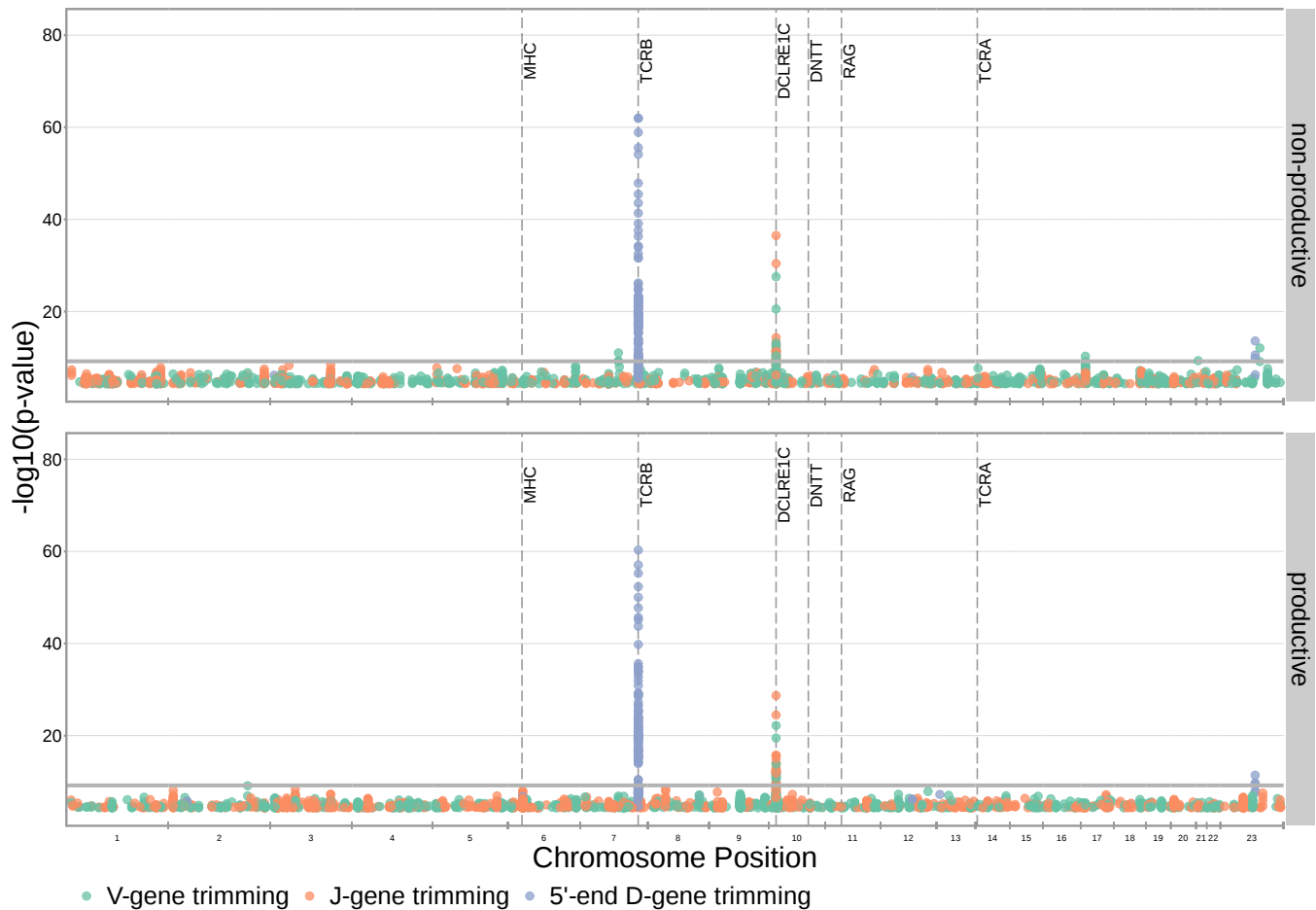


Figure 3. SNP associations for all four trimming types reveal the most significant associations to be located within the *TCRB* and *DCLRE1C* loci for 5' D-gene trimming and V-gene trimming, respectively, when conditioning out effects mediated by gene choice when calculating the strength of association. Only SNP associations whose $P < 5 \times 10^{-5}$ are shown here. The gray horizontal line corresponds to a Bonferroni-corrected P-value significance threshold of 9.68×10^{-10} .

Figure 3-source data 1. There are 317 significant SNP associations with the extent of nucleotide trimming for various trimming types. The model type and Bonferroni-corrected P-value significance threshold used to identify these significant associations are described in [Table 1](#).

Figure 3-source data 2. Genomic inflation factor values are less than 1.03 for all paired nucleotide trimming, productivity GWAS analyses. This suggests that we have properly controlled for population-substructure-related biases in all of the nucleotide trimming analyses. Genomic inflation factor values were calculated as described in Methods.

Figure 3-Figure supplement 1. The SNP genotype for the SNP most significantly associated with 5' end D-gene trimming within the *TCRB* locus is also associated with *TRBD2* allele genotype.

Figure 3-Figure supplement 2. Significant associations are no longer observed between 5' end D-gene trimming and variation in the *TCRB* locus after correcting for *TRBD2* allele genotype in our model formulation.

Figure 3-Figure supplement 3. Significant associations are also no longer observed between 5' end D-gene trimming and variation in the *TCRB* locus when restricting the analysis to TCRs which contain *TRBJ1* genes (and consequently contain *TRBD1*).

Figure 3-Figure supplement 4. The extent of nucleotide deletion varies by the gene allele identity for all gene types.

Figure 3-Figure supplement 5. Significant SNP associations are located within the MHC, *TCRB* and *DCLRE1C* loci for all four trimming types when calculating the strength of association without conditioning out effects mediated by gene choice.

Figure 3-Figure supplement 6. SNP associations for all fractions of non-gene-trimmed TCRs containing P-nucleotides are not significant within the *DCLRE1C* locus.

Figure 3-Figure supplement 7. SNP associations for the number of P-nucleotides are also not significant within the *DCLRE1C* locus.

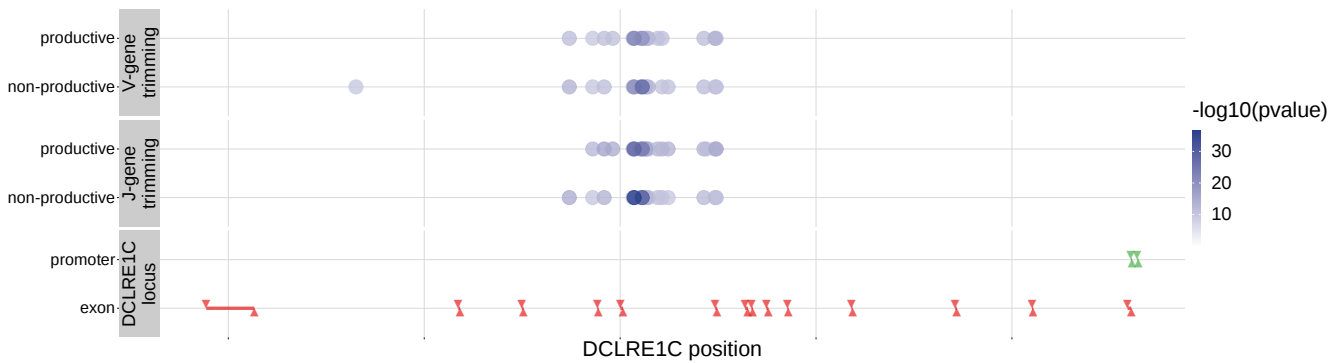


Figure 4. Within the *DCLRE1C* locus, 93.8% of these significantly associated SNPs were located within introns. Additionally, many of these significant SNP associations overlapped between trimming types. Downward arrows represent promoter/exon starting positions and upward arrows represent promoter/exon ending positions.

Figure 4–source data 1. *DCLRE1C* locus SNP association P-values and locus positions.

Figure 4–source data 2. There are two independent SNP signals within the *DCLRE1C* locus for J-gene trimming of non-productive TCRs. A conditional analysis was performed (as described in Methods) to identify these independent signals.

Figure 4–Figure supplement 1. The extent of J-gene trimming changes as a function of SNP genotype for the SNP (rs41298872) most significantly associated with J-gene trimming within the *DCLRE1C* locus.

174 extent of trimming with *TCRB* gene choice, we designed a linear fixed effects model to measure the
175 correlation between each SNP and the number of nucleotide deletions, while conditioning out the
176 effect mediated by gene choice. We fit this “gene-conditioned model” for each of the four trimming
177 types (V-gene trimming, 5’ end D-gene trimming, 3’ end D-gene trimming, and J-gene trimming)
178 on our paired data set. We performed the analysis, as above, incorporating ancestry-informative
179 principal components in each model (detailed in Methods). Diagnostic statistics show that this
180 correction for population-substructure-related biases is sufficient (**Figure 3–source data 2**). Here,
181 we considered the significance of associations at a Bonferroni-corrected whole-genome P-value
182 significance threshold of 9.68×10^{-10} (see Methods).

183 With these methods, we identified 317 significant SNP associations with the extent of nucleotide
184 trimming for various trimming types (**Figure 3** and **Figure 4–source data 1**). We found 66 highly
185 significant associations between V- and J-gene trimming and SNPs within the *DCLRE1C* gene locus
186 for both productive and non-productive TCRs when considered in the whole-genome context. The
187 *DCLRE1C* gene encodes the Artemis protein, an endonuclease responsible for cutting the hairpin in-
188 termediate prior to nucleotide trimming and insertion during V(D)J recombination. Many of the SNPs
189 responsible for these 66 significant associations within the *DCLRE1C* locus were shared between
190 trimming and productivity types (**Figure 4**). The most significantly-associated SNP (rs41298872)
191 within this locus had a P-value of 3.18×10^{-37} for J-gene trimming of non-productive TCRs (**Figure 3–**
192 **Figure Supplement 1**). This SNP was also significantly-associated with J-gene trimming of productive
193 ($P = 1.99 \times 10^{-29}$) TCRs and V-gene trimming of productive ($P = 6.23 \times 10^{-23}$) and non-productive
194 ($P = 2.81 \times 10^{-21}$) TCRs. We performed a conditional analysis to identify potential independent
195 secondary signals by including this SNP as an additional covariate within the model. This analysis
196 revealed a second, independent SNP signal (rs35441642) within the *DCLRE1C* locus for J-gene trim-

197 ming of non-productive TCRs (**Figure 4–source data 2**). None of the other nucleotide trimming type,
198 productivity status combinations had significant evidence for secondary independent signals.

199 Our procedure also identified many highly significant associations between 5' end D-gene
200 trimming and SNPs within the *TCRB* gene locus, however these appear to result from correlations
201 between SNP genotype and *TRBD2* allele genotype (**Figure 3–Figure Supplement 1**). If we correct
202 for *TRBD2* allele genotype in our model formulation (see Methods), we no longer observe these
203 associations between SNPs within the *TCRB* gene locus and the extent of 5' end D-gene trimming
204 (**Figure 3–Figure Supplement 2**). *TRBD2* allele genotype could be acting as a confounding variable
205 due to linked local genetic variation which influences nucleotide trimming and/or D-gene assignment
206 ambiguity variation as a function of *TRBD2* allele genotype. To explore the extent of possible D-gene
207 assignment ambiguity variation, we restricted our analysis to TCRs which contain *TRBJ1* genes (and
208 consequently contain *TRBD1* due to topological constraints during V(D)J recombination (**Robins et al.,**
209 **2010; Murphy and Weaver, 2016**)). With this approach, we also no longer observe associations
210 between SNPs within the *TCRB* gene locus and the extent of 5' end D-gene trimming, and additionally,
211 we do observe significant associations between SNPs within the *DCLRE1C* locus and 5' and 3' end
212 D-gene trimming which were not observed in the original genome-wide analysis (**Figure 3–Figure**
213 **Supplement 3**).

214 Our fixed effects model formulation for these inferences is important: if we don't condition
215 on gene choice then additional, and presumably spurious, associations arise. Indeed, when
216 implementing the “simple model” designed to quantify the association between the four trimming
217 types and genome-wide SNP genotypes, without conditioning out the effect mediated by gene
218 choice, we observe additional associations between SNPs within the MHC locus and V-gene trimming
219 of productive TCRs and between SNPs within the *TCRB* locus and V-gene and 3' end D-gene trimming
220 of, again, productive TCRs (**Figure 3–Figure Supplement 5**). This is perhaps not surprising, as we
221 noted earlier that variations in the MHC and *TCRB* loci are associated with gene usage frequencies in
222 productive TCRs (**Figure 1**), and different genes have different trimming distributions (determined
223 in part by the nucleotide sequences at their termini).

224 Because P-nucleotides can be present at V(D)J junctions in the absence of nucleotide trim-
225 ming (**Murphy and Weaver, 2016**), we hypothesized that similar *DCLRE1C* locus variation may also
226 be associated with P-addition. Interestingly, we did not identify any strong associations between
227 SNPs within the *DCLRE1C* locus and the fraction of non-gene-trimmed TCRs containing P-nucleotides
228 when implementing our “gene-conditioned model”, despite the known role of the Artemis protein
229 in functioning as an endonuclease responsible for cutting the hairpin intermediate, and thus,
230 potentially creating P-nucleotides during V(D)J recombination (**Figure 3–Figure Supplement 6**). We
231 observe similar results when quantifying the effect of genome-wide SNPs on the number of V-, D-,
232 and J-gene P-nucleotides per TCR (**Figure 3–Figure Supplement 7**).

233 ***DNTT* locus variation is associated with the number of V-D and D-J N-insertions**

234 Unlike V-, D-, or J-gene nucleotide trimming length, the number of nucleotide N-insertions between
235 V-D and D-J genes does not vary substantially with V(D)J *TCRB* gene choice (**Figure 5–Figure Supple-**
236 **ment 1**) (*Murugan et al., 2012*). Thus, to infer the association between SNPs and the number of
237 nucleotide N-insertions, we implemented a “simple model”, without conditioning out any effect
238 mediated by gene choice. Again, because of the potential for population-substructure-related
239 effects to inflate associations between each SNP and the number of N-insertions, we incorporated
240 ancestry-informative principal components as covariates in each model (detailed in Methods).
241 Diagnostic statistics show that this bias correction is sufficient (**Figure 5–source data 3**).

242 With these methods, we identified three associations between SNPs and the number of nu-
243 cleotide N-insertions using a Bonferroni-corrected whole-genome P-value significance threshold
244 of 1.94×10^{-9} (see Methods) (**Figure 5** and **Figure 5–source data 1**). Two SNPs within the *DNTT*
245 gene locus (rs2273892 and rs12569756) were responsible for these associations. The *DNTT* gene
246 encodes the terminal deoxynucleotidyl transferase (TdT) protein which is a specialized DNA poly-
247 merase responsible for adding non-templated (N) nucleotides to coding junctions during V(D)J
248 recombination. When we restrict our analysis to TCRs which contain *TRBJ1* genes and consequently
249 eliminate potential D-gene assignment ambiguity, we continue to observe these *DNTT* associations
250 (**Figure 5–Figure Supplement 2**).

251 Since the TdT protein has an important mechanistic role in the N-insertion process and because
252 we already identified SNPs within the *DNTT* locus to be weakly associated with the number of
253 N-insertions at V(D)J gene junctions, we wanted to explore the locus further. Restricting the
254 analysis to the extended *DNTT* locus reduced the multiple testing burden such that 232 significant
255 associations emerged (**Figure 5** and **Figure 5–source data 2**). Many of the SNPs responsible for
256 these 232 significant associations within the extended *DNTT* locus were shared between insertion
257 and productivity types (**Figure 6**). While most of these associations are likely the result of a single
258 independent signal for each insertion and productivity type, we performed a conditional analysis
259 to identify potential independent secondary signals. To do so, we included the most significant
260 SNP within the *DNTT* locus for each insertion and productivity type as a covariate in the model.
261 With this approach, we identified rs2273892 as the primary independent signal for D-J N-insertion
262 of non-productive TCRs and rs12569756 as the primary independent signal for D-J N-insertion of
263 productive TCRs and V-D N-insertion of productive and non-productive TCRs. However, these two
264 SNPs are tightly linked and, thus, likely both represent the same, primary independent signal. This
265 analysis did not reveal any significant evidence for secondary independent signals.

266 We found that correcting for population-substructure-related effects was especially important
267 in our primary genome-wide analysis, which led us to discover differences in the extent of N-
268 insertion by ancestry-informative PCA cluster. Indeed, if we don't incorporate correction terms

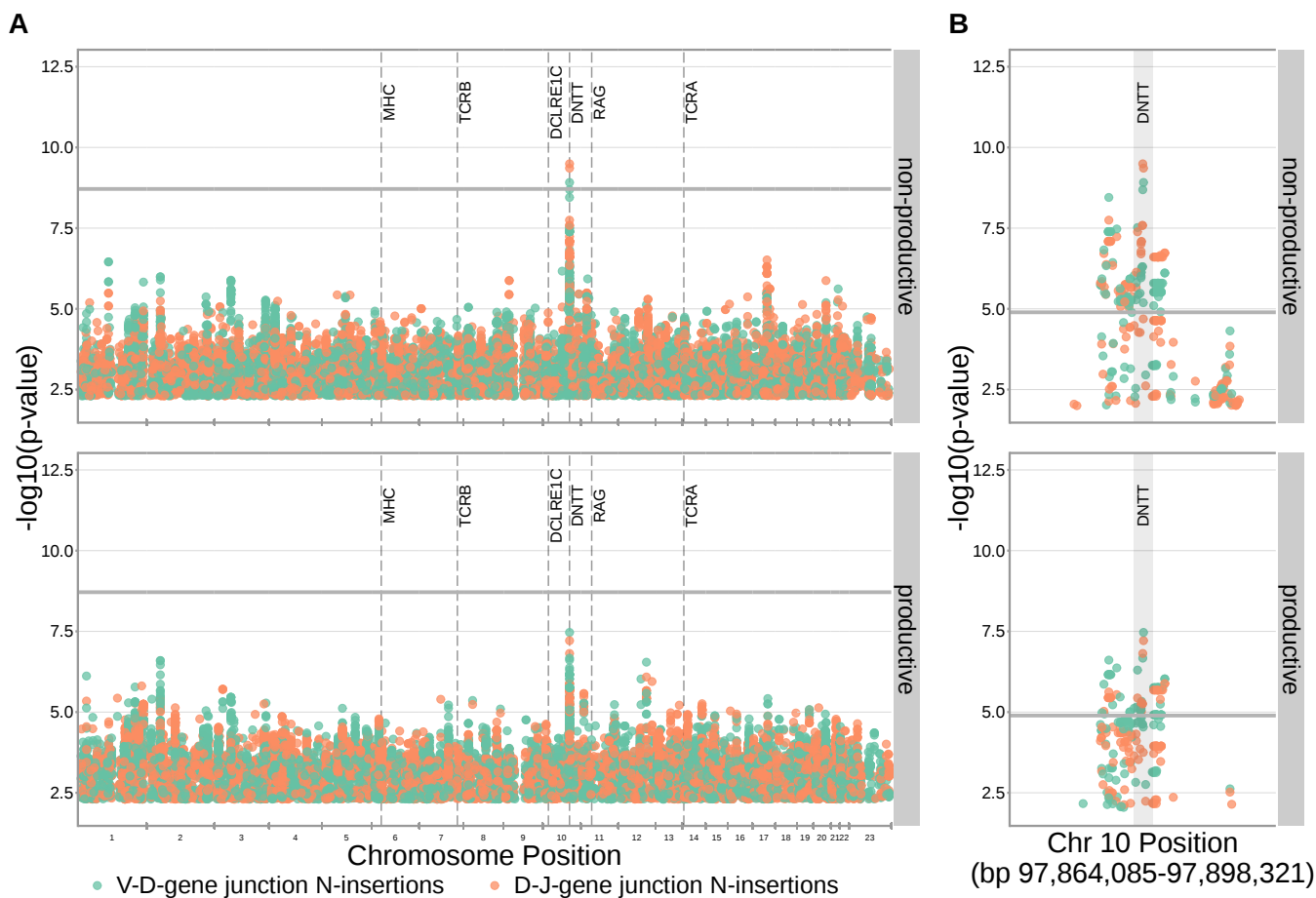


Figure 5. SNPs within the *DNTT* locus are associated with the extent of N-insertion. **(A)** There are three associations for SNPs within the *DNTT* locus which are significant when considered in the whole-genome context. The gray horizontal line corresponds to a whole-genome Bonferroni-corrected P-value significance threshold of 1.94×10^{-9} . **(B)** Using a *DNTT* gene-level significance threshold, many more SNPs within the extended *DNTT* locus have significant associations for both N-insertion types. Here, the gray horizontal line corresponds to a gene-level Bonferroni-corrected P-value significance threshold of 1.28×10^{-5} (calculated using gene-level Bonferroni correction for the 977 SNPs within 200kb of the *DNTT* locus, see Methods). For both (A) and (B), only SNP associations whose $P < 5 \times 10^{-3}$ are shown.

Figure 5-source data 1. There are three significant associations between SNPs genome-wide and the number of nucleotide N-insertions. The model type and Bonferroni-corrected P-value significance threshold used to identify these significant associations are described in [Table 1](#).

Figure 5-source data 2. There are 232 significant associations between SNPs genome-wide and the number of nucleotide N-insertions when restricting the analysis to the extended *DNTT* locus.

Figure 5-source data 3. Genomic inflation factor values are less than 1.03 for all paired N-insertion, productivity GWAS analyses. This suggests that we have properly controlled for population-substructure-related biases in all of the N-insertion analyses. Genomic inflation factor values were calculated as described in Methods.

Figure 5-figure supplement 1. The extent of N-insertion does not vary substantially by the gene allele identity for any gene type.

Figure 5-figure supplement 2. Significant associations continue to be observed within the *DNTT* locus for both V-D- and D-J-gene-junction N-insertions when restricting the analysis to TCRs which contain *TRBJ1* genes (and consequently contain *TRBD1*).

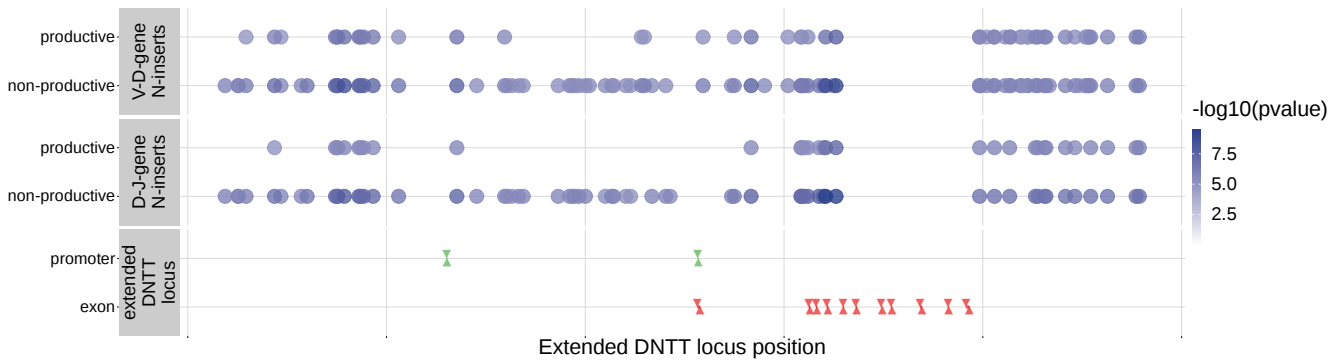


Figure 6. Within the *DNTT* locus, many of the significant SNP associations overlapped between N-insertion types when using *DNTT* gene-level Bonferroni-corrected P-value significance threshold of 1.28×10^{-5} . Downward arrows represent promoter/exon starting positions and upward arrows represent promoter/exon ending positions.

Figure 6-source data 1. *DNTT* locus SNP association P-values and locus positions.

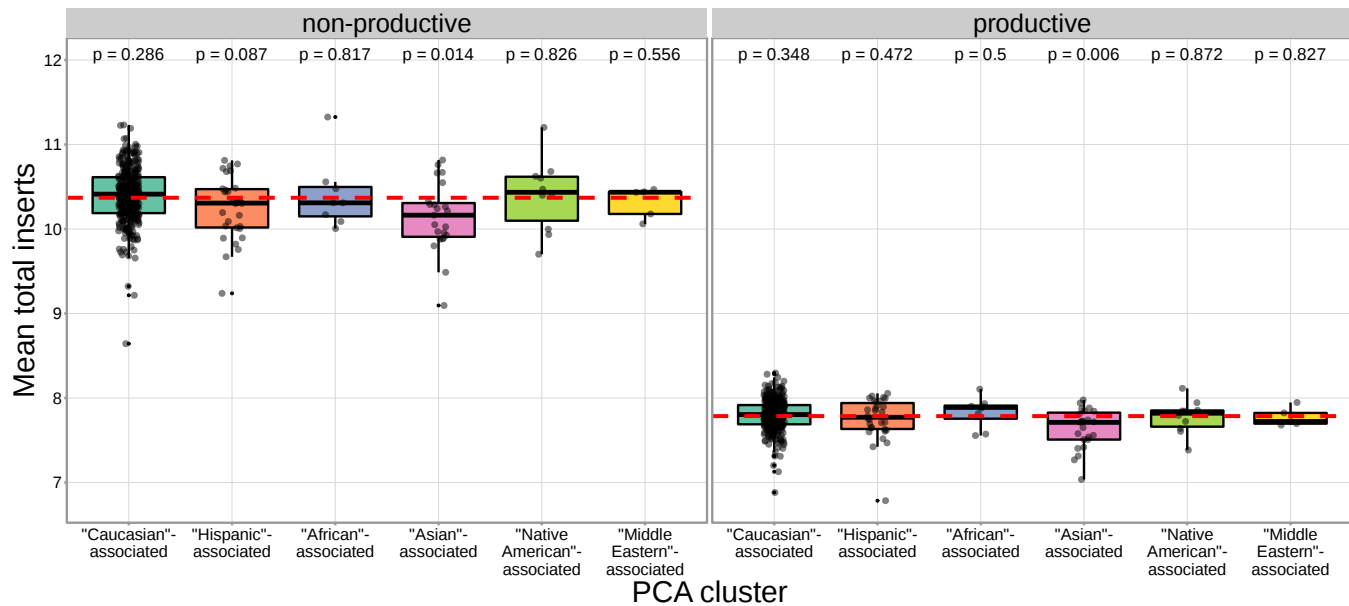


Figure 7. The TCR repertoires for subjects in the “Asian”-associated PCA-cluster contain fewer N-insertions for productive TCRs when compared to the population mean computed across all 666 subjects (dashed, red horizontal line). The P-values from a one-sample t-test (without Bonferroni multiple testing correction) for each PCA cluster compared to the population mean are reported at the top of the plot.

Figure 7-source data 1. PCA-cluster and average number of N-insertions by subject.

Figure 7-Figure supplement 1. The population mean is dominated by subjects in the “Caucasian”-associated PCA-cluster.

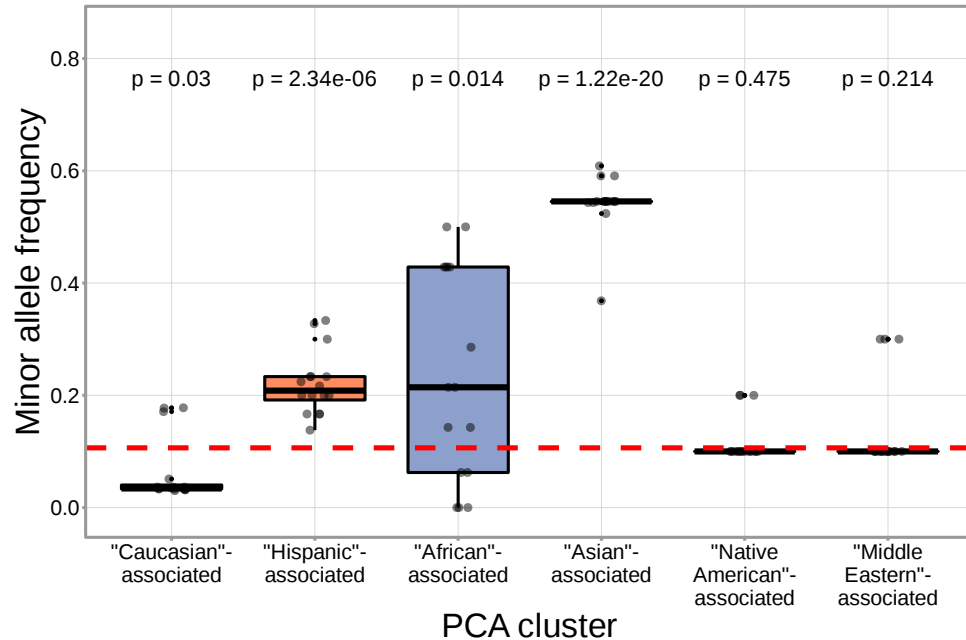


Figure 8. N-insertion associated SNPs within the *DNTT* region have a higher mean minor allele frequency within the "Asian"-associated PCA-cluster when compared to the population mean minor allele frequency computed across the 398 discovery cohort subjects (dashed, red horizontal line). The P-values from a one-sample t-test (without Bonferroni multiple testing correction) for each PCA cluster compared to the population mean are reported at the top of the plot. The population mean is dominated by subjects in the "Caucasian"-associated PCA cluster (*Figure 7–Figure Supplement 1*).

Figure 8–source data 1. Minor allele frequency for N-insertion associated SNPs within the *DNTT* locus by PCA-cluster.

269 for population-substructure-related biases in our model formulation, we observe many strongly
270 significant associations, particularly within the *DNTT* locus. This hinted at important PCA-cluster
271 level effects. When we look closely at the average number of N-insertions (combining the number
272 of V-D and D-J N-insertions) across TCR repertoires by PCA cluster, we note that subjects from the
273 "Asian"-associated PCA cluster have significantly fewer total N-insertions for productive ($P = 0.006$
274 without Bonferroni correction) and non-productive ($P = 0.014$ without Bonferroni correction) TCRs
275 when compared to the population mean (using a one-sample t-test) (*Figure 7*). The total N-insertions
276 for productive TCRs within the "Asian"-associated PCA cluster remain significantly different from the
277 population mean after Bonferroni multiple testing correction (corrected $P = 0.036$). Furthermore,
278 the "Asian"- and "Hispanic"-associated PCA clusters had significantly higher mean SNP minor allele
279 frequencies for N-insertion associated SNPs within the extended *DNTT* region when compared
280 to the mean population minor allele frequency ($P = 7.32 \times 10^{-20}$ for the "Asian"-associated PCA
281 cluster and $P = 1.17 \times 10^{-5}$ for the "Hispanic"-associated PCA cluster using a one-sample t-test with
282 Bonferroni multiple testing correction) (*Figure 8*).

Table 2. We inferred the associations between SNP genotype and TCR repertoire features for two SNPs overlapping between discovery-cohort and validation-cohort SNP sets. We considered the significance of the validation cohort associations at a Bonferroni-corrected SNP-level P-value significance threshold of 0.0042 for trimming and 0.0083 for N-insertion (see Methods). Validation cohort P-values are one-tailed. * discovery-cohort associations were only significant when considered at the *DNTT* -gene level significance threshold, not at the whole-genome significance threshold.

SNP	TCR chain	Repertoire feature	Productivity type	Discovery cohort signif. association	Validation cohort signif. association
rs12768894	TCR β	V-gene trimming	Productive	Yes (2.16×10^{-14})	Yes (7.17×10^{-7})
			Non-productive	Yes (7.21×10^{-14})	Yes (8.75×10^{-6})
	TCR α	J-gene trimming	Productive	Yes (1.23×10^{-11})	Yes (5.16×10^{-10})
			Non-productive	Yes (6.62×10^{-12})	No (4.18×10^{-2})
		V-gene trimming	Productive	N/A	Yes (2.59×10^{-5})
			Non-productive	N/A	Yes (2.68×10^{-7})
J-gene trimming	Productive	N/A	Yes (6.29×10^{-12})		
	Non-productive	N/A	No (9.99×10^{-3})		
rs3762093	TCR β	V-D N-insertion	Productive	Yes* (1.37×10^{-6})	No (0.153)
			Non-productive	Yes* (1.50×10^{-7})	No (0.059)
	TCR α	D-J N-insertion	Productive	Yes* (9.43×10^{-6})	No (0.137)
			Non-productive	Yes* (1.94×10^{-7})	No (0.067)
		V-J N-insertion	Productive	N/A	Yes (0.006)
			Non-productive	N/A	No (0.031)

Table 2-Figure supplement 1. The extent of V- and J-gene trimming of productive and non-productive TCR β chains changes as a function of SNP genotype within the discovery cohort for a non-synonymous *DCLRE1C* SNP (rs12768894, c.728A>G).

Table 2-Figure supplement 2. The extent of J-gene trimming of productive TCR β chains and V-gene trimming of productive and non-productive TCR β chains also changes as a function of rs12768894 genotype within the validation cohort.

Table 2-Figure supplement 3. The extent of V- and J-gene trimming of productive and non-productive TCR α chains also changes as a function of SNP genotype within the validation cohort for this SNP (rs12768894, c.728A>G).

Table 2-Figure supplement 4. The extent of V-D and D-J N-insertion of productive and non-productive TCR β chains changes as a function of SNP genotype within the discovery cohort for an intronic *DNTT* SNP (rs3762093).

Table 2-Figure supplement 5. rs3762093 genotype is not significantly associated with the number of V-D or D-J N-inserts within productive or non-productive TCR β chains in the validation cohort, but the direction of the effect is the same as the discovery cohort for all N-insertion and productivity types.

Table 2-Figure supplement 6. This SNP (rs3762093) is significantly associated with the number of V-J N-inserts for productive TCR α chains, but not for non-productive TCR α chains, in the validation cohort. However, the effect is stronger for both productivity types compared to TCR β chains.

283 Validation Analysis

284 To validate our results, we worked with paired ancestry-informative marker (AIM) SNP array and
 285 TCR α - and TCR β -immunosequencing data representing 94 individuals and 2 SNPs (which overlap
 286 with the discovery dataset) from an independent validation cohort (see Methods). In contrast
 287 to the discovery cohort, this cohort contains different demographics, shallower RNA-seq based
 288 TCR-sequencing, and a sparser set of SNPs. However, TCR-sequencing for both TCR α and TCR β
 289 chains is available.

290 We were able to validate a discovery-cohort significantly associated *DCLRE1C* SNP within this
 291 validation cohort. While none of the independent *DCLRE1C* SNPs from the discovery-cohort anal-
 292 ysis overlapped with the validation cohort SNP set, a single, non-synonymous SNP (rs12768894,
 293 c.728A>G) within the *DCLRE1C* locus was present in both SNP sets. This SNP was one of the signifi-
 294 cant associations we observed for V-gene trimming (productive $P = 2.16 \times 10^{-14}$; non-productive
 295 $P = 7.21 \times 10^{-14}$) and J-gene trimming (productive $P = 1.23 \times 10^{-11}$; non-productive $P = 6.62 \times 10^{-12}$)
 296 of TCR β chains in the genome-wide discovery cohort analysis (**Table 2-Figure Supplement 1**). Using

297 the same methods, we identified significant associations between this SNP and J-gene trimming
298 of productive TCR α and TCR β chains and V-gene trimming of both productive and non-productive
299 TCR α and TCR β chains within the validation cohort (**Table 2**, **Table 2-Figure Supplement 2**, and **Table 2-Figure Supplement 3**). Associations between rs12768894 and both types of D-gene trimming
300 of TCR β chains were not significant for either cohort.
301

302 We were unable to validate the most significantly associated *DNTT* SNPs due to lack of overlap
303 between the SNP sets for the discovery and validation cohorts; a discovery-cohort weakly associated
304 SNP (rs3762093) failed to reach statistical significance for all N-insertion types, but had the same
305 direction of effect in the validation cohort as follows. Within the discovery cohort, rs3762093
306 genotype was weakly associated with the number of V-D N-insertions (productive $P = 1.37 \times 10^{-6}$;
307 non-productive $P = 1.50 \times 10^{-7}$) and D-J N-insertions (productive $P = 9.43 \times 10^{-6}$; non-productive
308 $P = 1.94 \times 10^{-7}$) within TCR β chains (**Table 2-Figure Supplement 4**). Within the validation cohort, this
309 SNP was significantly associated with the number of V-J N-insertions within productive TCR α chains
310 (**Table 2** and **Table 2-Figure Supplement 6**). However, this SNP was not significantly associated with
311 the number of V-D or D-J N-insertions within productive or non-productive TCR β chains or the
312 number of V-J N-insertions within non-productive TCR α chains within the validation cohort (**Table 2**,
313 **Table 2-Figure Supplement 5**, and **Table 2-Figure Supplement 6**). Despite the lack of significance,
314 we noted that the model coefficients for rs3762093 genotype were in the same direction (i.e., the
315 minor allele was associated with fewer N-insertions) for all N-insertion and productivity types within
316 TCR β chains for both cohorts. Further, while TCR α chain sequencing was not available for the
317 discovery cohort, we observed stronger associations between rs3762093 genotype and the extent
318 of N-insertion for both productivity types within TCR α chains compared to TCR β chains within the
319 validation cohort. Perhaps with a larger validation cohort, significant associations would be present
320 for all N-insertion types.

321 Discussion

322 V(D)J recombination is a complex stochastic process that enables the generation of diverse TCR
323 repertoires. Our results show that genetic variation in various V(D)J recombination genes has a
324 key role in shaping the TCR repertoire through biasing V(D)J gene choice, nucleotide trimming, and
325 N-insertion in a broad population sample. While we recognize that there may be a complicated
326 entanglement between allelic variation and local *cis*-acting effects, we were primarily interested
327 in identifying strong, *trans*-acting associations. By leveraging the unique pairing of TCR β chain
328 immunosequencing and genome-wide genotype data, we have (1) confirmed and extended previous
329 studies on the genetic determinants of TCR V-gene usage, (2) discovered associations between
330 common genetic variants within the *DCLRE1C* and *DNTT* loci and V(D)J junctional trimming and
331 N-insertions, respectively, (3) developed a method for quantifying the extent of the associations
332 between genetic variations and junctional features, directly, without confounding gene choice

333 effects, and (4) revealed differences in the extent of N-insertion by ancestry-informative PCA cluster.

334 We note an abundance of associations between variation in the *TCRB* locus and V(D)J gene usage
335 biases for both productive and non-productive TCRs. Although previous reports have revealed
336 similar patterns of association for productive TCRs (*Sharon et al., 2016; Gao et al., 2019*), our results
337 refine and extend this result by quantifying the extent of *TCRB* locus variation on V(D)J gene usage for
338 non-productive TCRs. This highlights that locus variation is associated with TCR generation-related
339 gene usage biases, in addition to potential thymic selection biases for productive TCRs. These
340 TCR generation-related gene usage biases likely reflect local gene regulation and/or recombination
341 efficiency effects. For example, one of the SNPs most significantly associated with *TRBV28* expression
342 (rs17213) is located within the recombination signal sequence at the 3'-end of the gene and, thus,
343 could be involved directly in changing the recombination efficiency of *TRBV28*. Thus, different
344 expression levels of various genes could be promoted by variation within non-coding regions
345 such as promoters, 5'UTRs and leader sequences, introns, or recombination signal sequences.
346 Polymorphisms within these regions have been suggested to influence V(D)J gene expression levels
347 within B-cell receptor repertoires (*Mikocziova et al., 2021*). We also observed that variation in the
348 MHC locus is associated with V-gene usage biases for productive TCRs, but not non-productive
349 TCRs. These MHC locus associations are likely only observed for V-gene usage since the V-gene
350 locus, exclusively, encodes the TCR regions (complementarity-determining regions 1 and 2) which
351 directly contact MHC during peptide presentation (*Murphy and Weaver, 2016*). Previous work has
352 suggested that the thymic selection of certain V-genes may be biased by germline-encoded TCR-
353 MHC compatibilities in an MHC dependent manner (*Sharon et al., 2016; Gao et al., 2019*). Because
354 of our observed distinction between associations present between MHC variation and V-gene usage
355 in productive versus non-productive TCRs, our work supports this hypothesis.

356 We have identified, for the first time, specific genetic variants which are associated with modify-
357 ing the extent of N-insertion and nucleotide trimming. While many previous studies have reported
358 evidence of genetic influences on overall gene usage (*Zvyagin et al., 2014; Qi et al., 2016; Rubelt
359 et al., 2016; Pogorelyy et al., 2018; Tanno et al., 2020; Fischer et al., 2021*) and repertoire similarity
360 in response to acute infection (*Qi et al., 2016; Pogorelyy et al., 2018*), there have been few ex-
361 plorations into how heritable factors may bias TCR junctional features beyond reports of genetic
362 similarity implying overall TCR repertoire similarity (*Krishna et al., 2020; Rubelt et al., 2016*). Here,
363 we noted that variation in the gene encoding the Artemis protein (*DCLRE1C*) is associated with
364 the extent of V- and J-gene nucleotide trimming for both productive and non-productive TCRs.
365 These associations are strongest for non-productive TCRs suggesting a TCR generation-related
366 repertoire bias. It is well established that the Artemis protein, in complex with DNA-PKcs, functions
367 as an endonuclease responsible for cutting the hairpin intermediate, and thus, potentially creat-
368 ing P-nucleotides prior to nucleotide trimming during V(D)J recombination (*Weigert et al., 1978;
369 Moshous et al., 2001; Ma et al., 2002; Lu et al., 2007*). The direct involvement of Artemis in the

370 nucleotide trimming mechanism, however, has yet to be confirmed. It has been shown that the
371 Artemis protein possesses single-strand-specific 5' to 3' exonuclease activity (*Ma et al., 2002; Li*
372 *et al., 2014*) and, thus, may be properly positioned to trim nucleotides. A non-synonymous SNP
373 within *DCLRE1C* (rs12768894, c.728A>G) was one of the significant associations we observed for V-
374 and J-gene nucleotide trimming in both the primary cohort and the independent validation cohort.
375 Perhaps this mutation, or other linked non-synonymous *DCLRE1C* variation that was not studied
376 here, is directly involved in the trimming changes we observe. We did not observe strong associ-
377 ations between variation in the *DCLRE1C* locus and the number of P-nucleotides or the fraction
378 of non-gene-trimmed TCRs containing P-nucleotides, despite the established mutually exclusive
379 relationship between P-addition and nucleotide trimming (*Gauss and Lieber, 1996; Srivastava and*
380 *Robins, 2012; Murphy and Weaver, 2016*). However, the absence of P-nucleotide associations at the
381 *DCLRE1C* locus could be the result of restricting the analyses to the non-gene-trimmed repertoire
382 subset. Perhaps with a larger dataset these associations would be present.

383 Further, we have identified associations between variation in the gene encoding the TdT protein
384 (*DNTT*) and the number of N-insertions for both productive and non-productive TCRs. Because of
385 the established, direct involvement of the TdT protein in the N-insertion mechanism, these *DNTT*
386 locus variations could be influencing the function of the TdT protein. These significant associations
387 were slightly stronger for non-productive TCRs perhaps suggesting that thymic selection may limit
388 the mechanistic effects of locus variation. Interestingly, we noted that the extent of N-insertion
389 varies by ancestry-informative PCA cluster. Specifically, we found that the "Asian"-associated PCA
390 cluster had significantly fewer N-insertions for productive TCRs when compared to the population
391 mean which is dominated by the "Caucasian"-associated PCA cluster. This finding is, perhaps,
392 related to the influence of broad heritable factors biasing the extent of N-insertions.

393 More work is required to elucidate the mechanistic relationship between *DCLRE1C* locus variation
394 and nucleotide trimming changes. Future work can also focus on identifying correlations between
395 TCR repertoires and host immune exposures while accounting for genetically determined repertoire
396 biases identified here. These directions would allow us to continue disentangling the genetic and
397 environmental determinants governing TCR repertoire diversity.

398 One limitation of our approach is the possibility that the SNP array data used here does not
399 capture all potential causal variation. Further, the lack of overlap between SNP sets for the discovery
400 and validation cohorts limited our ability to directly validate our strongest inferences. Another key
401 constraint is the challenge of inferring the V(D)J rearrangements from the final nucleotide sequences.
402 Therefore, there is the potential for biases resulting from incorrect V(D)J -gene assignment. We have
403 found that controlling for D-gene assignment ambiguity in the nucleotide trimming and N-insertion
404 analyses results in similar significant associations within the *DNTT* and *DCLRE1C* loci. Although we
405 cannot rule out some effect of incorrect V(D)J -gene assignment bias for *trans* associations resulting
406 from the signal being "masked" by stronger *TCRB* locus signals, these biases seem to be mostly

407 restricted to *cis* associations.

408 In summary, we have found that the usage of *TCRB* genes is associated with variation in MHC and
409 *TCRB* loci, the number of N-insertions is associated with *DNTT* variation, and the extent of nucleotide
410 trimming is associated with *DCLRE1C* variation. Our results clearly demonstrate how variation in
411 V(D)J recombination-related genes can bias TCR repertoire combinatorial and junctional diversity. In
412 the case of B cells, genetically determined V(D)J gene usage biases within B-cell receptor repertoires
413 have been linked to functional consequences for the overall immune response to specific antigens
414 and, thus, an increased susceptibility to certain diseases (*Mikocziova et al., 2021*). As such, the
415 genetic TCR repertoire biases identified here lay the groundwork for further exploration into the
416 diversity of immune responses and disease susceptibilities between individuals. Such studies will
417 enhance our understanding of how an individual's diverse TCR repertoire can support a unique,
418 robust immune response to disease and vaccination. Our findings also provide a step towards the
419 ability to understand and predict an individual's TCR repertoire composition which will be critical for
420 the future development of personalized therapeutic interventions and rational vaccine design.

421 **Methods and Materials**

422 **Discovery cohort dataset**

423 *TCR β* repertoire sequence data for 666 healthy bone marrow donor subjects was downloaded from
424 the Adaptive Biotechnologies website using the link provided in the original publication (*Emerson*
425 *et al., 2017*). For both the discovery and validation cohorts, V, D, and J genes were assigned by
426 comparing the *TCR β* -chain (and *TCR α* -chain for the validation cohort) nucleotide sequences to the
427 human IMGT/GENE-DB *TCRB* (or *TCRA*) allele sequences (*Giudicelli et al., 2005*). To infer the extent
428 of nucleotide trimming, N-insertion, and P-addition for each *TCR β* -chain (and *TCR α* -chain) nucleotide
429 sequence, the most parsimonious V(D)J recombination scenario was assigned to each sequence
430 using the TCRdist pipeline (*Dash et al., 2017*). The V(D)J recombination scenario requiring the fewest
431 N-insertions was defined as the most parsimonious scenario.

432 SNP array data corresponding to 398 of these subjects was downloaded from The database
433 of Genotypes and Phenotypes (accession number: phs001918). Details of the SNP array dataset,
434 genotype imputation, and quality control have been described previously (*Martin et al., 2020*).

435 **Validation cohort dataset**

436 Peripheral blood mononuclear cell (PBMC) samples were collected from 150 healthy subjects
437 recruited at the Health Center Sócrates Flores Vivas (HCSFV) in Managua, Nicaragua (*Ng et al., 2016*).
438 Healthy participants were recruited as contacts of influenza infected index patients and blood
439 samples were collected at both the initial visit and a 30 day follow-up visit. Participants provided
440 written informed consent and parental permission was obtained from parents or legal guardians
441 of children, in addition to verbal assent from children aged six years and older. This study was

442 approved by the Institutional Review Boards at the University of Michigan, Centro Nacional de
443 Diagnóstico y Referencia (Ministry of Health, Nicaragua), and University of California, Berkeley.

444 With these samples, PBMCs were stained with CD3-PerCP eFluor710 (Thermo Cat. 46-0037-42),
445 CD4-BV650 (BD Biosciences Cat. 563875), CD8-APC Fire750 (Biolegend Cat. 344746), and gdCy7
446 (Biolegend Cat. 331222). Briefly, after thawing from cryopreservation and plating in a 96-well round
447 bottom plate, cells were spun down and resuspended in 50 μ L of human Fc block (BD Biosciences
448 Cat. 564220) in Dulbecco's phosphate-buffered saline (DPBS) at 1 μ L per test (1 test = 1.0×10^6 cells)
449 and incubated for 10 minutes at room temperature. Afterwards, 50 μ L of a Live/Dead Aqua (Tonbo
450 Cat. 13-0870-T100, 1 μ L per test, 1 test = 1.0×10^6 cells) and pre-titrated surface antibody cocktail
451 in DPBS were added to each well and cells were incubated for 30 minutes on ice and in the dark.
452 Cells were washed, resuspended in sort buffer and bulk sorted into polystyrene tubes. Afterwards,
453 samples were spun down, pellets were resuspended in 350 μ L of RNA lysis buffer, and stored at -80
454 C in labeled epitubes.

455 From here, DNA was extracted from 200 μ L of neutrophil pellets using the Qiagen QIAamp
456 DNA Mini Kit (Cat. 51306). Bulk repertoires for sorted CD4 and CD8 T cells were generated in
457 accordance with the protocol developed by *Egorov et al. (2015)*, and sequencing was performed on
458 the NovaSeq by the Hartwell Center at St. Jude. Raw cDNA sequencing data were processed with the
459 MIGEC software package (*Shugay et al., 2014*) to define error-corrected TCRA and TCRB transcript
460 sequences, which were then analyzed as described above for the discovery cohort data (*Emerson*
461 *et al., 2017*).

462 Genotypes for SNPs of interest corresponding to 94 of these subjects were pulled from Infinium
463 Global Screening Array-24 v3.0 BeadChip results, which measures 654,027 SNP makers including
464 multi-ethnic genome-wide content, curated clinical research variants, and quality control markers.
465 High quality DNA was extracted using the Qiagen QIAamp DNA Mini Kit (Cat. 51306), and submitted
466 to the St. Jude Hartwell Center for preparation and processing. Two SNPs, rs72640001 and
467 rs72772435, were not included on this chip and were determined using Thermo Fisher TaqMan SNP
468 Genotyping Assays (Cat. 4351379, Assay ID C_99271581_10 and C_99587751_10, respectively) and
469 TaqMan Genotyping Master Mix (Cat. 4371353) according to the kit manual.

470 **Data preparation**

471 With these paired SNP array and TCR-immunosequencing for both the discovery and validation
472 cohorts, we aimed to identify significant associations between these SNPs and various TCR reper-
473 toire features. Because we would expect a difference in these phenotypes depending on whether
474 a TCR sequence is classified as productive or non-productive, we split the data based on this TCR
475 productivity status and computed associations separately for the two groups.

476 We also subset the SNP data further based on several quality control metrics. We filtered the
477 SNP array data to use only SNPs with a minor allele frequency above 0.05 in our analyses which

478 excluded SNPs for which all subjects had the same genotype. For the discovery cohort, this filtering
479 procedure and previous quality control (*Martin et al., 2020*) left 6,456,824 SNPs (of the original 35
480 million SNPs) remaining for our analyses. Only 2 SNPs from the validation cohort overlapped with
481 this discovery cohort SNP set. For each of these discovery and validation cohort SNPs, when fitting
482 each association model, we excluded observations which contained a missing SNP genotype. Next,
483 for the TCR repertoire data, we excluded repertoires which contained a relatively small number
484 of TCRs ($\log_{10}(\text{TCR count}) < 4.25$ for productive TCRs and $\log_{10}(\text{TCR count}) < 3.5$ for non-productive
485 TCRs) from the analyses. Lastly, for TCR β -chains, if a D-gene is trimmed so much that the D-gene
486 is unidentifiable, the inference pipeline used to infer *TCRB* genes for each sequenced TCR does
487 not report a D-gene. Instead, this D-gene (if it is indeed present) is reported as a V-J N-insertion.
488 Because of this, we excluded these observations when fitting models for TCR features involving the
489 D-gene (i.e. D-gene usage, both V-D and D-J junction N-insertions, D-gene P-additions, and D-gene
490 nucleotide trimming).

491 **Notation**

492 The discovery dataset contains observations for a total of $I = 398$ subjects and the validation dataset
493 contains observations for a total of $I = 94$ subjects. Within each cohort, for subject $i \in \{1, \dots, I\}$,
494 we observe a total of N_i TCRs which, here, represents the number of TCRs which compose each
495 subject's TCR repertoire. Thus, for each TCR $k \in \{1, \dots, N_i\}$, we measure a TCR feature of interest, y_{ik} ,
496 such as the number of V-D N-insertions, the extent of V-trimming, etc. We also have SNP genotype
497 data for a total of J SNPs such that for each SNP $j \in \{1, \dots, J\}$ and subject $i \in \{1, \dots, I\}$, we measure
498 the number of minor alleles in the genotype, $x_{ij} \in \{0, 1, 2\}$.

499 **Quantifying the association strength between each SNP and TCR feature using the** 500 **"simple model"**

501 We first describe what we call the "simple model". We will describe more complex models, as well
502 as each model with added correction for population-substructure-related effects, in the sections
503 following.

504 We began by calculating the average occurrence of the TCR feature of interest, \bar{y}_i , within the
505 repertoire of each subject, i . By condensing the data in this way, for each subject $i \in \{1, \dots, I\}$,
506 we are left with $N_i = 1$ observations. For example, for the discovery cohort, we can fit the model
507 across $\sum_{i=1}^I N_i = 398$ observations. Using this condensed dataset, for each SNP, TCR feature, and
508 productivity status, we can fit the model:

$$\bar{y}_i = x_{ij} \cdot \beta_{1j} + \beta_0 + \epsilon_{ij} \quad (1)$$

509 where β_{1j} is the allele effect for SNP j on the TCR feature of interest \bar{y}_i , β_0 is the intercept, and ϵ_{ij} is
510 the random error for subject i and SNP j such that $\epsilon_{ij} \sim \mathcal{N}(0, \sigma^2)$.

511 To estimate each regression coefficient, we solved the least squares problem:

$$(\hat{\beta}_0, \hat{\beta}_{1j}) = \operatorname{argmin}_{\beta_0, \beta_{1j}} \sum_{i=1}^n (\bar{y}_i - (x_{ij} \cdot \beta_{1j} + \beta_0))^2 \quad (2)$$

512 using the function `lm` in R. With each estimate of the j -th SNP effect on the TCR feature of interest,
513 $\hat{\beta}_{1j}$, generated by fitting the least squares problem (**Equation 2**), we quantified the association
514 strength between each SNP and the TCR feature of interest by testing whether $\hat{\beta}_{1j} = 0$. To do this,
515 we calculate the test statistic:

$$T_j = \frac{\hat{\beta}_{1j}}{\operatorname{se}(\hat{\beta}_{1j})} \quad (3)$$

516 and compare T_j to a $N(0, 1)$ distribution to obtain each P-value.

517 **Quantifying the association strength between each SNP and TCR feature, condi-** 518 **tional on *TCRB* gene type using the “gene-conditioned model”**

519 We noted that the amount of certain TCR features (such as the extent of all types of nucleotide
520 trimming) vary by V(D)J *TCRB* gene choice. Thus, we can condition on this gene choice to quantify
521 the direct association between each SNP and the amount of each TCR feature, without confounding
522 gene choice effects. In this way, we condition on each gene type $t \in \{\text{V-gene, J-gene, D-gene}\}$
523 corresponding to the TCR feature of interest (i.e. $t = \text{V-gene}$ for V-gene trimming, $t = \text{J-gene}$ for
524 J-gene trimming, etc.). We will refer to the following model as the “gene-conditioned model” in the
525 main text. Many similarities exist between the “simple model” described in the previous section and
526 this “gene-conditioned model.” Thus, we will focus on the differences between the two models here.
527 We will describe both models with added correction for population-substructure-related effects, in
528 the sections following.

529 As in the previous section, we, again, want to reduce the number of data observations. For
530 each subject $i \in \{1, \dots, I\}$, we can calculate the average amount of each TCR feature \bar{y}_{im} by each
531 candidate *TCRB* gene allele group m for the given gene type t such that $m \in \{1, \dots, M_t\}$. In calculating
532 the average amount of each TCR feature across TCRs with the same candidate *TCRB* gene allele, we
533 combined *TCRB* gene alleles which had identical CDR3 sequences and were of the same candidate
534 *TCRB* gene into *TCRB* gene allele groups. As such, the number of observations per subject N_i in
535 this condensed dataset will equal M_t and, thus, we will need to fit each model across $\sum_{i=1}^I M_t$
536 observations. In our data, for TCR β chains, we observe 141 possible *TCRB* V-gene allele groups, 16
537 J-gene allele groups, and 3 D-gene allele groups. Thus, using the extent of nucleotide trimming as
538 an example TCR feature within the discovery cohort, with this condensed formulation, for each SNP
539 and productivity status, we have $\sim 56,000$ observations for V-gene trimming, $\sim 6,000$ observations
540 for J-gene trimming, and $\sim 1,200$ observations for both types of D-gene trimming.

541 Using this condensed dataset, for each SNP, TCR feature, and productivity status, we fit the

542 following “gene-conditioned model”:

$$\bar{y}_{im} = x_{ij} \cdot \beta_{1j} + \beta_0 + \gamma_{jm} + \epsilon_{ijm} \quad (4)$$

543 where γ_{jm} represents the gene-effect on the amount of the TCR feature of interest for SNP j and
544 gene-allele-group m , and ϵ_{ijm} is the random error for subject i , SNP j , and gene-allele-group m such
545 that $\epsilon_{ijm} \sim \mathcal{N}(0, \sigma^2)$. The variables x_{ij} , β_{1j} , and β_0 are defined as in the “simple model” description
546 (**Equation 1**) in the previous section. However, since each subject had a different number of TCRs
547 measured and varying *TCRB* gene usage, we calculated the proportion of TCRs from each candidate
548 *TCRB* gene allele group, m , to define a weight, W_{im} , for each observation:

$$W_{im} = \frac{N_{im}}{\sum_{m=1}^{M_i} N_{im}}.$$

549 With this, we solved the following weighted least squares problem for each SNP, TCR feature, and
550 productivity status combination:

$$(\hat{\beta}_0, \hat{\beta}_{1j}, \hat{\gamma}_j) = \underset{\beta_0, \beta_{1j}, \gamma_j}{\operatorname{argmin}} \sum_{i=1}^n \sum_{m=1}^{M_i} W_{im} \cdot (\bar{y}_{im} - (\beta_0 + \gamma_{jm} + \beta_{1j} x_{ij}))^2 \quad (5)$$

551 using the `lm` function in R.

552 With each estimate of the j -th SNP effect on the amount of the TCR feature of interest, $\hat{\beta}_{1j}$,
553 generated using the models described above, we quantified the association strength between
554 each SNP and the amount of the TCR feature by testing whether $\hat{\beta}_{1j} = 0$. To do this, we applied a
555 t-test (described in the previous section) using the test statistic (**Equation 3**) to obtain each P-value.
556 However, because our condensed dataset contains a total of M_i observations from each subject i ,
557 these P-values may be inflated due to intra-subject observations being potentially correlated. Thus,
558 to increase the accuracy of the P-value calculation, for each association P-value below a certain
559 threshold (we chose $P < 5 \times 10^{-5}$), we recalculated the P-value using a clustered bootstrap (with
560 subjects as the sampling unit). To do so, for each bootstrap iterate, we resampled subjects from the
561 condensed dataset with replacement. Using this re-sampled data, we fit the model in **Equation 5** to
562 estimate each coefficient. We repeated this bootstrap process 100 times and used the resulting 100
563 coefficient estimates to estimate a standard error for each model coefficient. With this re-calculated
564 standard error of the estimate of the j -th SNP effect on the amount of the TCR feature of interest,
565 $se(\hat{\beta}_{1j})$, we wanted to test whether $\hat{\beta}_{1j} = 0$ by recalculating the test-statistic, **Equation 3**, and applying
566 a t-test to obtain each “corrected” P-value. As noted in the multiple testing correction methods
567 section, when accounting for multiple testing via Bonferroni correction, we used the entire number
568 of TCR features and SNPs considered (not just those that were sufficiently promising to warrant
569 use of the bootstrap to get a more accurate P-value): This ensures that our correction will not be
570 anti-conservative.

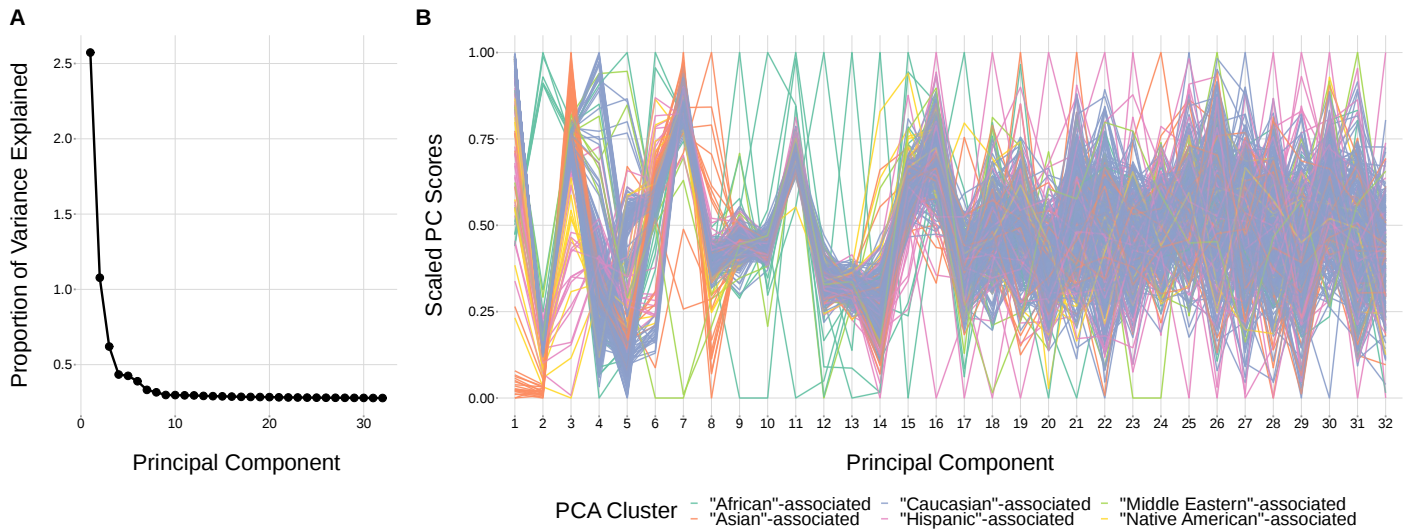


Figure 9. The top principal components calculated from genotype data reflect ancestry structure among samples. **(A)** The majority of the ancestry-informative principal component analysis variance is explained by the first 8 principal components. **(B)** The first 8 principal components show distinct separation by PCA cluster. Each colored line represents one of the 398 samples. The first 32 principal components are shown on the X-axis and their scaled component values for each subject on the Y-axis.

Figure 9–source data 1. Percent variance explained by each principal component.

Figure 9–source data 2. Scaled principal component values by subject.

571 Correcting for population-substructure-related effects

572 Structure within our SNP genotype data (such as population-substructure-related biases due to
 573 ancestry), if present, may produce false positive associations when quantifying the association
 574 strength between each SNP and our phenotype of interest. To account for this, we implemented
 575 principal component analysis as commonly applied to genome-wide genotype data for population
 576 substructure inference. Specifically, we used the PC-AiR algorithm (*Conomos et al., 2015*) which
 577 identifies principal components that capture ancestry while accounting for relatedness in the sam-
 578 ples. As such, the top principal components calculated from the genotype data reflect population
 579 substructure among the samples. When plotting the proportion of variance explained by each PC,
 580 we find that the majority of variability appears to be explained by the top eight PCs (*Figure 9*). This
 581 conclusion is supported when plotting each PC score by ancestral group (*Figure 9*). With this, we
 582 incorporated the top eight principal components as covariates into our GWAS models described
 583 above.

584 As such, to quantify the association strength between each SNP and TCR feature without
 585 conditioning on gene usage as in *Equation 1*, while incorporating principal component terms to
 586 correct for population-substructure-related bias due to ancestry, we fit the model:

$$\bar{y}_i = x_{ij} \cdot \beta_{1j} + \beta_0 + \sum_{p=1}^8 \beta_{2jp} \cdot P_{ip} + \epsilon_{ij} \quad (6)$$

587 where \bar{y}_i , x_{ij} , β_{1j} , β_0 , and ϵ_{ij} are defined as in *Equation 1*, β_{2jp} is the population-substructure-related
 588 bias correction term for SNP j and the p -th principal component, and P_{ip} is the p -th principal

589 component for subject i as calculated above. To estimate each regression coefficient, we solved the
590 following least squares problem for each SNP, TCR feature, and productivity status combination:

$$(\hat{\beta}_0, \hat{\beta}_{1j}, \vec{\beta}_{2j}) = \operatorname{argmin}_{\beta_0, \beta_{1j}, \vec{\beta}_{2j}} \sum_{i=1}^n (\bar{y}_i - (x_{ij} \cdot \beta_{1j} + \beta_0 + \sum_{p=1}^8 \beta_{2jp} \cdot P_{ip}))^2.$$

591 Furthermore, to quantify the association strength between each SNP and TCR feature, condi-
592 tional on gene usage as in **Equation 4**, while incorporating principal component terms to correct
593 for population-substructure-related bias due to ancestry, we fit the model:

$$\bar{y}_{im} = x_{ij} \cdot \beta_{1j} + \beta_0 + \gamma_{jm} + \sum_{p=1}^8 \beta_{2jp} \cdot P_{ip} + \epsilon_{ijm} \quad (7)$$

594 where \bar{y}_{im} , x_{ij} , β_{1j} , β_0 , γ_{jm} , and ϵ_{ij} are defined as in **Equation 4** and β_{2jp} and P_{ip} are defined as in
595 **Equation 6**. Again, to estimate each regression coefficient, we solved the following weighted least
596 squares problem for each SNP, TCR feature, and productivity status combination:

$$(\hat{\beta}_0, \hat{\beta}_{1j}, \hat{\gamma}_j, \vec{\beta}_{2j}) = \operatorname{argmin}_{\beta_0, \beta_{1j}, \gamma_j, \vec{\beta}_{2j}} \sum_{i=1}^n \sum_{m=1}^{M_i} W_{im} \cdot (\bar{y}_{im} - (\beta_0 + \gamma_{jm} + \beta_{1j} x_{ij} + \sum_{p=1}^8 \beta_{2jp} \cdot P_{ip}))^2.$$

597 With these estimates for the population-substructure-corrected j -th SNP effect on the amount of
598 the TCR feature of interest, $\hat{\beta}_{1j}$, we calculated a P-value using the methods described in the methods
599 section for each model type.

600 **Correcting for *TRBD2* allele genotype, SNP genotype linkage when quantifying SNP, 601 TCR feature associations within the *TCRB* locus**

602 Within the *TCRB* locus, we noted that SNP genotypes were associated with *TRBD2* allele genotype
603 (**Figure 3–Figure Supplement 1**). Associations between gene-alleles and *TCRB* locus SNP genotypes,
604 if present, may produce false positive associations when implementing the “gene-conditioned
605 model” to infer associations between SNPs and TCR repertoire features, conditional on gene
606 usage. To explore this phenomenon further, we zoomed in to the *TCRB* locus and incorporated a
607 *TRBD2* allele genotype correction procedure into our model formulation. As such, to quantify the
608 association strength between each *TCRB* locus SNP and TCR feature, conditional on gene usage and
609 correcting for population-substructure-related effects as in **Equation 7**, while incorporating *TRBD2*
610 allele genotype correction terms, we fit the model:

$$\bar{y}_{im} = z_i \cdot \alpha_j + x_{ij} \cdot \beta_{1j} + \beta_0 + \gamma_{jm} + \sum_{p=1}^8 \beta_{2jp} \cdot P_{ip} + \epsilon_{ijm}$$

611 where z_i represents the qualitative *TRBD2* allele genotype status for subject i such that $z_i \in$
612 {“*TRBD2**01 homozygous”, “heterozygous”, “*TRBD2**02 homozygous”}, α_j is the *TRBD2* allele geno-
613 type effect for SNP j , and the remaining variables are defined as in **Equation 7**. With this model
614 formulation, we can estimate each regression coefficient by solving the following weighted least

615 squares problem for each *TCRB* SNP, TCR feature, and productivity status combination:

$$(\hat{\alpha}_j, \hat{\beta}_0, \hat{\beta}_{1j}, \hat{\gamma}_j, \vec{\hat{\beta}}_{2j}) = \underset{\alpha_j, \beta_0, \beta_{1j}, \gamma_j, \vec{\beta}_{2j}}{\operatorname{argmin}} \sum_{i=1}^n \sum_{m=1}^{M_i} W_{im} \cdot (\bar{y}_{im} - (\alpha_j z_i + \beta_0 + \gamma_{jm} + \beta_{1j} x_{ij} + \sum_{p=1}^8 \beta_{2jp} \cdot P_{ip}))^2.$$

616 With these estimates for the *TRBD2* allele genotype and population-substructure-corrected *j*-th
617 SNP effect on the amount of the TCR feature of interest, $\hat{\beta}_{1j}$, we calculated a P-value using the
618 methods described in the methods section for the “gene-conditioned model”.

619 **Multiple testing correction for associations**

620 For each TCR feature (i.e. extent of trimming, number of N-insertions, etc.), we considered the
621 significance of associations using a Bonferroni-corrected threshold. To establish each threshold,
622 we corrected for each TCR feature subtype (i.e. V-gene trimming, J-gene trimming, etc. for the TCR
623 trimming feature), the two TCR productivity types (productive and non-productive), and the total
624 number of SNPs tested. When considering associations in the whole-genome context, we corrected
625 for the approximately 6.5 million SNPs (remaining after filtering). When considering associations in
626 a gene-level context, we corrected for the number of SNPs within 200 kb of the gene of interest. For
627 the validation analysis, we considered associations in a SNP-level context and did not correct for
628 multiple SNPs. However, for the validation analysis, we considered the significance of associations
629 within both *TCRα* and *TCRβ* chains and, thus, corrected the significance threshold accordingly.

630 **Genomic inflation factor calculations**

631 We defined the genomic inflation factor λ to be the ratio of the median of the empirically observed
632 squared test statistic to the expected median (*Devlin and Roeder, 1999; Freedman et al., 2004;*
633 *Price et al., 2010*). For each GWAS analysis implemented using the “simple model”, we used the
634 test statistic T_j given by *Equation 3* for each SNP $j = \{1 \dots J\}$ tested genome-wide. For each GWAS
635 analysis implemented using the “gene-conditioned model”, it was not computational feasible to
636 calculate a test statistic T_j for all SNPs tested genome-wide using the bootstrapping protocol
637 described in the “gene-conditioned model” methods section. Thus, instead, we randomly sampled
638 10,000 SNPs and calculated the test statistic T_j for each SNP in the random subset. Let $S =$
639 $\{T_1^2, \dots, T_J^2\}$ be the set of all squared test statistics. As such,

$$\lambda = \frac{\operatorname{median}(S)}{0.456}$$

640 where 0.456 is the median of a chi-squared distribution with one degree of freedom. If the GWAS
641 analysis results follow the chi-squared distribution, the expected value of λ is 1. Thus, when $\lambda < 1.03$,
642 we concluded that there was no evidence of systemic population-substructure-related bias in the
643 analysis (*Price et al., 2010; Conomos et al., 2016*).

644 **Conditional analysis to test for multiple independent association signals**

645 Within the *DNTT* and *DCLRE1C* loci, we performed a stepwise series of nested regression analyses to
646 test for independent SNP associations within each locus for N-insertion and nucleotide trimming,
647 respectively. We used the same models and covariates as the primary analyses (“simple model”
648 for associations between N-insertion and *DNTT* variation and the “gene-conditioned model” for
649 associations between nucleotide trimming and *DCLRE1C* variation) and included the most significant
650 SNP within each locus as an additional covariate. We inferred the association between each SNP
651 within each locus and the TCR feature of interest using this new conditional model and considered
652 significant associations at a gene-level Bonferroni-corrected significance threshold for each locus.
653 From here, we repeated this analysis (if necessary), identifying and adding additional SNPs one-by-
654 one as a covariate to each successive model. Once the P-value of top SNP within the locus was no
655 longer significant, we concluded the analysis. SNPs which were added as additional covariates in
656 the final conditional model were considered to be independent signals.

657 **Ancestry-informative PCA cluster classification**

658 In order to correct for population-substructure-related biases due to ancestry in our GWAS analyses,
659 we used ancestry-informative principal component analysis. The original genotyping dataset (*Mar-*
660 *tin et al., 2020*) contained self-reported ancestry. However, a number of subjects did not self-report
661 ancestry in the original data collection. Further, for some subjects, their self-reported ancestry was
662 discordant with clusters observed in a principal component analysis. Therefore, for analysis pur-
663 poses, we used the minimum covariance determinant method (*Rousseeuw and Van Driessen, 1999*;
664 *Conomos et al., 2016*) with the original self-identified labels to group the subjects into six ancestry-
665 informative PCA clusters: “African”-associated (8), “Asian”-associated (23), “Caucasian”-associated
666 (322), “Hispanic”-associated (30), “Middle Eastern”-associated (5), and “Native American”-associated
667 (10).

668 **Quantifying associations between *TRBD2* allele genotype and SNP genotype within
669 the *TCRB* locus**

670 For each significantly associated SNP within the *TCRB* locus as shown in *Figure 3*, we compared SNP
671 genotype to *TRBD2* allele genotype across all subjects. We used Pearson correlation to measure the
672 correlation between the two genotypes.

673 **Quantifying TCR repertoire feature and SNP minor allele frequency variations by
674 ancestry-informative PCA cluster**

675 To quantify PCA cluster variation of TCR repertoire features (such as total N-insertions (V-D N-
676 insertion and D-J N-insertion)), we first calculated an average of each TCR repertoire feature by
677 subject and productivity status. We also calculated a population mean of each TCR repertoire

678 feature by productivity status. Each subject was classified into one of six PCA clusters. Thus, we
679 compared the mean of the TCR repertoire features within each PCA cluster to the population mean
680 using a one-sample t-test to compute each P-value. We used Bonferroni multiple testing correction
681 to adjust each P-value.

682 We also calculated SNP minor allele frequencies for the whole population and for each PCA
683 cluster individually such that

$$\text{MAF}_{jr} = \frac{\sum_{i=1}^{I_r} x_{ij}}{2 * I_r}. \quad (8)$$

684 Here, MAF_{jr} is the minor allele frequency for SNP marker j and PCA cluster r , I_r is the number of
685 individuals in the PCA cluster r , and x_{ij} is the number of alleles in the genotype of SNP marker
686 j for subject $i \in \{1, \dots, I_r\}$. For each SNP j , the minor allele was defined as the allele with the
687 lowest frequency in the total population. To quantify minor allele frequency differences by PCA
688 cluster for select SNPs within various loci of interest (i.e. *DNTT* gene), we compared the minor allele
689 frequencies calculated within PCA-clusters to the minor allele frequencies calculated for the entire
690 population using a one-sample t-test to compute each P-value. Again, we used Bonferroni multiple
691 testing correction to adjust each P-value.

692 For both of these analyses, we used the `t_test` function from the `rstatix` package in R.

693 **Implementation and code**

694 R code implementing the genome-wide association inferences described here is available at <https://github.com/phbradley/tcr-gwas>. The following tools were especially helpful:

- 696 • `data.table` (*Dowle and Srinivasan, 2021*)
- 697 • `tidyverse` (*Wickham et al., 2019*)
- 698 • `doParallel` (*Corporation and Weston, 2020*)
- 699 • `SNPRelate` (*Zheng et al., 2012*)
- 700 • `GWASTools` (*Gogarten et al., 2012*)
- 701 • `GENESIS` (*Gogarten et al., 2019*)
- 702 • `cowplot` (*Wilke, 2020*)

703 **Acknowledgments**

704 The authors thank Christopher Carlson, William DeWitt, and Michael Lieber for helpful discussions
705 regarding this paper.

706 **Additional Information**

707 **Competing interests**

708 Paul G Thomas consults for Johnson and Johnson, Immunoscapes, Cytoagents, and PACT Pharma. He
709 has received travel reimbursement from 10X Genomics and Illumina. He has patents on methods

710 related to T cell receptor biology. The other authors declare that no competing interests exist.

711 **Funding**

Funder	Grant reference number	Author
National Institutes of Health	R01 AI146028	Magdalena L Russell Frederick A Matsen IV Noah Simon Philip Bradley
The Simons Foundation and Howard Hughes Medical Institute	55108544	Frederick A Matsen IV
National Institutes of Health	R01 AI136514	Aisha Souquette E Kaitlynn Allen Paul G Thomas Philip Bradley
National Institutes of Health	R01 AI120997	Guillermina Kuan Angel Balmaseda Aubree Gordon
National Institutes of Health	R01 AI107625	Aisha Souquette E Kaitlynn Allen Paul G Thomas
National Institute of Allergy and Infectious Diseases via Centers of Excellence for Influenza Research and Surveillance	HHSN272201 400006C	Aisha Souquette E Kaitlynn Allen Guillermina Kuan Angel Balmaseda Aubree Gordon Paul G Thomas
National Institute of Allergy and Infectious Diseases via Centers of Excellence for Influenza Research and Response	75N93021C00016	Aisha Souquette E Kaitlynn Allen Guillermina Kuan Angel Balmaseda Aubree Gordon Paul G Thomas
National Institute of Allergy and Infectious Diseases	AI33484	David M Levine
National Institute of Allergy and Infectious Diseases	AI149213	David M Levine
National Cancer Institute	CA015704	David M Levine
National Heart, Lung, and Blood Institute	HL087690	David M Levine
National Heart, Lung, and Blood Institute	HL088201	David M Levine
National Heart, Lung, and Blood Institute	HL094260	David M Levine
National Heart, Lung, and Blood Institute	HL105914	David M Levine
National Heart, Lung, and Blood Institute	K23HL69860	David M Levine
National Institutes of Health	ORIP S10OD028685	Scientific Computing Infrastructure at Fred Hutch

712 **Additional Files**

713 **Data availability**

714 Data required to reproduce the findings reported here and a table mapping subject identifiers
715 between the TCR repertoire and SNP data for the discovery cohort will be deposited in the Zenodo
716 database prior to publication.

717 The following new dataset was generated:

Author	Year	Dataset title	Dataset URL	Database, license, and accessibility information
Aisha Souquette, E Kaitlynn Allen, Guillermina Kuan, Angel Balmaseda, Aubree Gordon, Paul G Thomas	2021	The Nicaraguan Influenza Cohort Study	https://www.ncbi.nlm.nih.gov/bioproject/PRJNA762269	Publicly available in The BioProject database (accession number: PRJNA762269)

718 The following previously published datasets were used:

Author	Year	Dataset title	Dataset URL	Database, license, and accessibility information
Emerson RO, DeWitt WS, Vignali M, Gravley J, Hu JK, Osborne EJ, Desmarais C, Klinger M, Carlson CS, Hansen JA, Rieder M, Robins HS	2017	Immunosequencing identifies signatures of cytomegalovirus exposure history and HLA mediated effects on the T cell repertoire	https://doi.org/10.21417/B7001Z	Publicly available in ImmuneACCESS database
Martin PJ, Levine DM, Storer BE, Nelson SC, Dong X, Hansen JA	2020	Recipient and donor genetic variants associated with mortality after allogeneic hematopoietic cell transplantation	https://www.ncbi.nlm.nih.gov/projects/gap/cgi-bin/study.cgi?study_id=phs001918.v1.p1	Publicly available in The database of Genotypes and Phenotypes (accession number: phs001918)

719 **References**

720 **Conomos MP**, Laurie CA, Stilp AM, Gogarten SM, McHugh CP, Nelson SC, Sofer T, Fernández-Rhodes L, Justice
721 AE, Graff M, Young KL, Seyerle AA, Avery CL, Taylor KD, Rotter JJ, Talavera GA, Daviglus ML, Wassertheil-
722 Smoller S, Schneiderman N, Heiss G, et al. Genetic Diversity and Association Studies in US Hispanic/Latino
723 Populations: Applications in the Hispanic Community Health Study/Study of Latinos. *Am J Hum Genet.* 2016
724 Jan; 98(1):165–184.

- 725 **Conomos MP**, Miller MB, Thornton TA. Robust inference of population structure for ancestry prediction and
726 correction of stratification in the presence of relatedness. *Genet Epidemiol*. 2015 May; 39(4):276–293.
- 727 **Corporation M**, Weston S. doParallel: Foreach Parallel Adaptor for the 'parallel' Package; 2020, [https://CRAN.](https://CRAN.R-project.org/package=doParallel)
728 [R-project.org/package=doParallel](https://CRAN.R-project.org/package=doParallel), r package version 1.0.16.
- 729 **Dash P**, Fiore-Gartland AJ, Hertz T, Wang GC, Sharma S, Souquette A, Crawford JC, Clemens EB, Nguyen THO,
730 Kedzierska K, La Gruta NL, Bradley P, Thomas PG. Quantifiable predictive features define epitope-specific T
731 cell receptor repertoires. *Nature*. 2017 Jul; 547(7661):89–93.
- 732 **Devlin B**, Roeder K. Genomic control for association studies. *Biometrics*. 1999 Dec; 55(4):997–1004.
- 733 **DeWitt WS 3rd**, Smith A, Schoch G, Hansen JA, Matsen FA 4th, Bradley P. Human T cell receptor occurrence
734 patterns encode immune history, genetic background, and receptor specificity. *Elife*. 2018 Aug; 7.
- 735 **Dowle M**, Srinivasan A. data.table: Extension of 'data.frame'; 2021, [https://CRAN.R-project.org/package=data.](https://CRAN.R-project.org/package=data.table)
736 [table](https://CRAN.R-project.org/package=data.table), r package version 1.14.0.
- 737 **Egorov ES**, Merzlyak EM, Shelenkov AA, Britanova OV, Sharonov GV, Staroverov DB, Bolotin DA, Davydov AN,
738 Barsova E, Lebedev YB, Shugay M, Chudakov DM. Quantitative profiling of immune repertoires for minor
739 lymphocyte counts using unique molecular identifiers. *J Immunol*. 2015 Jun; 194(12):6155–6163.
- 740 **Emerson RO**, DeWitt WS, Vignali M, Gravley J, Hu JK, Osborne EJ, Desmarais C, Klinger M, Carlson CS, Hansen
741 JA, Rieder M, Robins HS. Immunosequencing identifies signatures of cytomegalovirus exposure history and
742 HLA-mediated effects on the T cell repertoire. *Nat Genet*. 2017 May; 49(5):659–665.
- 743 **Feeney AJ**, Victor KD, Vu K, Nadel B, Chukwuocha RU. Influence of the V(D)J recombination mechanism on the
744 formation of the primary T and B cell repertoires. *Semin Immunol*. 1994 Jun; 6(3):155–163.
- 745 **Fischer S**, Stanke F, Tümmler B. VJ Segment Usage of TCR-Beta Repertoire in Monozygotic Cystic Fibrosis Twins.
746 *Front Immunol*. 2021 Feb; 12:599133.
- 747 **Freedman ML**, Reich D, Penney KL, McDonald GJ, Mignault AA, Patterson N, Gabriel SB, Topol EJ, Smoller JW, Pato
748 CN, Pato MT, Petryshen TL, Kolonel LN, Lander ES, Sklar P, Henderson B, Hirschhorn JN, Altshuler D. Assessing
749 the impact of population stratification on genetic association studies. *Nat Genet*. 2004 Apr; 36(4):388–393.
- 750 **Fugmann SD**, Lee AI, Shockett PE, Villey IJ, Schatz DG. The RAG proteins and V(D)J recombination: complexes,
751 ends, and transposition. *Annu Rev Immunol*. 2000; 18(1):495–527.
- 752 **Gao K**, Chen L, Zhang Y, Zhao Y, Wan Z, Wu J, Lin L, Kuang Y, Lu J, Zhang X, Tian L, Liu X, Qiu X. Germline-encoded
753 TCR-MHC contacts promote TCR V gene bias in umbilical cord blood T cell repertoire. *Front Immunol*. 2019
754 Aug; 10:2064.
- 755 **Gauss GH**, Lieber MR. Mechanistic constraints on diversity in human V(D)J recombination. *Mol Cell Biol*. 1996
756 Jan; 16(1):258–269.
- 757 **Gellert M**. DNA double-strand breaks and hairpins in V(D)J recombination. *Semin Immunol*. 1994 Jun; 6(3):125–
758 130.
- 759 **Gilfillan S**, Dierich A, Lemeur M, Benoist C, Mathis D. Mice lacking TdT: mature animals with an immature
760 lymphocyte repertoire. *Science*. 1993 Aug; 261(5125):1175–1178.

- 761 **Giudicelli V**, Chaume D, Lefranc MP. IMGT/GENE-DB: a comprehensive database for human and mouse
762 immunoglobulin and T cell receptor genes. *Nucleic Acids Res.* 2005 Jan; 33(Database issue):D256–61.
- 763 **Gogarten SM**, Bhangale T, Conomos MP, Laurie CA, McHugh CP, Painter I, Zheng X, Crosslin DR, Levine D, Lumley
764 T, Nelson SC, Rice K, Shen J, Swarnkar R, Weir BS, Laurie CC. GWASTools: an R/Bioconductor package for
765 quality control and analysis of genome-wide association studies. *Bioinformatics.* 2012; 28(24):3329–3331. doi:
766 10.1093/bioinformatics/bts610.
- 767 **Gogarten SM**, Sofer T, Chen H, Yu C, Brody JA, Thornton TA, Rice KM, Conomos MP. Genetic association testing
768 using the GENESIS R/Bioconductor package. *Bioinformatics.* 2019; doi: 10.1093/bioinformatics/btz567.
- 769 **Goldrath AW**, Bevan MJ. Selecting and maintaining a diverse T-cell repertoire. *Nature.* 1999 Nov; 402(6759):255–
770 262.
- 771 **Gu J**, Li S, Zhang X, Wang LC, Niewolik D, Schwarz K, Legerski RJ, Zandi E, Lieber MR. DNA-PKcs regulates a
772 single-stranded DNA endonuclease activity of Artemis. *DNA Repair (Amst).* 2010 Apr; 9(4):429–437.
- 773 **Jackson KJL**, Gaeta B, Sewell W, Collins AM. Exonuclease activity and P nucleotide addition in the generation of
774 the expressed immunoglobulin repertoire. *BMC Immunol.* 2004 Sep; 5:19.
- 775 **Kallenbach S**, Doyen N, Fanton d'Andon M, Rougeon F. Three lymphoid-specific factors account for all junctional
776 diversity characteristic of somatic assembly of T-cell receptor and immunoglobulin genes. *Proc Natl Acad Sci*
777 *U S A.* 1992 Apr; 89(7):2799–2803.
- 778 **Komori T**, Okada A, Stewart V, Alt FW. Lack of N regions in antigen receptor variable region genes of TdT-deficient
779 lymphocytes. *Science.* 1993 Aug; 261(5125):1171–1175.
- 780 **Krishna C**, Chowell D, Gönen M, Elhanati Y, Chan TA. Genetic and environmental determinants of human TCR
781 repertoire diversity. *Immun Ageing.* 2020 Dec; 17(1).
- 782 **Li S**, Chang HH, Niewolik D, Hedrick MP, Pinkerton AB, Hassig CA, Schwarz K, Lieber MR. Evidence that the DNA
783 endonuclease ARTEMIS also has intrinsic 5'-exonuclease activity. *J Biol Chem.* 2014 Mar; 289(11):7825–7834.
- 784 **Lu H**, Schwarz K, Lieber MR. Extent to which hairpin opening by the Artemis:DNA-PKcs complex can contribute
785 to junctional diversity in V(D)J recombination. *Nucleic Acids Res.* 2007 Oct; 35(20):6917–6923.
- 786 **Ma Y**, Pannicke U, Schwarz K, Lieber MR. Hairpin opening and overhang processing by an Artemis/DNA-
787 dependent protein kinase complex in nonhomologous end joining and V(D)J recombination. *Cell.* 2002 Mar;
788 108(6):781–794.
- 789 **Martin PJ**, Levine DM, Storer BE, Nelson SC, Dong X, Hansen JA. Recipient and donor genetic variants associated
790 with mortality after allogeneic hematopoietic cell transplantation. *Blood Adv.* 2020 Jul; 4(14):3224–3233.
- 791 **Mikocziova I**, Greiff V, Sollid LM. Immunoglobulin germline gene variation and its impact on human disease.
792 *Genes Immun.* 2021 Jun; p. 1–13.
- 793 **Moshous D**, Callebaut I, de Chasseval R, Corneo B, Cavazzana-Calvo M, Le Deist F, Tezcan I, Sanal O, Bertrand Y,
794 Philippe N, Fischer A, de Villartay JP. Artemis, a novel DNA double-strand break repair/V(D)J recombination
795 protein, is mutated in human severe combined immune deficiency. *Cell.* 2001 Apr; 105(2):177–186.
- 796 **Murphy K**, Weaver C. *Janeway's Immunobiology.* Garland Science; 2016.

- 797 **Murugan A**, Mora T, Walczak AM, Callan CG Jr. Statistical inference of the generation probability of T-cell
798 receptors from sequence repertoires. *Proc Natl Acad Sci U S A*. 2012 Oct; 109(40):16161–16166.
- 799 **Nadel B**, Feeney AJ. Influence of coding-end sequence on coding-end processing in V(D)J recombination. *J*
800 *Immunol*. 1995 Nov; 155(9):4322–4329.
- 801 **Nadel B**, Feeney AJ. Nucleotide deletion and P addition in V(D)J recombination: a determinant role of the
802 coding-end sequence. *Mol Cell Biol*. 1997 Jul; 17(7):3768–3778.
- 803 **Ng S**, Lopez R, Kuan G, Gresh L, Balmaseda A, Harris E, Gordon A. The timeline of influenza virus shedding in
804 children and adults in a household transmission study of influenza in Managua, Nicaragua. *Pediatr Infect Dis*
805 *J*. 2016; .
- 806 **Oltz EM**. Regulation of antigen receptor gene assembly in lymphocytes. *Immunol Res*. 2001; 23(2-3):121–133.
- 807 **Pogorelyy MV**, Minervina AA, Touzel MP, Sycheva AL, Komech EA, Kovalenko EI, Karganova GG, Egorov ES,
808 Komkov AY, Chudakov DM, Mamedov IZ, Mora T, Walczak AM, Lebedev YB. Precise tracking of vaccine-
809 responding T cell clones reveals convergent and personalized response in identical twins. *Proc Natl Acad Sci*
810 *U S A*. 2018 Dec; 115(50):12704–12709.
- 811 **Price AL**, Zaitlen NA, Reich D, Patterson N. New approaches to population stratification in genome-wide
812 association studies. *Nat Rev Genet*. 2010 Jul; 11(7):459–463.
- 813 **Qi Q**, Cavanagh MM, Le Saux S, NamKoong H, Kim C, Turgano E, Liu Y, Wang C, Mackey S, Swan GE, Dekker CL,
814 Olshen RA, Boyd SD, Weyand CM, Tian L, Goronzy JJ. Diversification of the antigen-specific T cell receptor
815 repertoire after varicella zoster vaccination. *Sci Transl Med*. 2016 Mar; 8(332):332ra46.
- 816 **Robins HS**, Srivastava SK, Campregher PV, Turtle CJ, Andriesen J, Riddell SR, Carlson CS, Warren EH. Overlap and
817 effective size of the human CD8+ T cell receptor repertoire. *Sci Transl Med*. 2010 Sep; 2(47):47ra64.
- 818 **Rousseuw PJ**, Van Driessen K. A Fast Algorithm for the Minimum Covariance Determinant Estimator. *Techno-*
819 *metrics*. 1999 Aug; 41(3):212–223.
- 820 **Rubelt F**, Bolen CR, McGuire HM, Vander Heiden JA, Gadala-Maria D, Levin M, Euskirchen GM, Mamedov MR,
821 Swan GE, Dekker CL, Cowell LG, Kleinstein SH, Davis MM. Individual heritable differences result in unique cell
822 lymphocyte receptor repertoires of naïve and antigen-experienced cells; 2016.
- 823 **Schatz DG**, Swanson PC. V(D)J recombination: mechanisms of initiation. *Annu Rev Genet*. 2011 Aug; 45(1):167–
824 202.
- 825 **Sharon E**, Sibener LV, Battle A, Fraser HB, Garcia KC, Pritchard JK. Genetic variation in MHC proteins is associated
826 with T cell receptor expression biases. *Nat Genet*. 2016 Sep; 48(9):995–1002.
- 827 **Shugay M**, Britanova OV, Merzlyak EM, Turchaninova MA, Mamedov IZ, Tuganbaev TR, Bolotin DA, Staroverov
828 DB, Putintseva EV, Plevova K, Linnemann C, Shagin D, Pospisilova S, Lukyanov S, Schumacher TN, Chudakov
829 DM. Towards error-free profiling of immune repertoires. *Nat Methods*. 2014 Jun; 11(6):653–655.
- 830 **Srivastava SK**, Robins HS. Palindromic nucleotide analysis in human T cell receptor rearrangements. *PLoS One*.
831 2012 Dec; 7(12):e52250.
- 832 **Tanno H**, Gould TM, McDaniel JR, Cao W, Tanno Y, Durrett RE, Park D, Cate SJ, Hildebrand WH, Dekker CL, Tian L,
833 Weyand CM, Georgiou G, Goronzy JJ. Determinants governing T cell receptor α/β -chain pairing in repertoire
834 formation of identical twins. *Proc Natl Acad Sci U S A*. 2020 Jan; 117(1):532–540.

- 835 **Thomas PG**, Crawford JC. Selected before selection: A case for inherent antigen bias in the T cell receptor
836 repertoire. *Curr Opin Syst Biol*. 2019 Dec; 18:36–43.
- 837 **Weigert M**, Gatmaitan L, Loh E, Schilling J, Hood L. Rearrangement of genetic information may produce
838 immunoglobulin diversity. *Nature*. 1978; 276(5690):785–790.
- 839 **Wickham H**, Averick M, Bryan J, Chang W, McGowan LD, François R, Grolemond G, Hayes A, Henry L, Hester J,
840 Kuhn M, Pedersen TL, Miller E, Bache SM, Müller K, Ooms J, Robinson D, Seidel DP, Spinu V, Takahashi K, et al.
841 Welcome to the tidyverse. *Journal of Open Source Software*. 2019; 4(43):1686. doi: [10.21105/joss.01686](https://doi.org/10.21105/joss.01686).
- 842 **Wilke CO**. cowplot: Streamlined Plot Theme and Plot Annotations for 'ggplot2'; 2020, <https://CRAN.R-project.org/package=cowplot>, r package version 1.1.1.
- 844 **Witzgall R**, O'Leary E, Leaf A, Onaldi D, Bonventre JV. The Krüppel-associated box-A (KRAB-A) domain of zinc
845 finger proteins mediates transcriptional repression. *Proc Natl Acad Sci U S A*. 1994 May; 91(10):4514–4518.
- 846 **Woodsworth DJ**, Castellarin M, Holt RA. Sequence analysis of T-cell repertoires in health and disease. *Genome*
847 *Med*. 2013 Oct; 5(10):98.
- 848 **Zhao B**, Rothenberg E, Ramsden DA, Lieber MR. The molecular basis and disease relevance of non-homologous
849 DNA end joining. *Nat Rev Mol Cell Biol*. 2020 Dec; 21(12):765–781.
- 850 **Zheng X**, Levine D, Shen J, Gogarten S, Laurie C, Weir B. A High-performance Computing Toolset for Relatedness
851 and Principal Component Analysis of SNP Data. *Bioinformatics*. 2012; 28(24):3326–3328. doi: [10.1093/bioinformatics/bts606](https://doi.org/10.1093/bioinformatics/bts606).
- 853 **Zvyagin IV**, Pogorelyy MV, Ivanova ME, Komech EA, Shugay M, Bolotin DA, Shelenkov AA, Kurnosov AA, Staroverov
854 DB, Chudakov DM, Lebedev YB, Mamedov IZ. Distinctive properties of identical twins' TCR repertoires revealed
855 by high-throughput sequencing. *Proc Natl Acad Sci U S A*. 2014 Apr; 111(16):5980–5985.

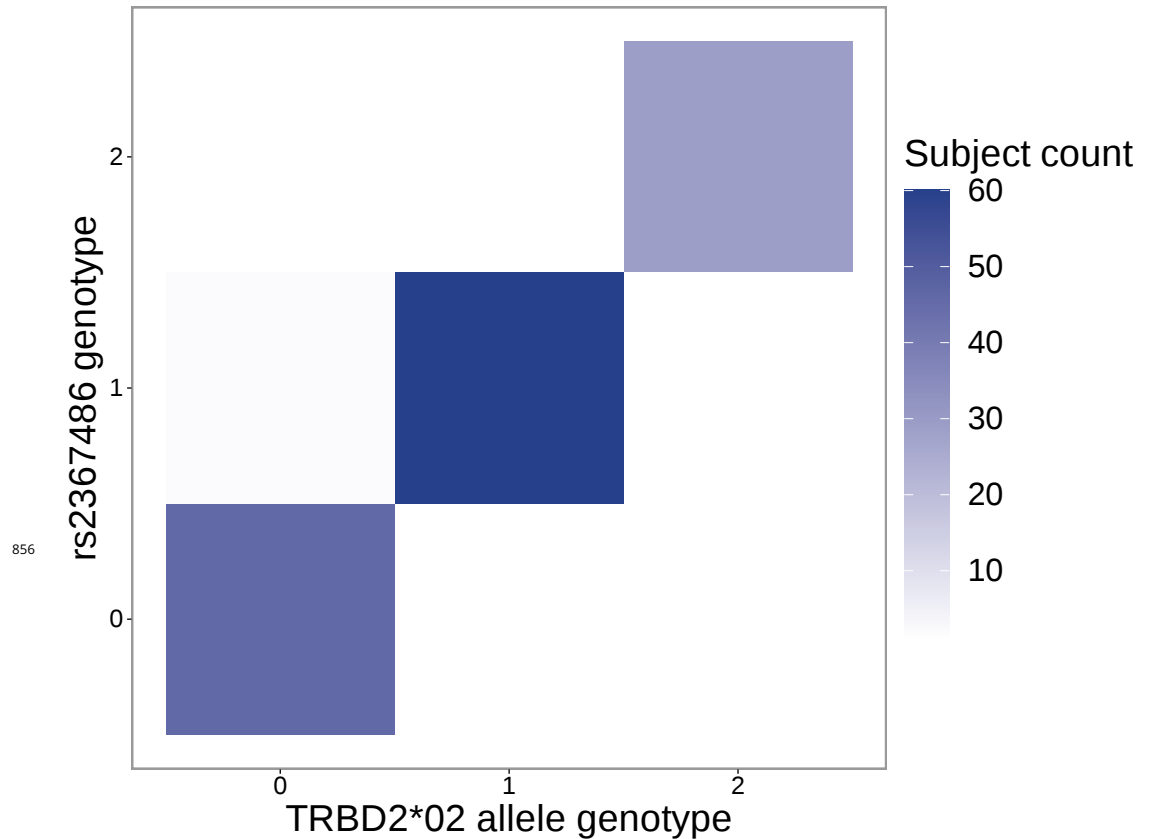


Figure 3-Figure supplement 1. The SNP genotype for the SNP (rs2367486) most significantly associated with 5' end D-gene trimming within the *TCRB* locus is also associated with *TRBD2*02* allele genotype. Specifically, SNP genotype and *TRBD2*02* allele genotype are significantly correlated ($P < 2.2 \times 10^{-16}$ and $\chi^2 = 259.3$) using a chi-square test of independence. The Y-axis integer genotypes correspond to the number of minor alleles within the rs2367486 SNP genotype. The X-axis integer genotypes correspond to the number of *TRBD2*02* alleles within the *TRBD2* gene locus genotype.

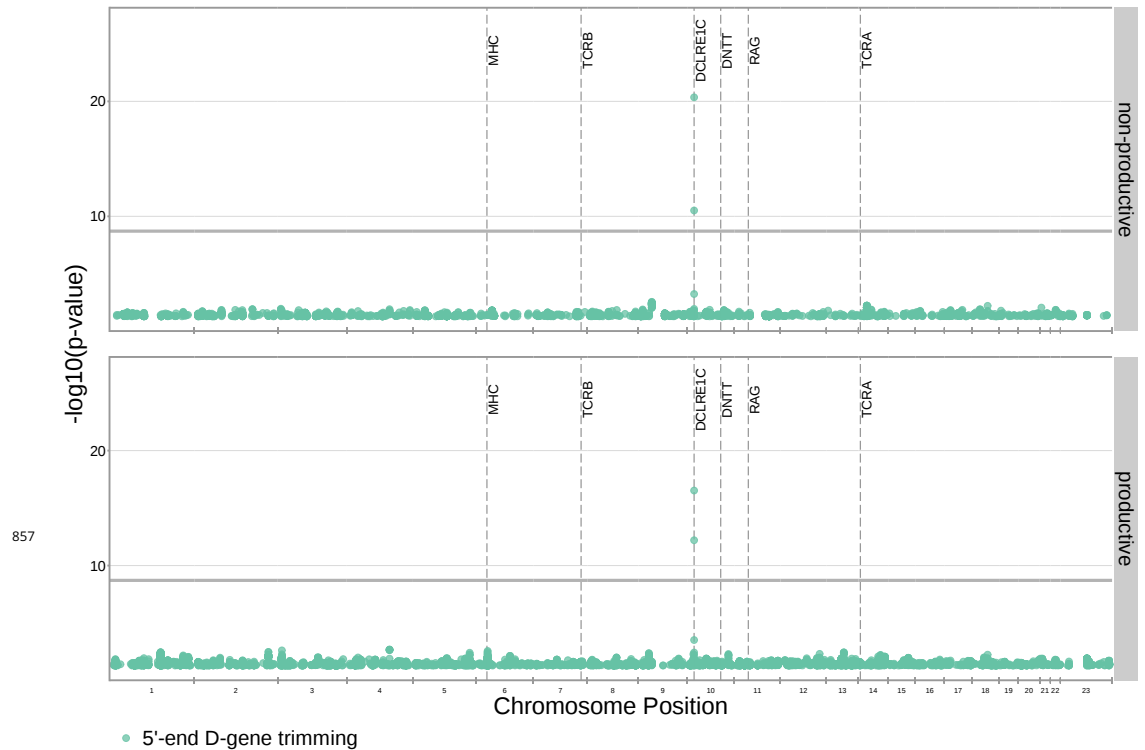


Figure 3–Figure supplement 2. Significant associations are no longer observed between 5' end D-gene trimming and variation in the *TCRB* locus after correcting for *TRBD2* allele genotype in our model formulation. Further, four new significant associations are present between 5' end D-gene trimming and variation in the *DCLRE1C* locus. Only SNP associations whose $P < 5 \times 10^{-2}$ are shown here. All genome-wide 3' end D-gene trimming associations fell above this plotting threshold. The gray horizontal line corresponds to a P-value of 1.94×10^{-9} (calculated using whole-genome Bonferroni correction, see Methods).

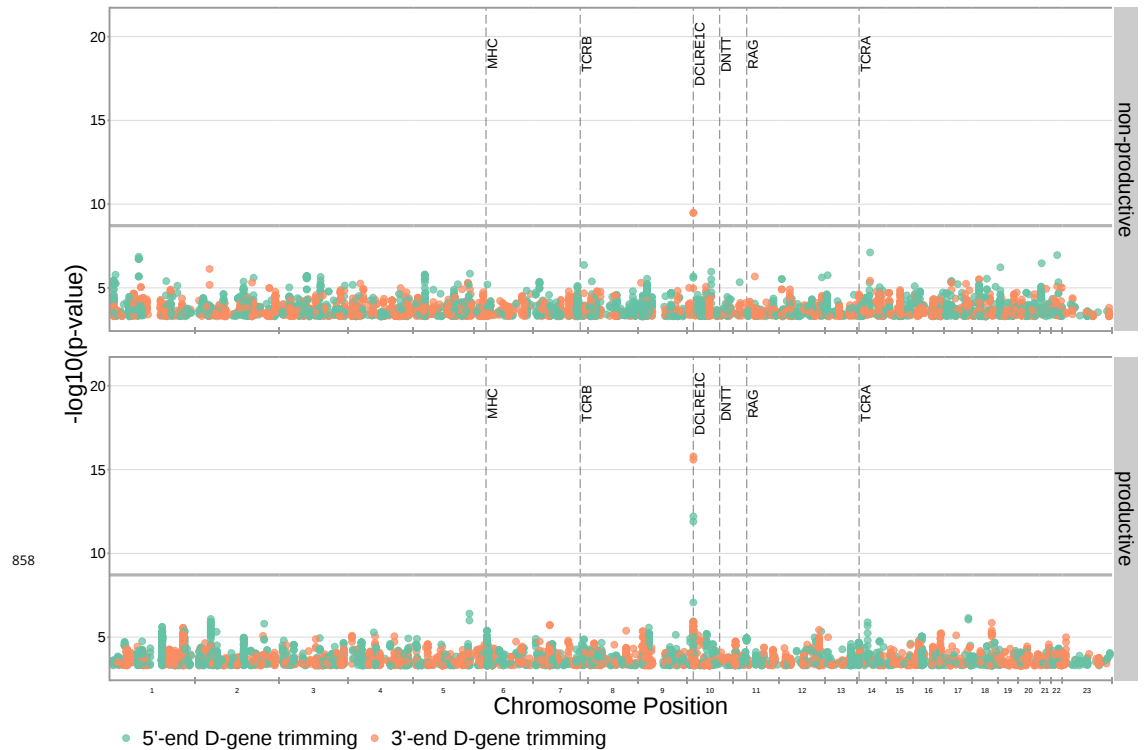


Figure 3-Figure supplement 3. Significant associations are also no longer observed between 5' end D-gene trimming and variation in the *TCRB* locus when restricting the analysis to TCRs which contain *TRBJ1* genes (and consequently contain *TRBD1*). Additionally, two new associations are present between 5' end D-gene trimming and variation in the *DCLRE1C* locus for productive TCRs. Four new associations are present between 3' end D-gene trimming and variation in the *DCLRE1C* locus. Only SNP associations whose $P < 5 \times 10^{-4}$ are shown here. The gray horizontal line corresponds to a P-value of 1.94×10^{-9} (calculated using whole-genome Bonferroni correction, see Methods).

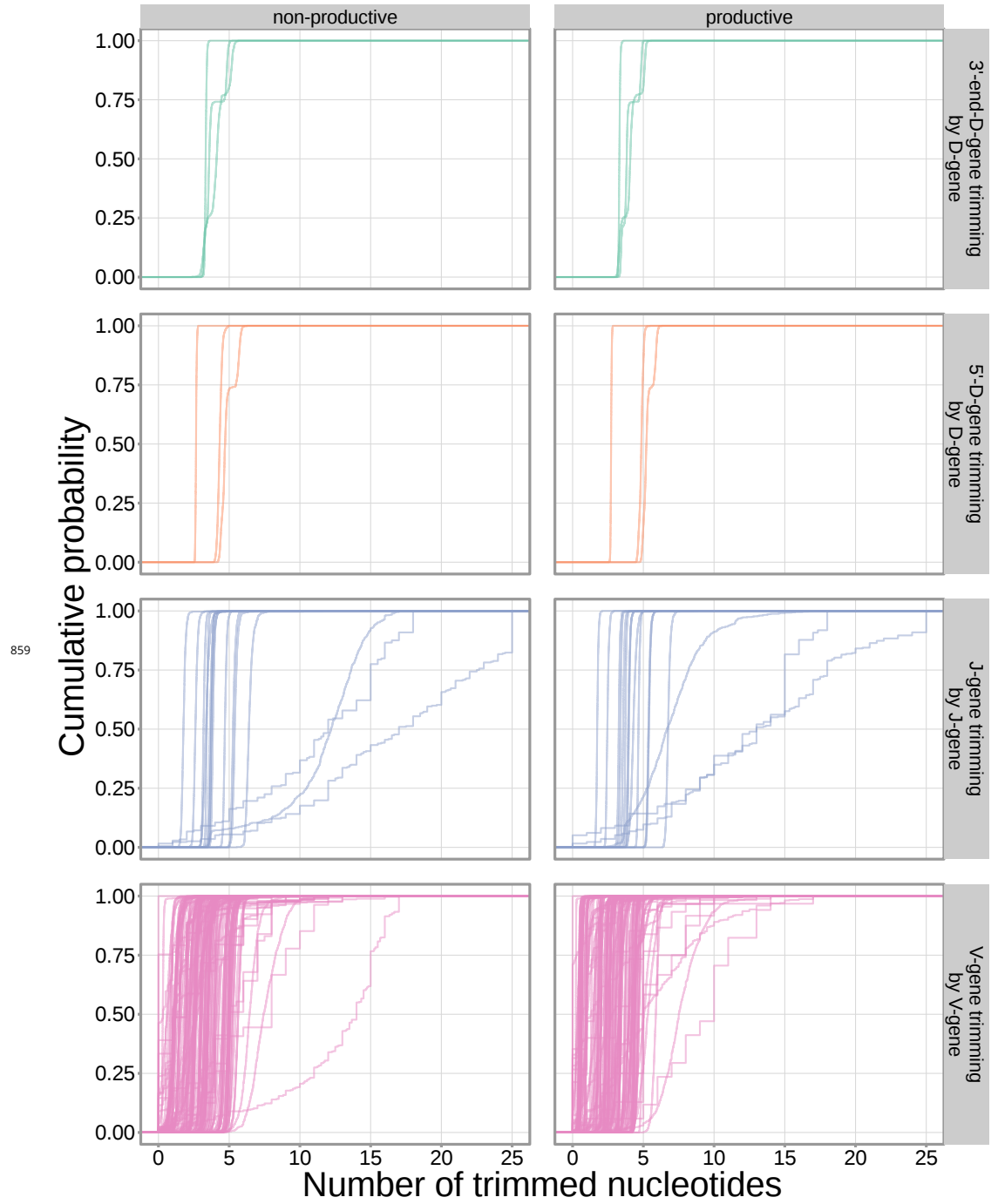


Figure 3–Figure supplement 4. The extent of nucleotide deletion varies by the gene allele identity for all gene types. An empirical cumulative distribution is drawn for each gene allele type within each indicated gene type (i.e. V-gene, D-gene, J-gene).

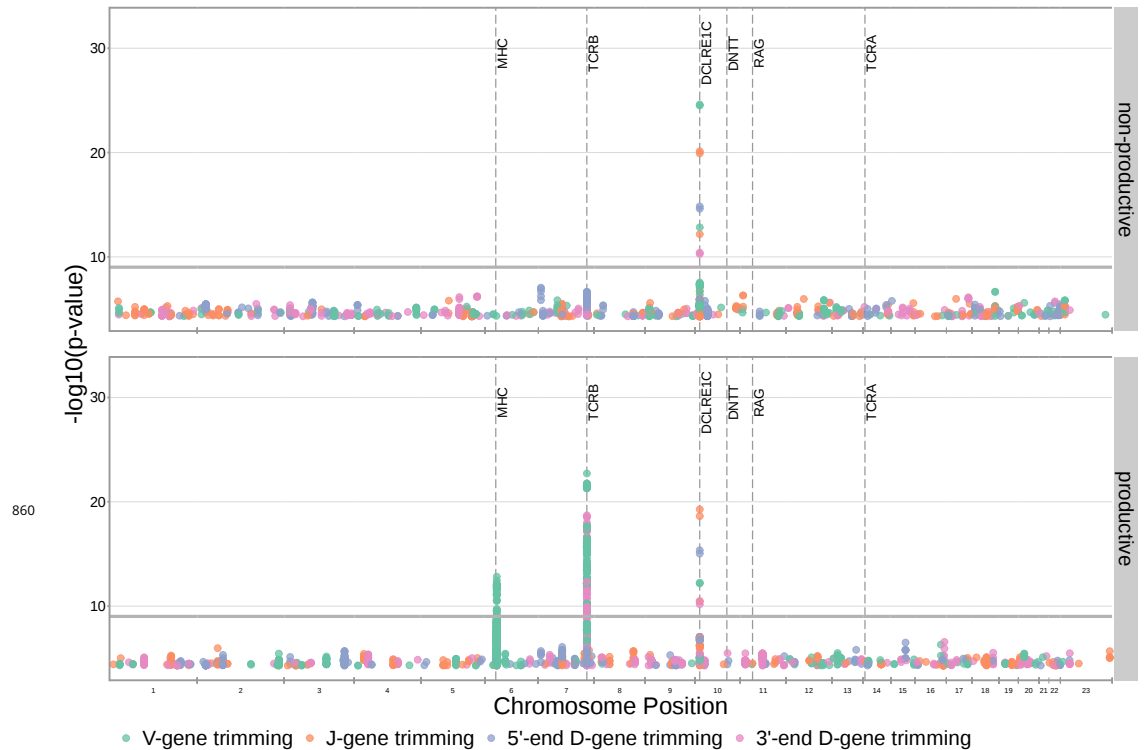


Figure 3-Figure supplement 5. Significant SNP associations are located within the MHC, *TCRB* and *DCLRE1C* loci for all four trimming types when calculating the strength of association without conditioning out effects mediated by gene choice. Earlier findings relating variations in MHC and *TCRB* to gene usage changes, however, indicate that many of these associations are likely artefactual. Only SNP associations whose $P < 5 \times 10^{-5}$ are shown here. The gray horizontal line corresponds to a P-value of 9.68×10^{-10} .

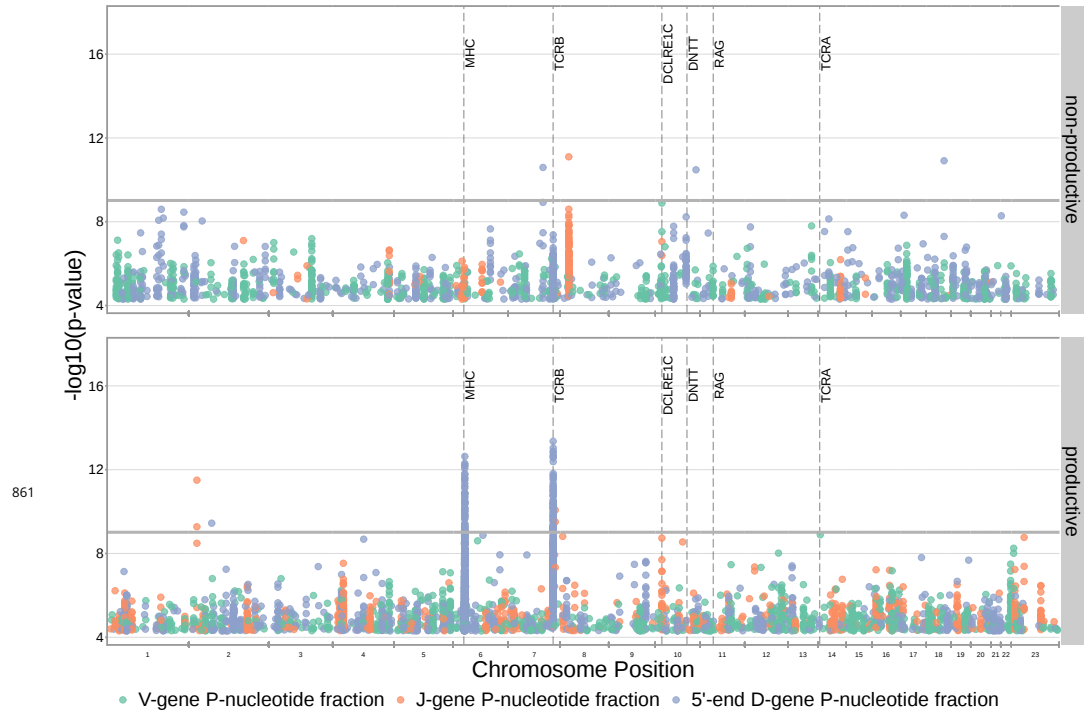


Figure 3-Figure supplement 6. SNP associations for all fractions of non-gene-trimmed TCRs containing P-nucleotides are not significant within the *DCLRE1C* locus. However, significant associations are present within the *TCRB* and *MHC* loci for the fraction of non-D-gene-trimmed, productive TCRs containing 5' end D-gene P-nucleotides. Only SNP associations whose $P < 5 \times 10^{-5}$ are shown here. The gray horizontal line corresponds to a P-value of 9.68×10^{-10} (calculated using whole-genome Bonferroni correction, see Methods).

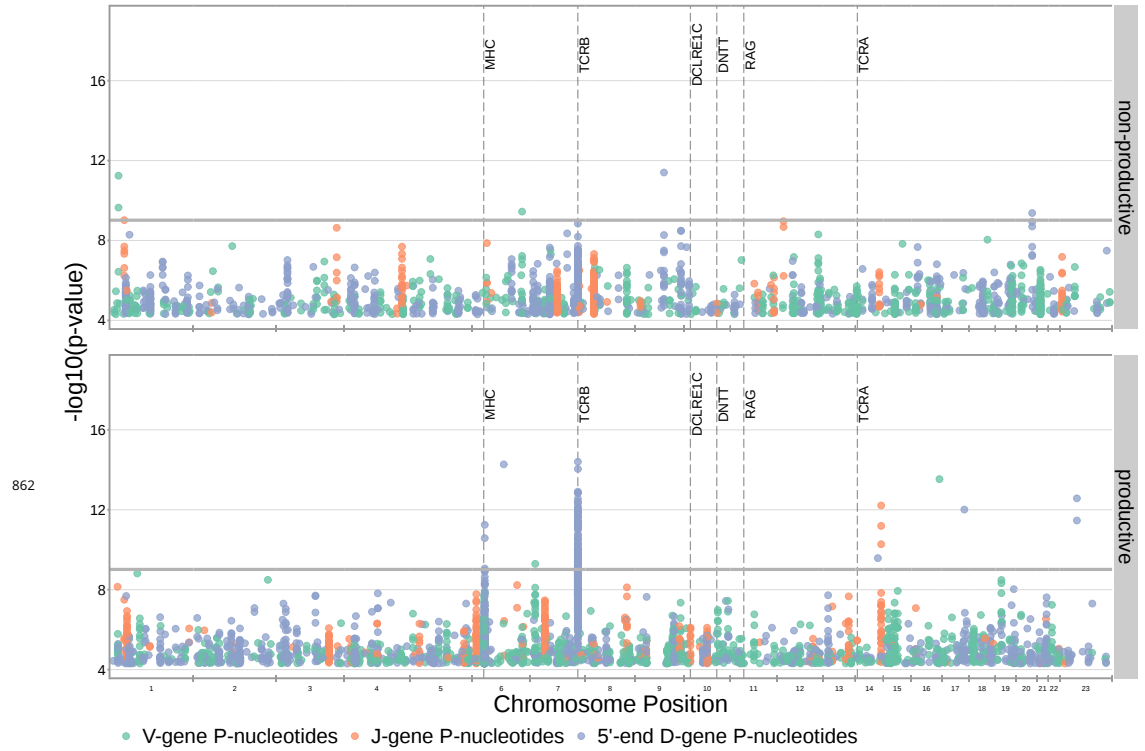


Figure 3—Figure supplement 7. SNP associations for the number of P-nucleotides are not significant within the *DCLRE1C* locus. However, significant associations are present within the *TCRB* and *MHC* loci. Only SNP associations whose $P < 5 \times 10^{-5}$ are shown here. The gray horizontal line corresponds to a Bonferroni-corrected whole-genome P-value significance threshold of 9.68×10^{-10} (see Methods).

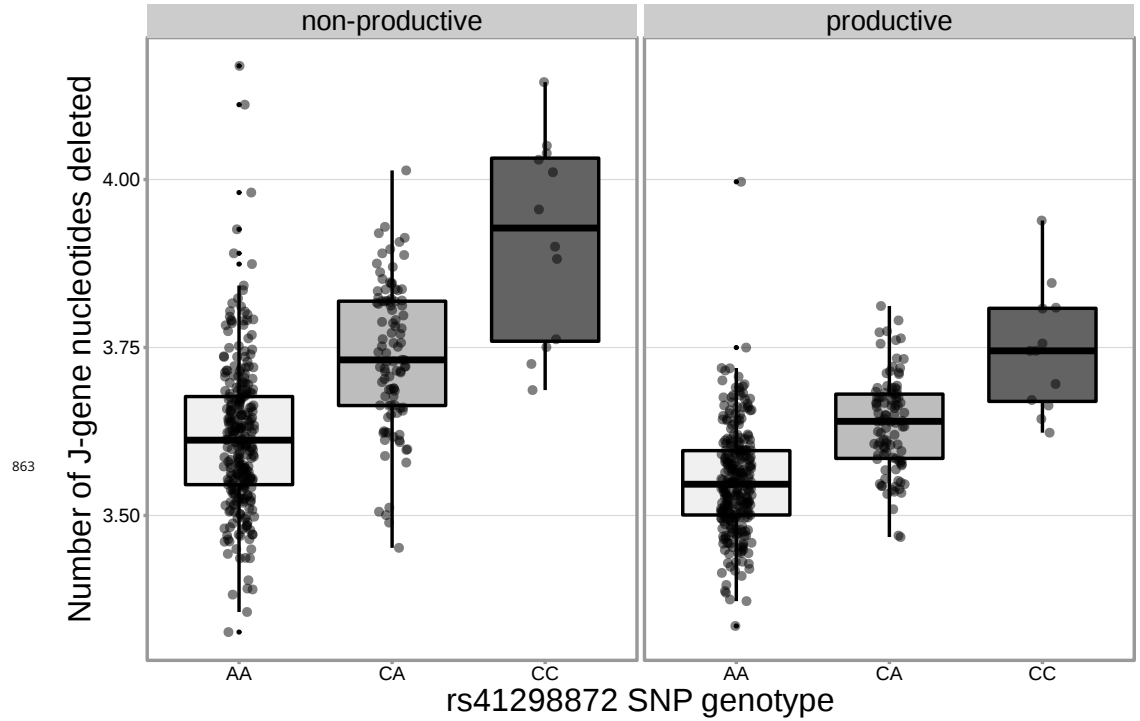


Figure 4-Figure supplement 1. The extent of J-gene trimming changes as a function of SNP genotype for the SNP (rs41298872) most significantly associated with J-gene trimming within the *DCLRE1C* locus. Only TCRs containing *TRBJ1-1*01* (the most frequently used *TRBJ1* gene across subjects) were included when calculating the average number of J-gene nucleotides deleted for each subject.

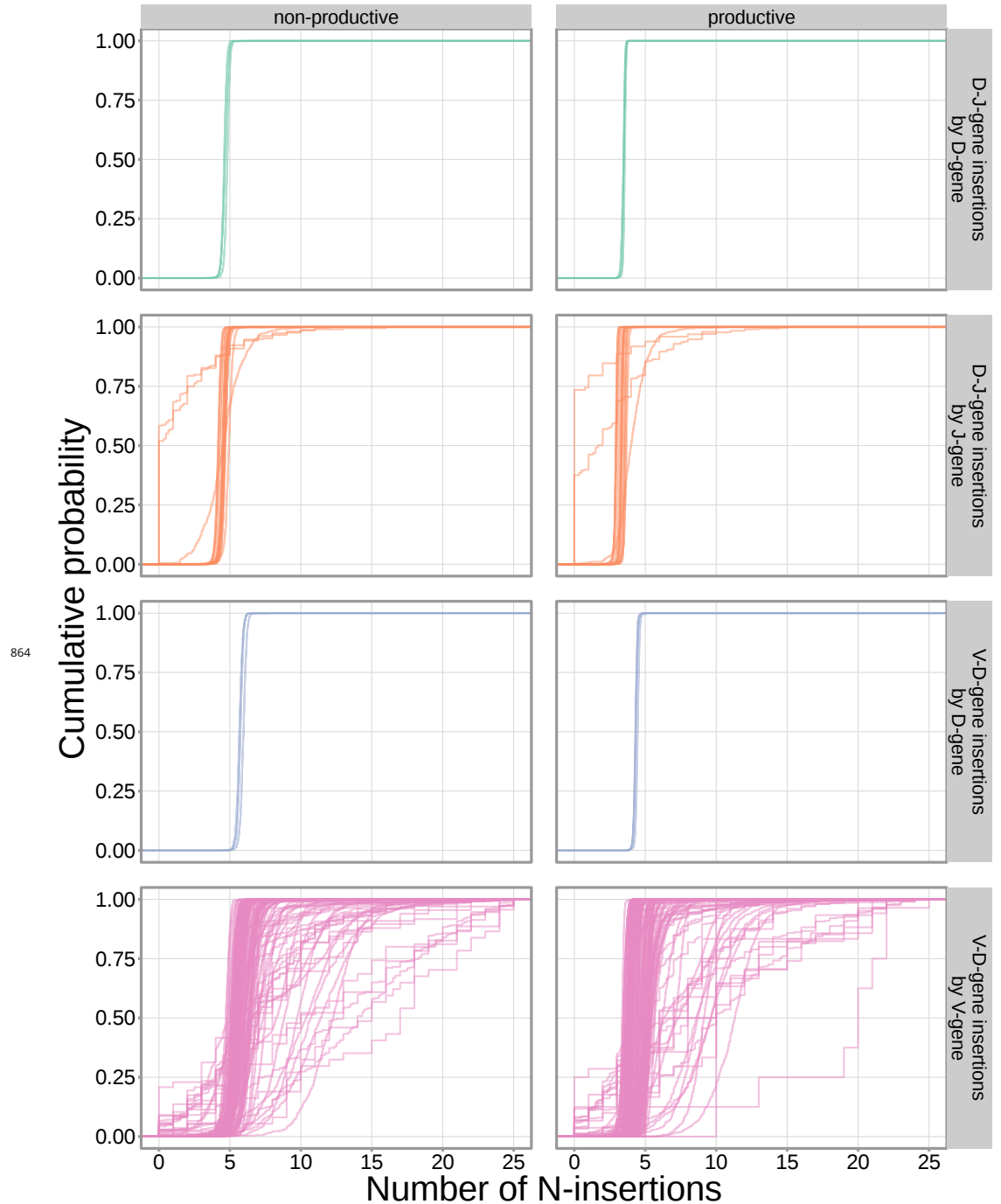


Figure 5-Figure supplement 1. The extent of N-insertion does not vary substantially by the gene allele identity for any gene type. An empirical cumulative distribution is drawn for each gene allele type within each indicated gene type (i.e. V-gene, D-gene, J-gene).

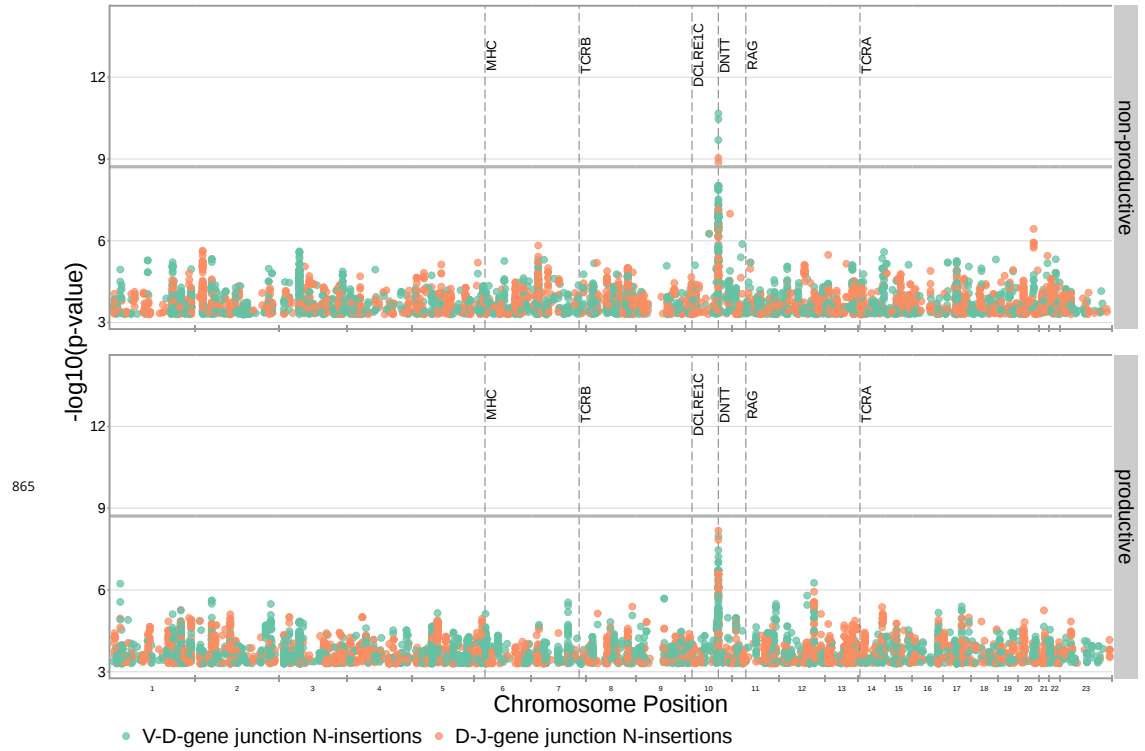


Figure 5-Figure supplement 2. Significant associations continue to be observed within the *DNNT* locus for both V-D- and D-J-gene-junction N-insertions when restricting the analysis to TCRs which contain *TRBJ1* genes (and consequently contain *TRBD1*). Only SNP associations whose $P < 5 \times 10^{-4}$ are shown here. The gray horizontal line corresponds to a Bonferroni-corrected P-value significance threshold of 1.94×10^{-9} (calculated using whole-genome Bonferroni correction, see Methods).

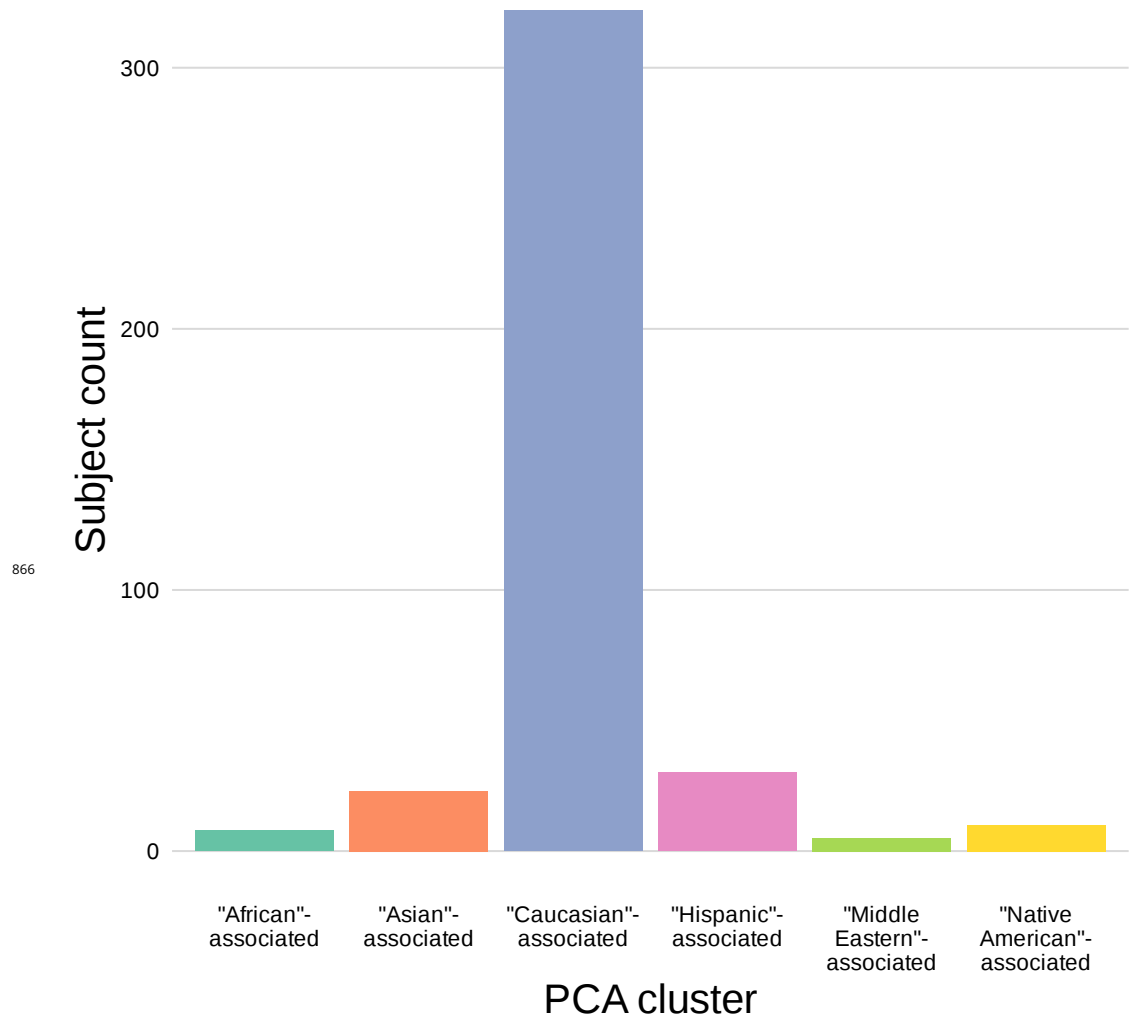


Figure 7-Figure supplement 1. The population mean is dominated by subjects in the "Caucasian"-associated PCA-cluster. Of the 398 subjects in the sample population, 81% are in the "Caucasian"-associated PCA-cluster.

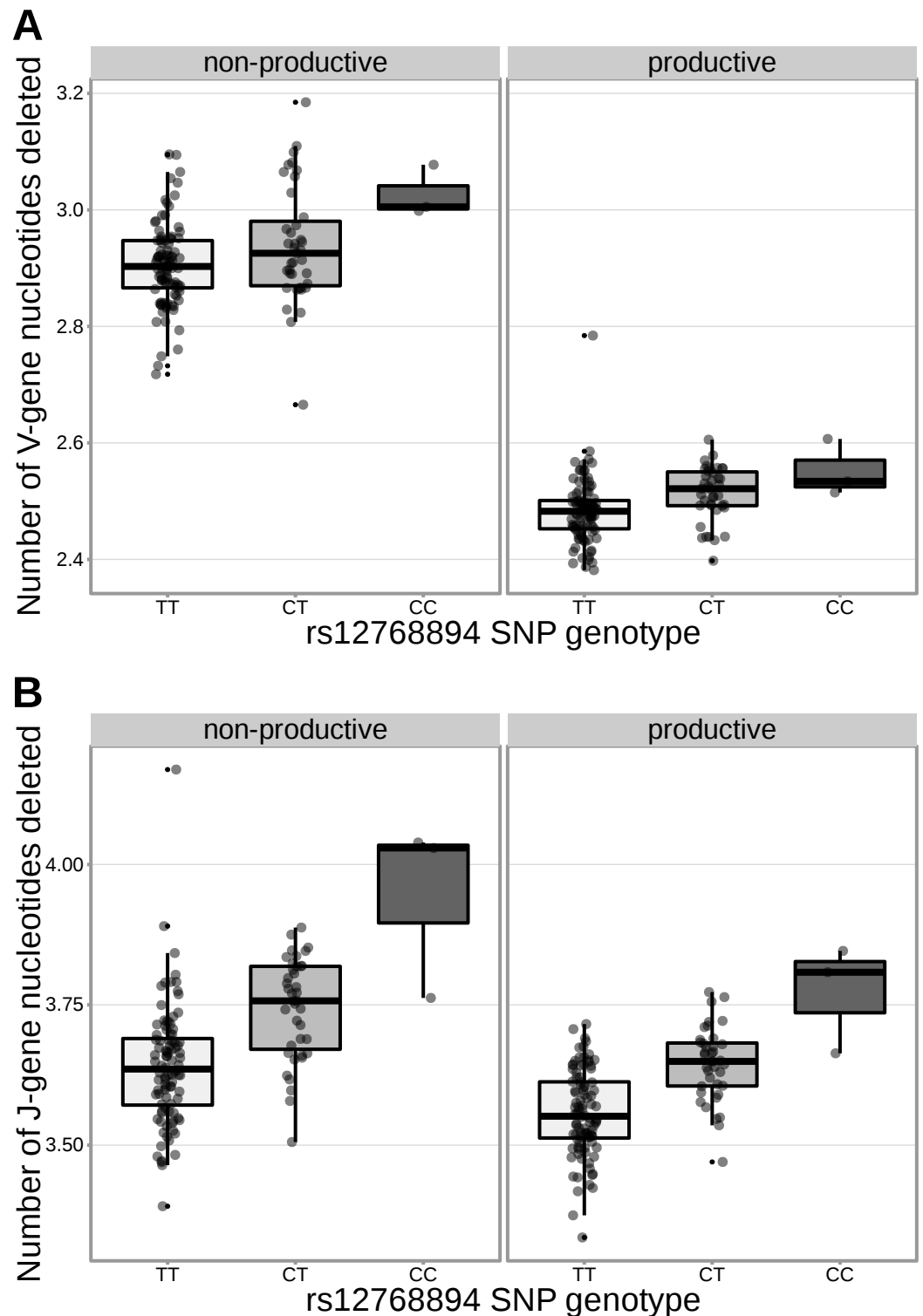


Table 2-Figure supplement 1. The extent of V- and J-gene trimming of productive and non-productive TCR β chains changes as a function of SNP genotype within the discovery cohort for a non-synonymous *DCLRE1C* SNP (rs12768894, c.728A>G). Only TCRs containing *TRBJ1-1*01* (the most frequently used *TRBJ1* gene across subjects) were included when calculating the average number of J-gene nucleotides deleted for each subject. Only TCRs containing *TRBV5-1*01* (the most frequently used *TRBV* gene across subjects) were included when calculating the average number of V-gene nucleotides deleted for each subject.

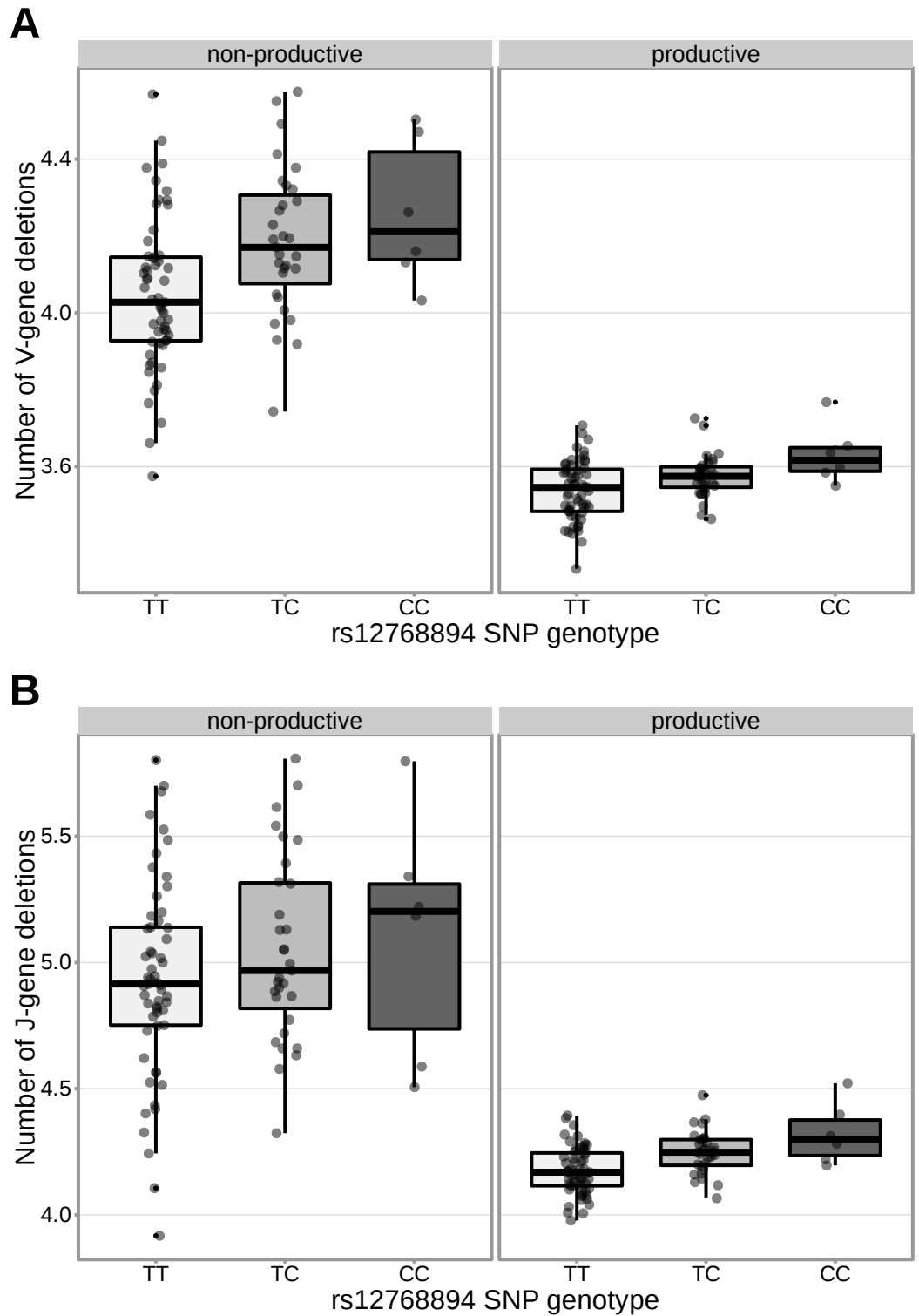


Table 2-Figure supplement 2. The extent of V-gene trimming (**A**) of productive and non-productive TCR β chains and J-gene trimming (**B**) of productive TCR β chains changes as a function of SNP genotype within the validation cohort for a non-synonymous *DCLRE1C* SNP (rs12768894, c.728A>G). The average number of nucleotides deleted was calculated across all TCR β chains for each subject, regardless of gene-usage.

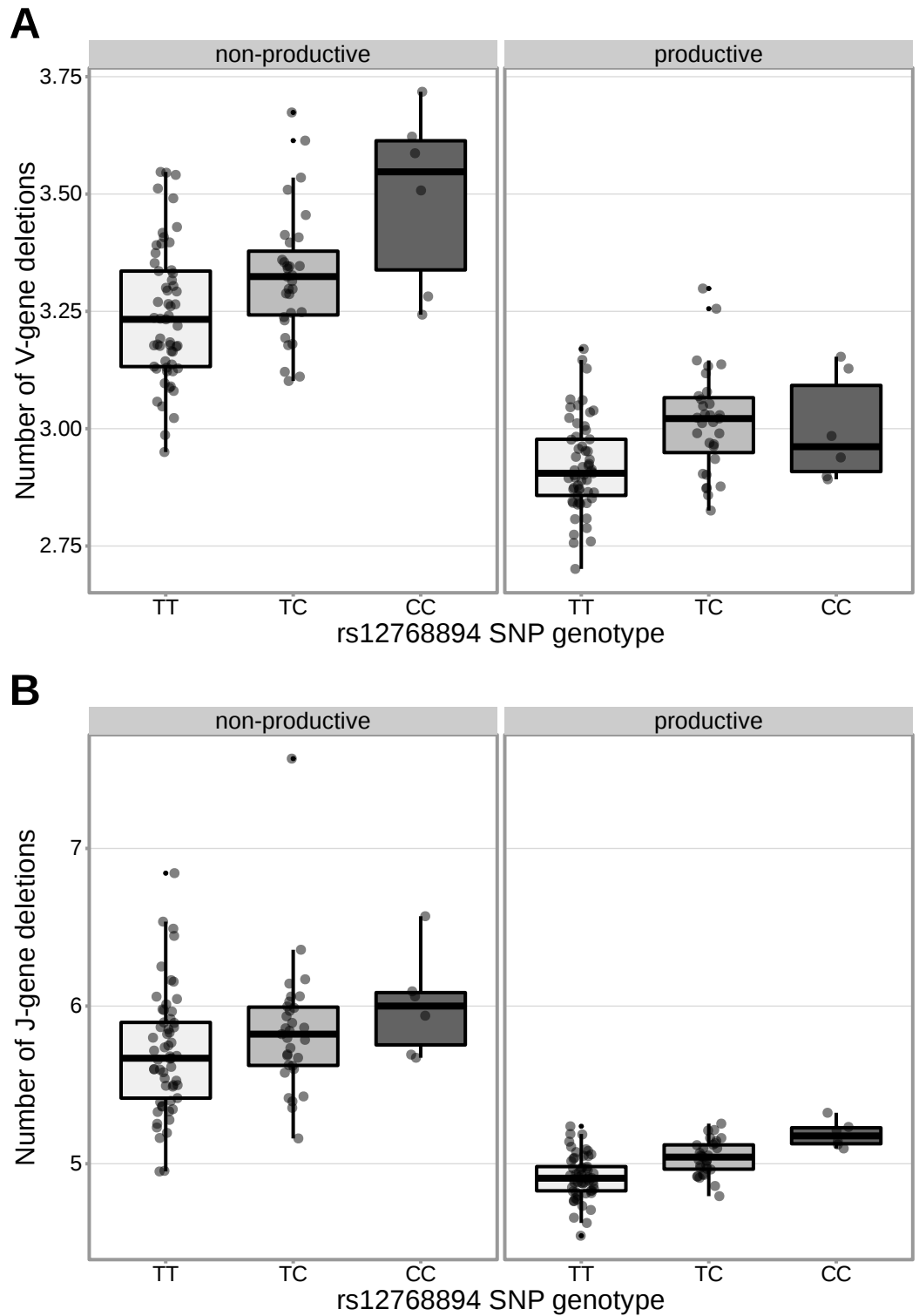


Table 2-Figure supplement 3. The extent of V- (A) and J-gene (B) trimming of productive and non-productive TCR α chains changes as a function of SNP genotype within the validation cohort for a non-synonymous *DCLRE1C* SNP (rs12768894, c.728A>G). The average number of nucleotides deleted was calculated across all TCR α chains for each subject, regardless of gene-usage.

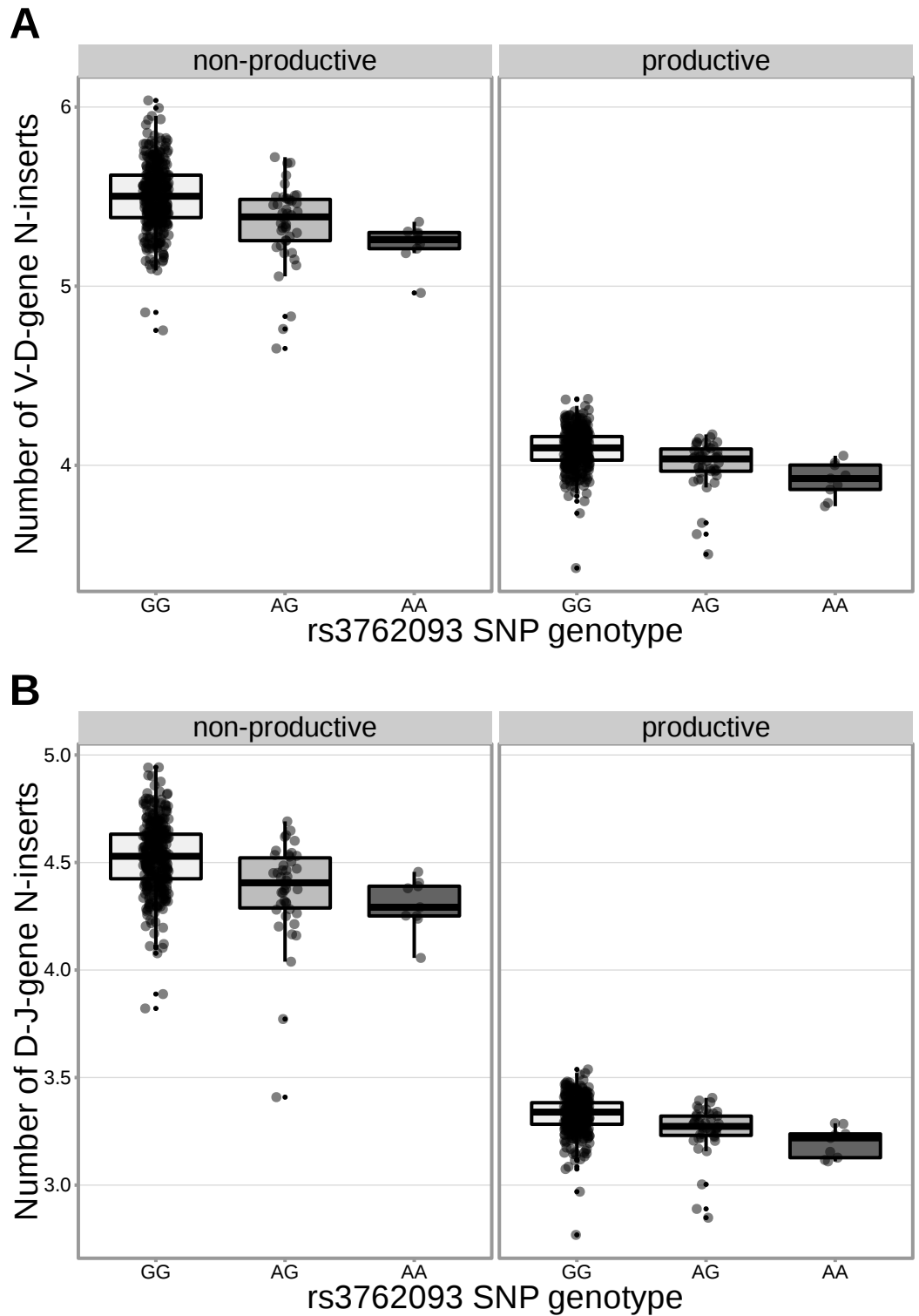


Table 2-Figure supplement 4. The extent of V-D and D-J N-insertion of productive and non-productive TCR β chains changes as a function of SNP genotype within the discovery cohort for an intronic *DNTT* SNP (rs3762093). The average number of N-insertions was calculated across all TCR β chains for each subject.

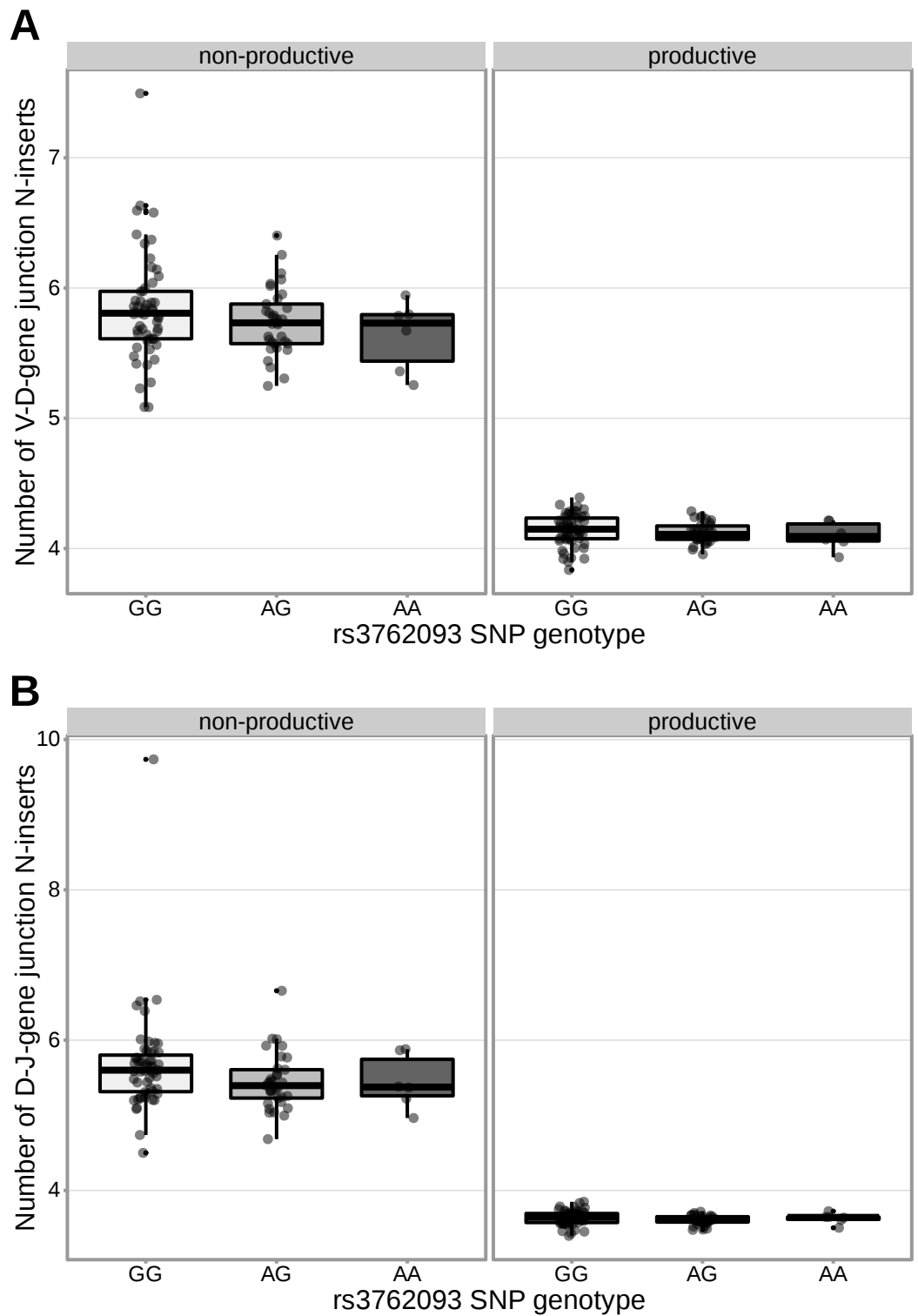


Table 2-Figure supplement 5. An intronic SNP (rs3762093) within the *DNTT* gene locus is not strongly associated with the number of V-D (**A**) or D-J (**B**) N-inserts within productive or non-productive TCR β chains in the validation cohort. However, the direction of the effect is the same as the discovery cohort for all N-insertion and productivity types. The average number of N-insertions was calculated across all TCR β chains for each subject.

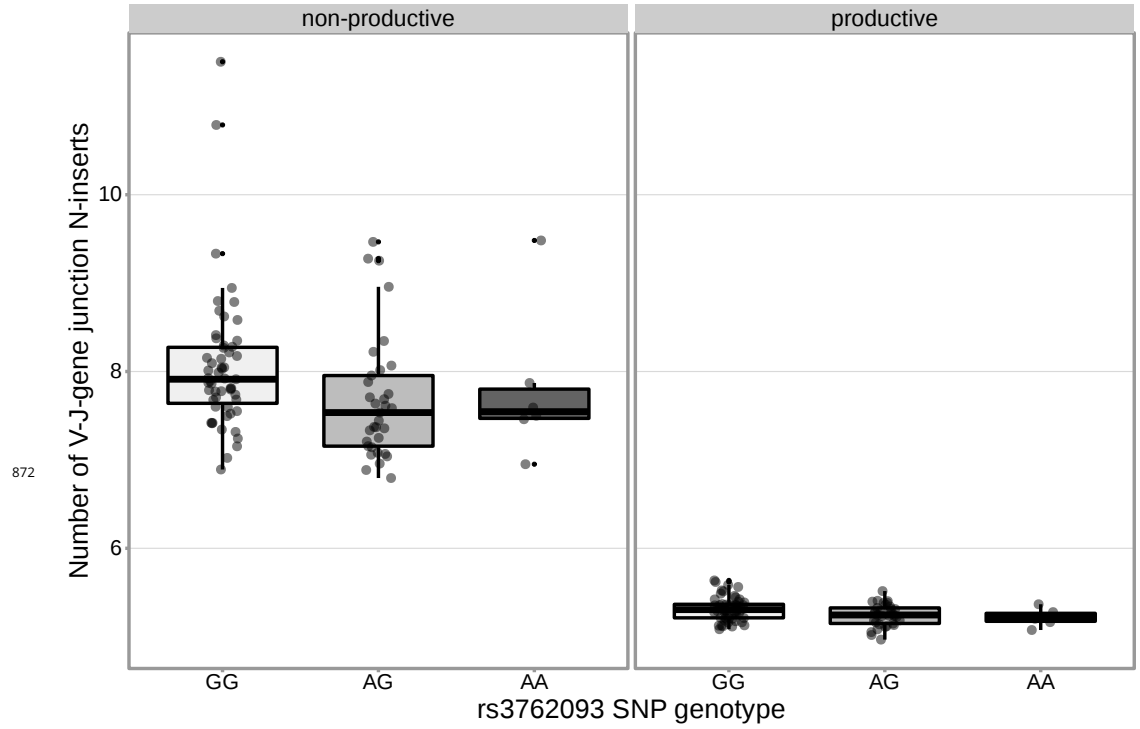
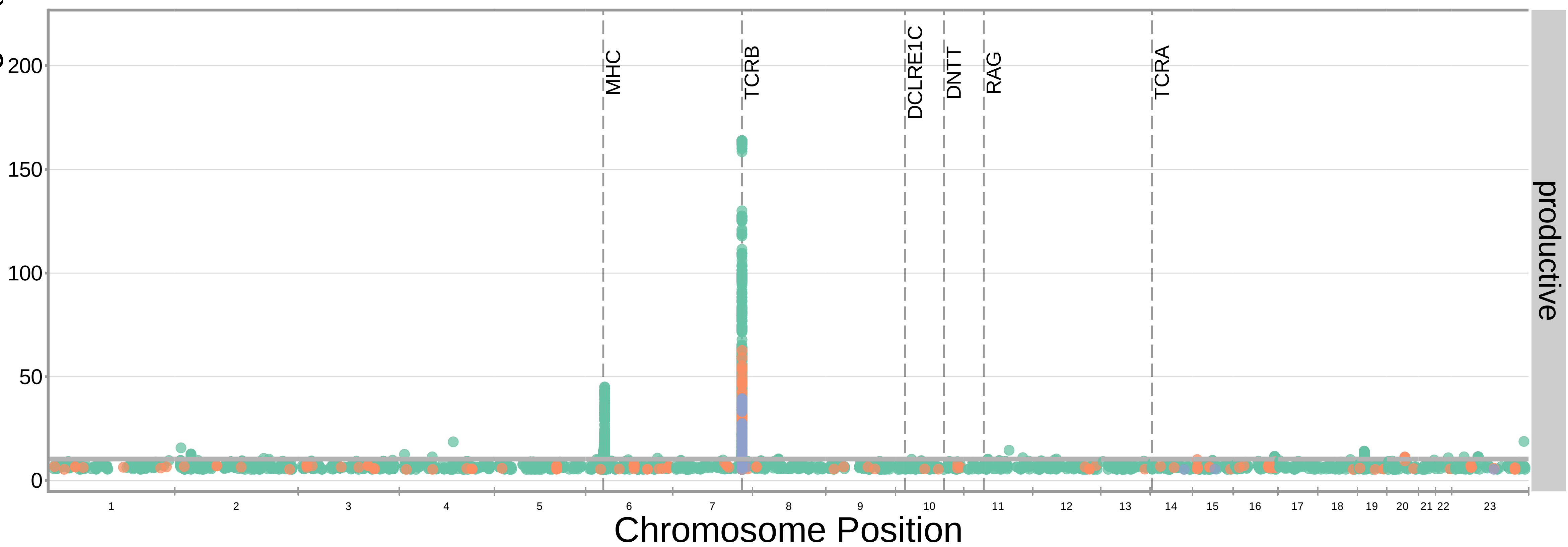
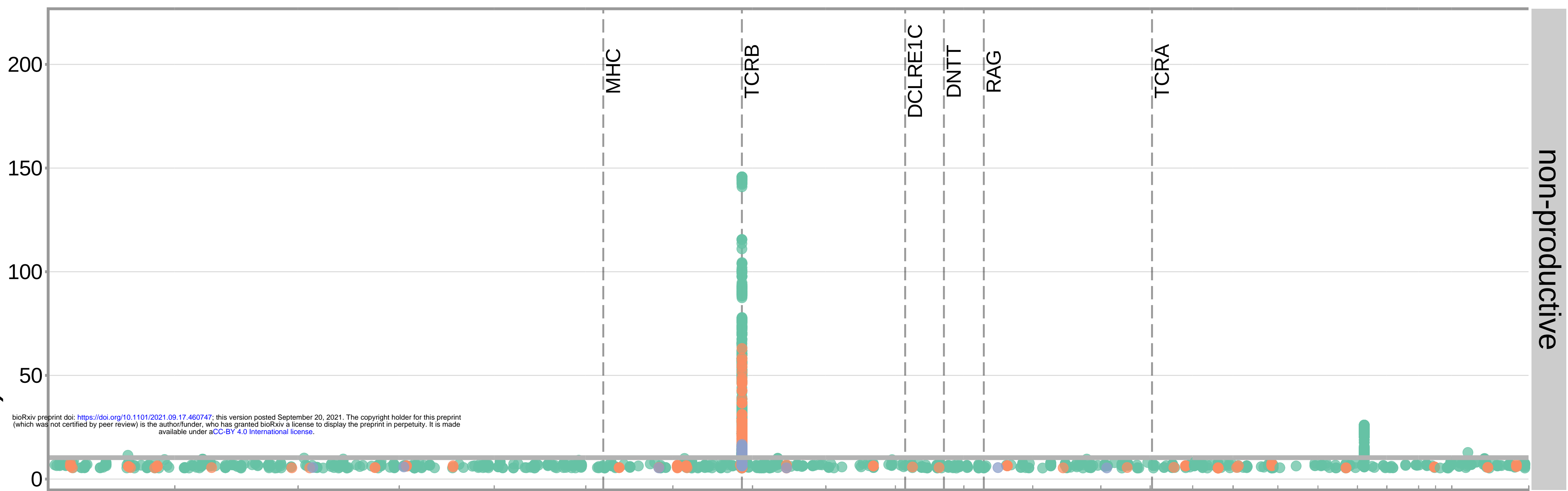
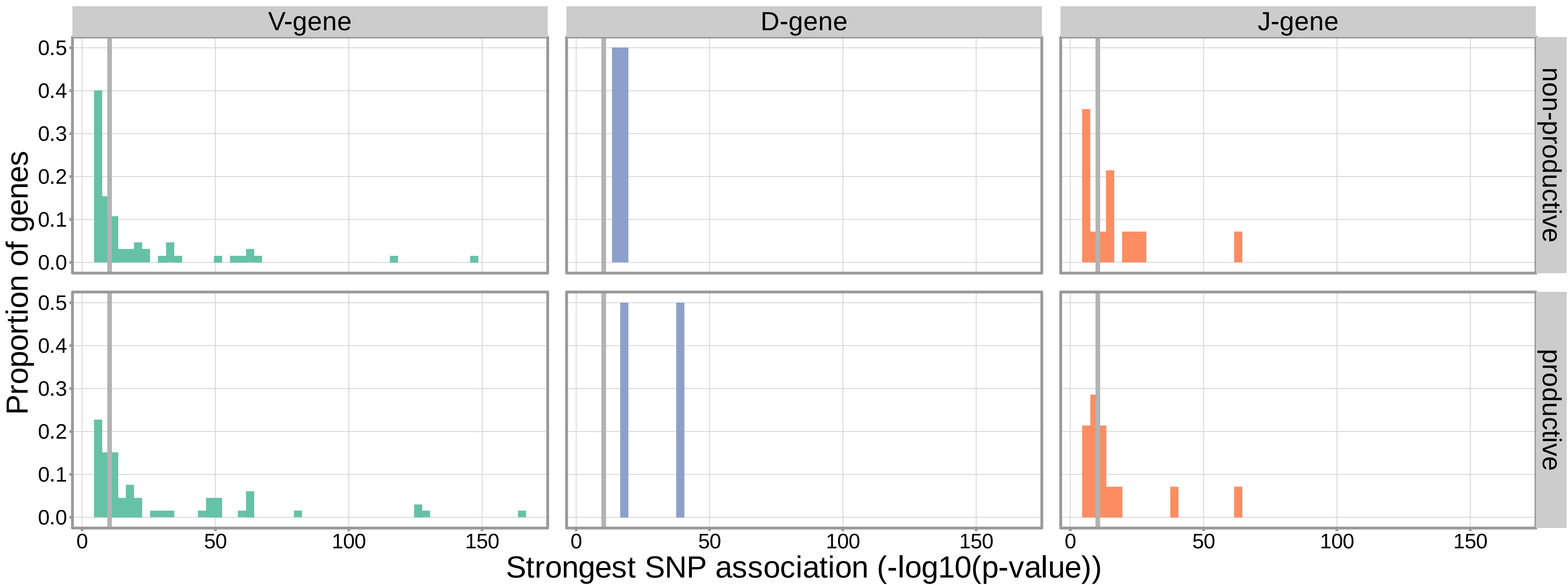


Table 2-Figure supplement 6. An intronic SNP (rs3762093) within the *DNTT* gene locus is significantly associated with the number of V-J N-inserts for productive TCR α chains in the validation cohort. This SNP is not significantly associated with the number of V-J N-inserts for non-productive TCR α chains in the validation cohort. The average number of N-insertions was calculated across all TCR α chains for each subject.

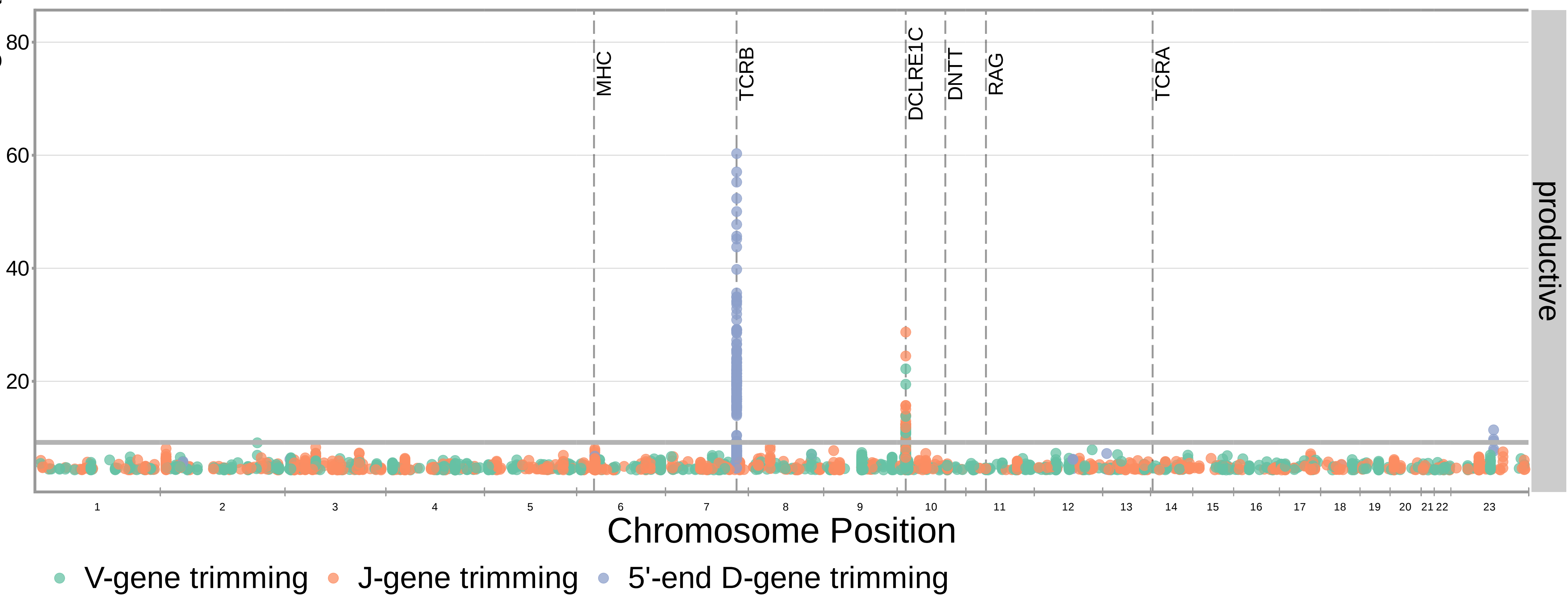
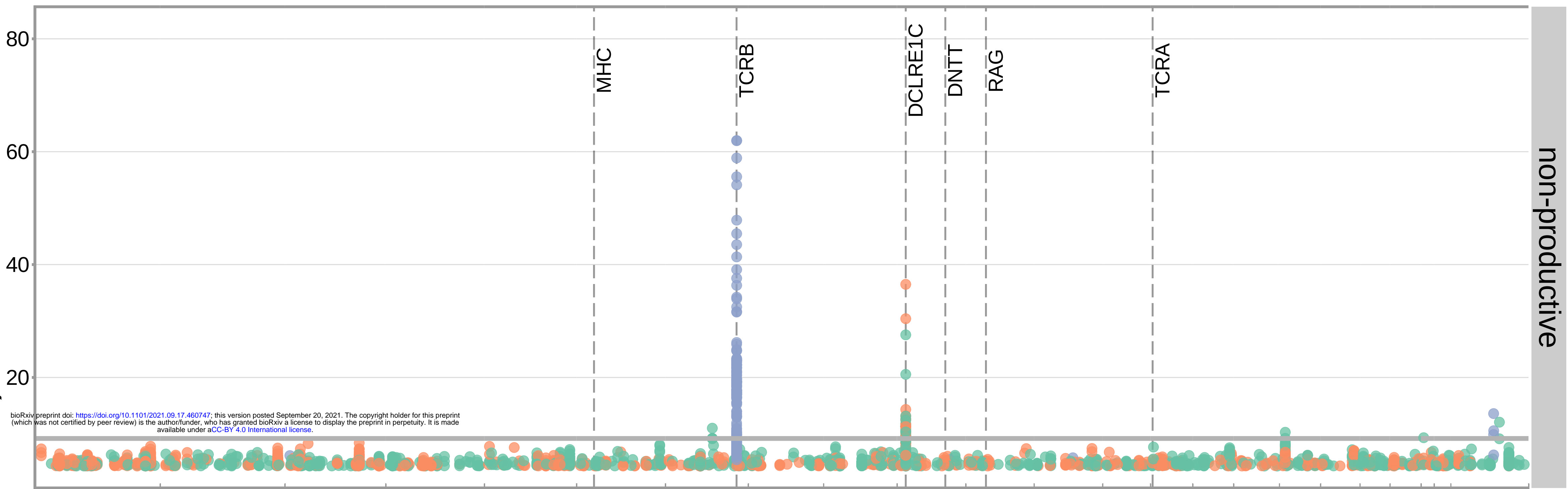
$-\log_{10}(\text{p-value})$



● D-gene usage ● J-gene usage ● V-gene usage



$-\log_{10}(\text{p-value})$



rs2367486 genotype

2

1

0

0

1

2

TRBD2*02 allele genotype

Subject count

60

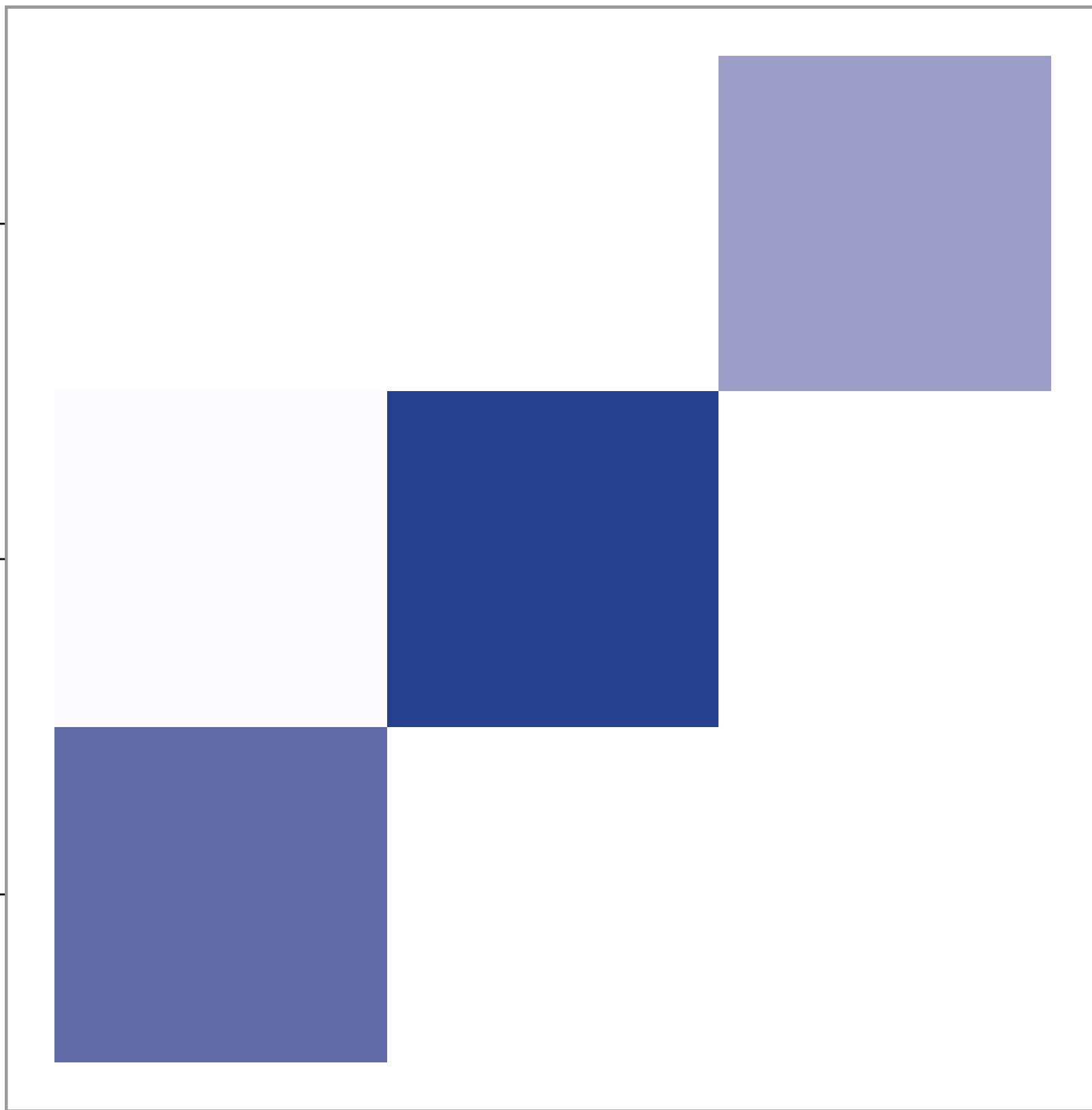
50

40

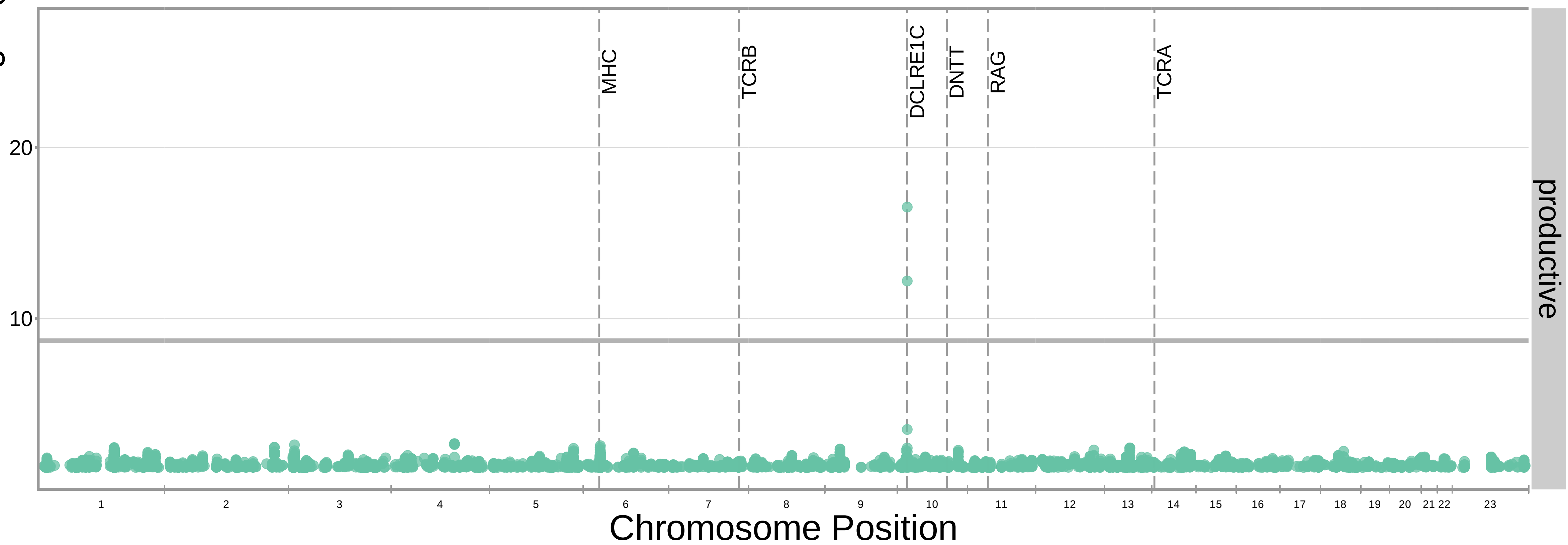
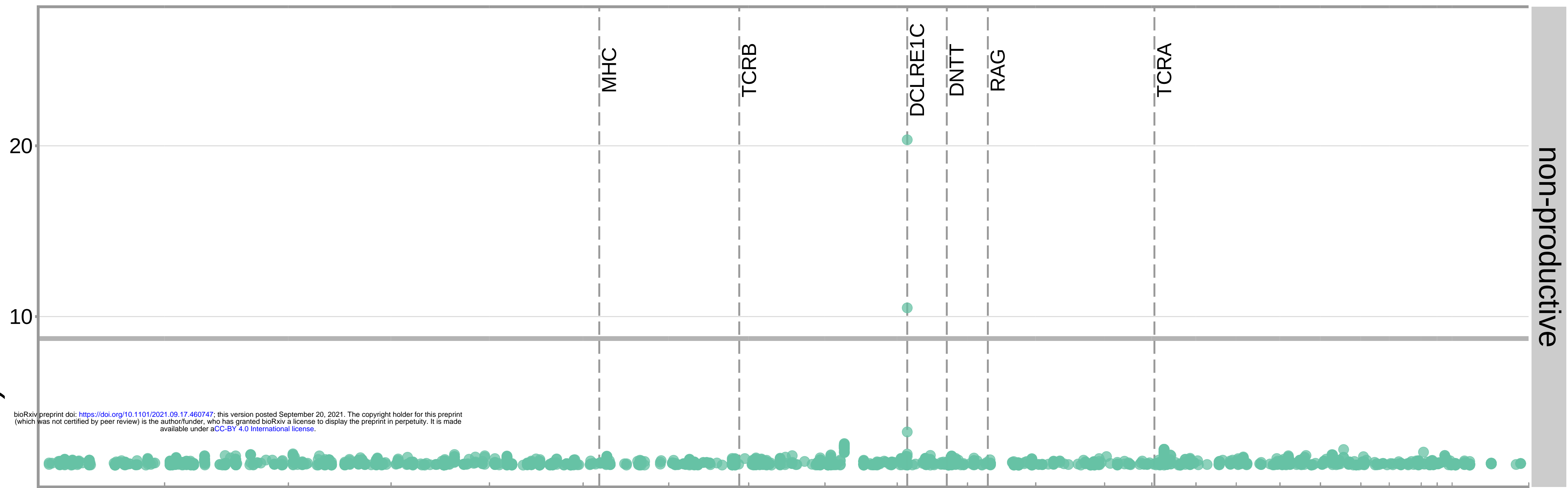
30

20

10

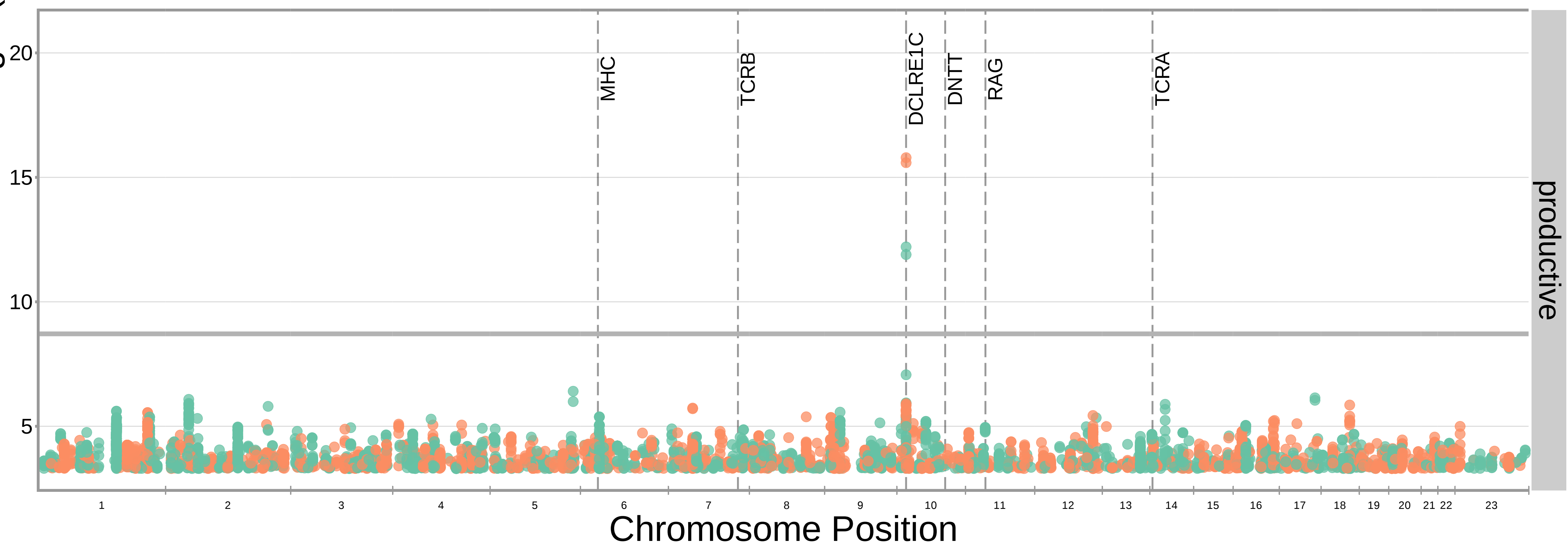
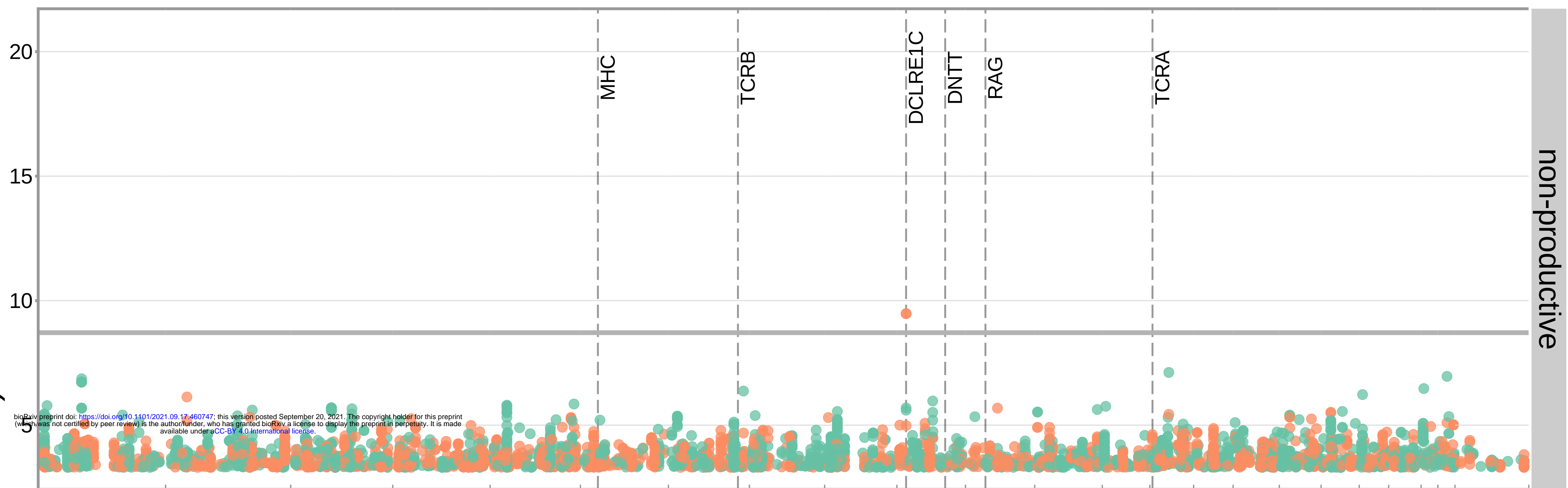


$-\log_{10}(\text{p-value})$



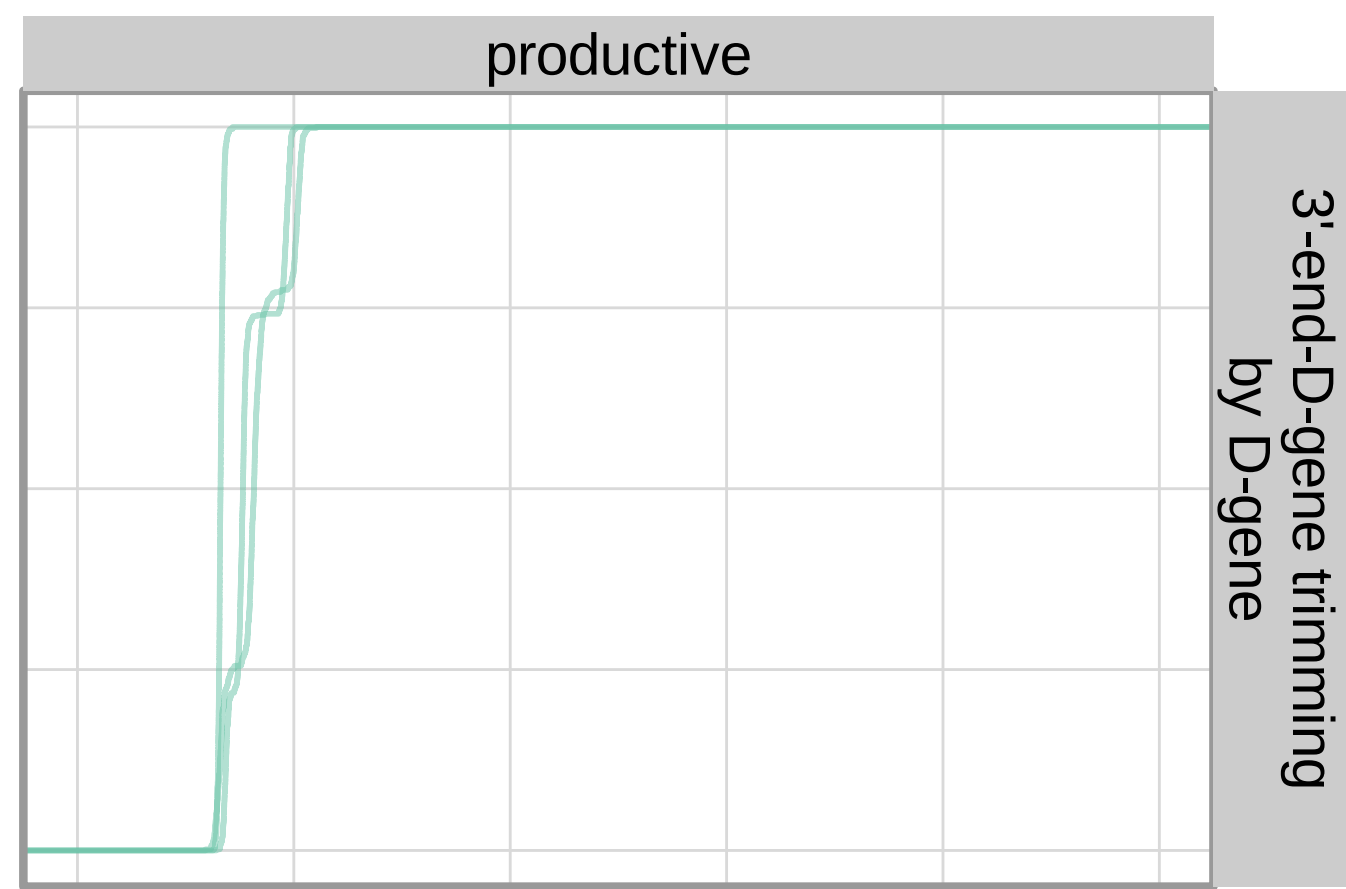
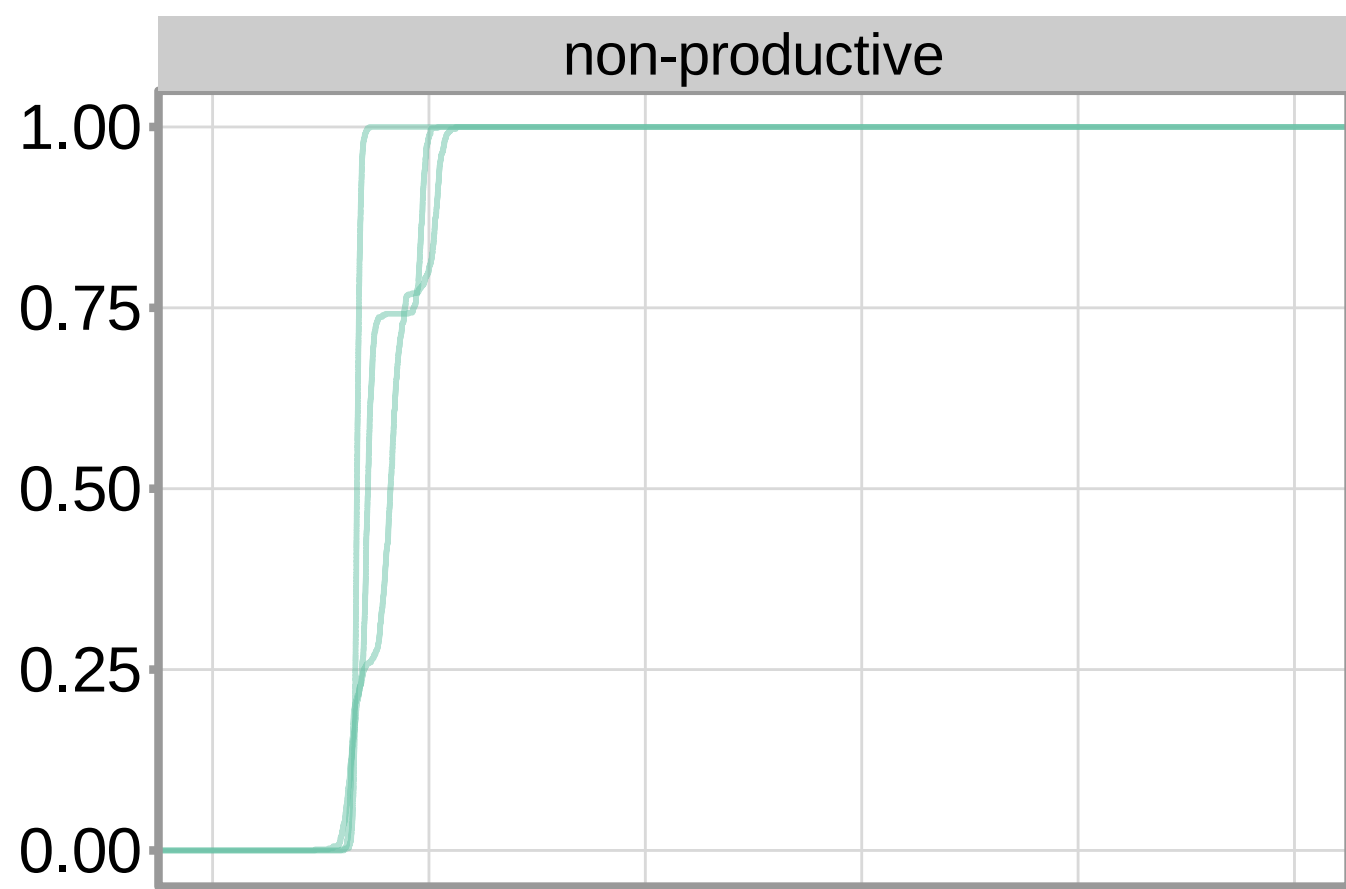
● 5'-end D-gene trimming

$-\log_{10}(\text{p-value})$

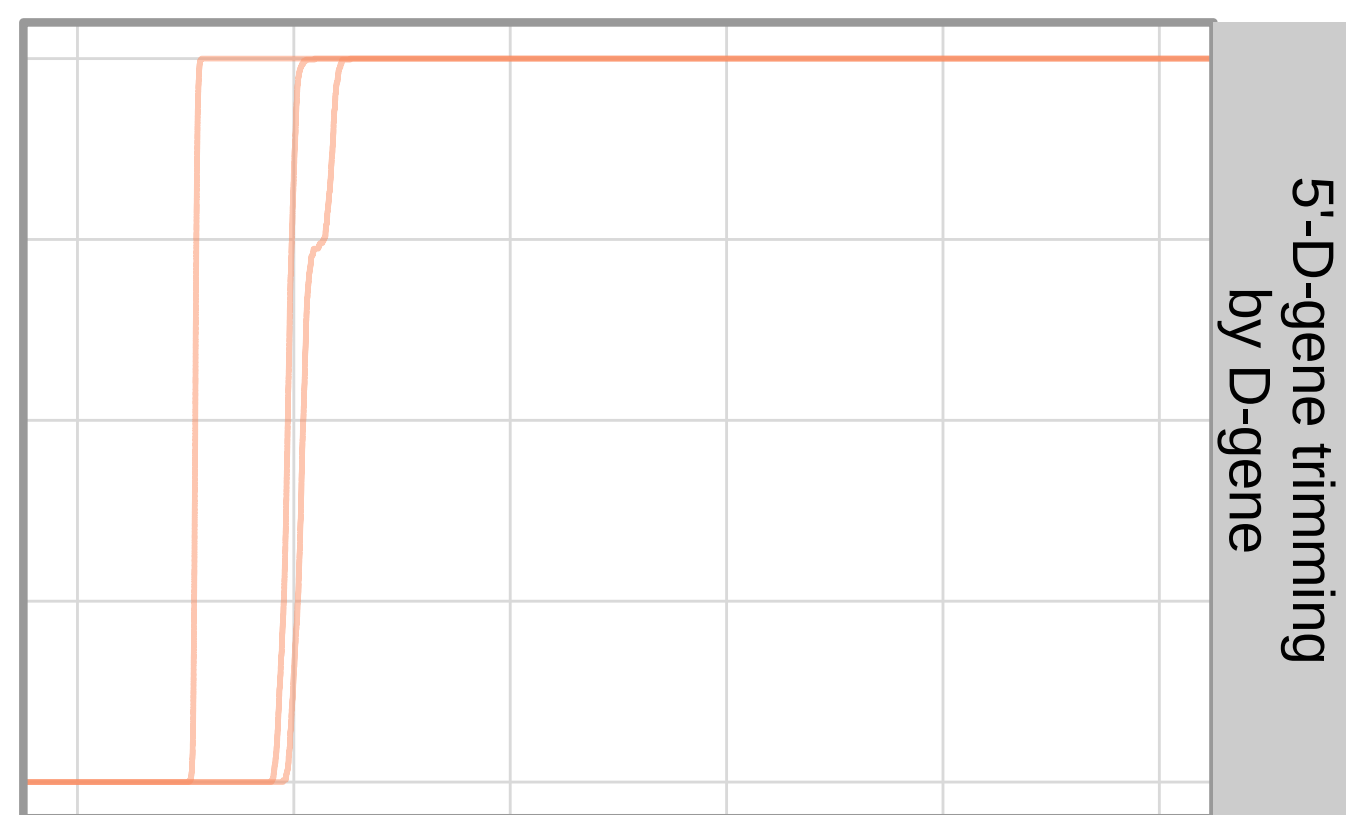
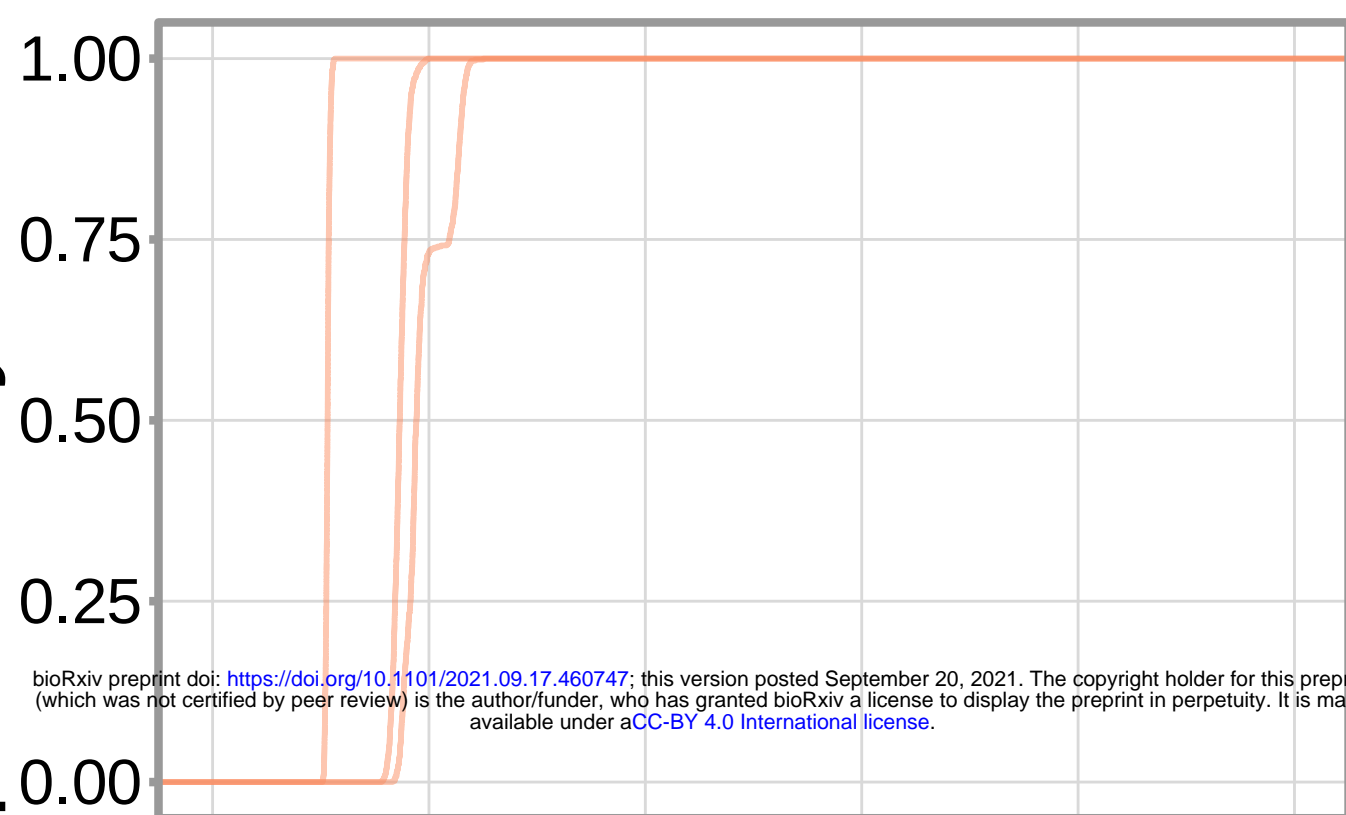


● 5'-end D-gene trimming ● 3'-end D-gene trimming

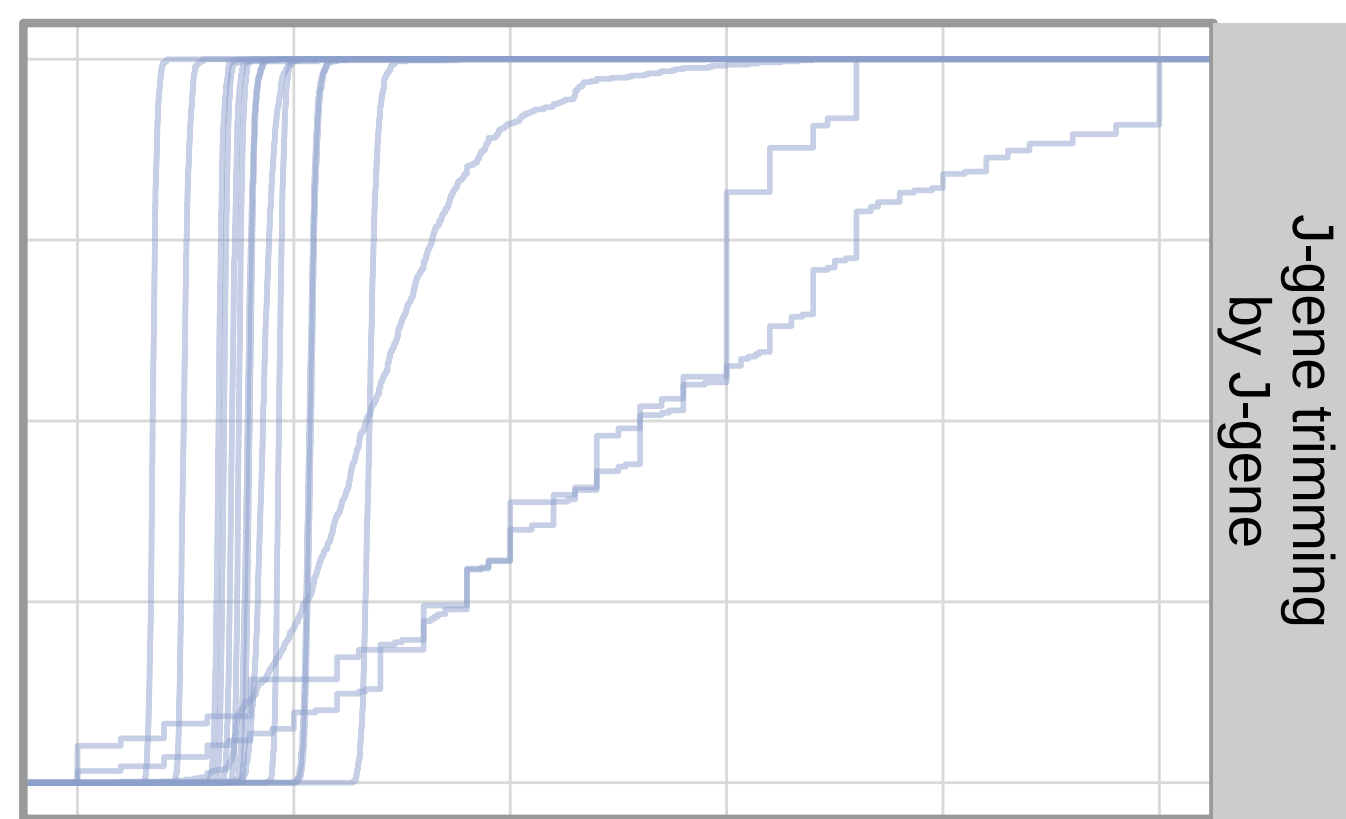
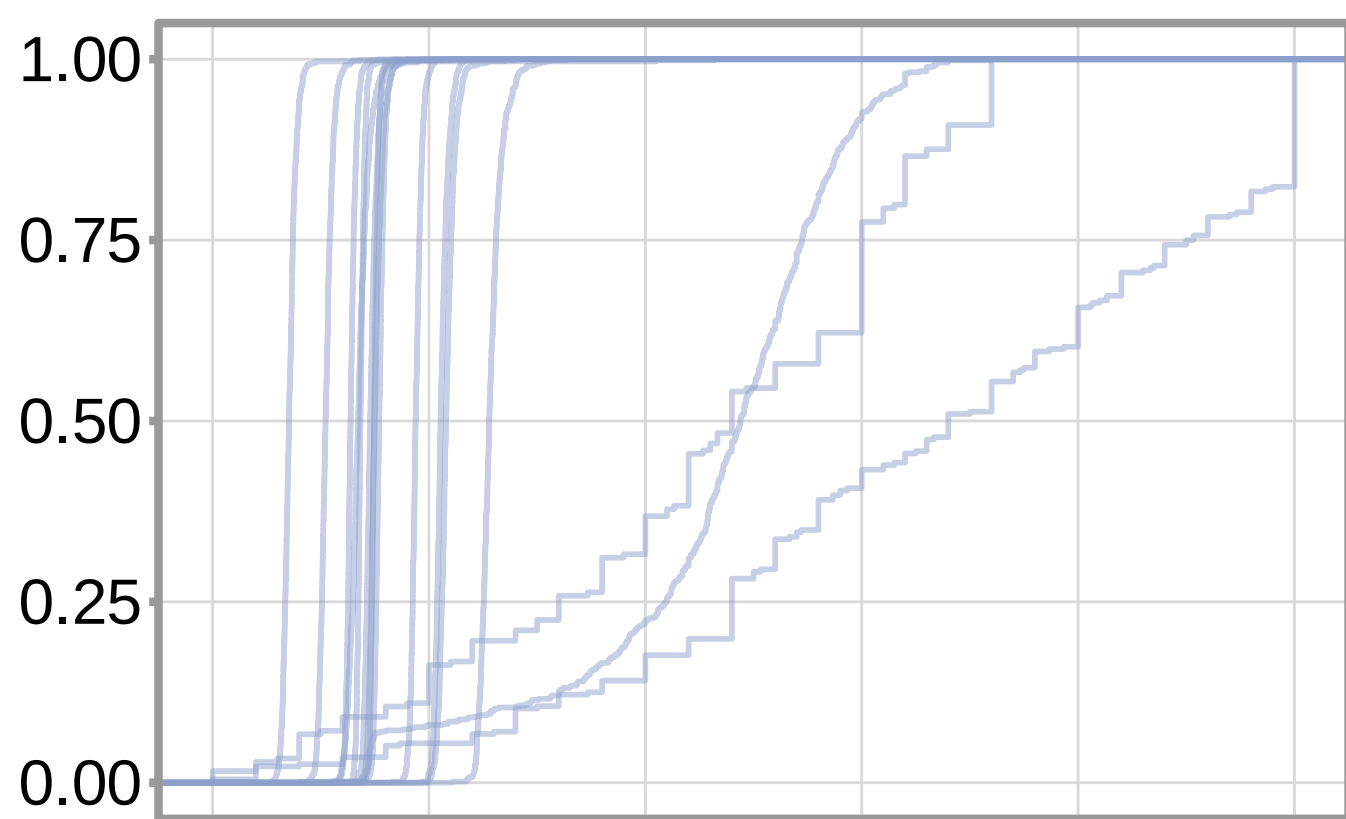
Cumulative probability



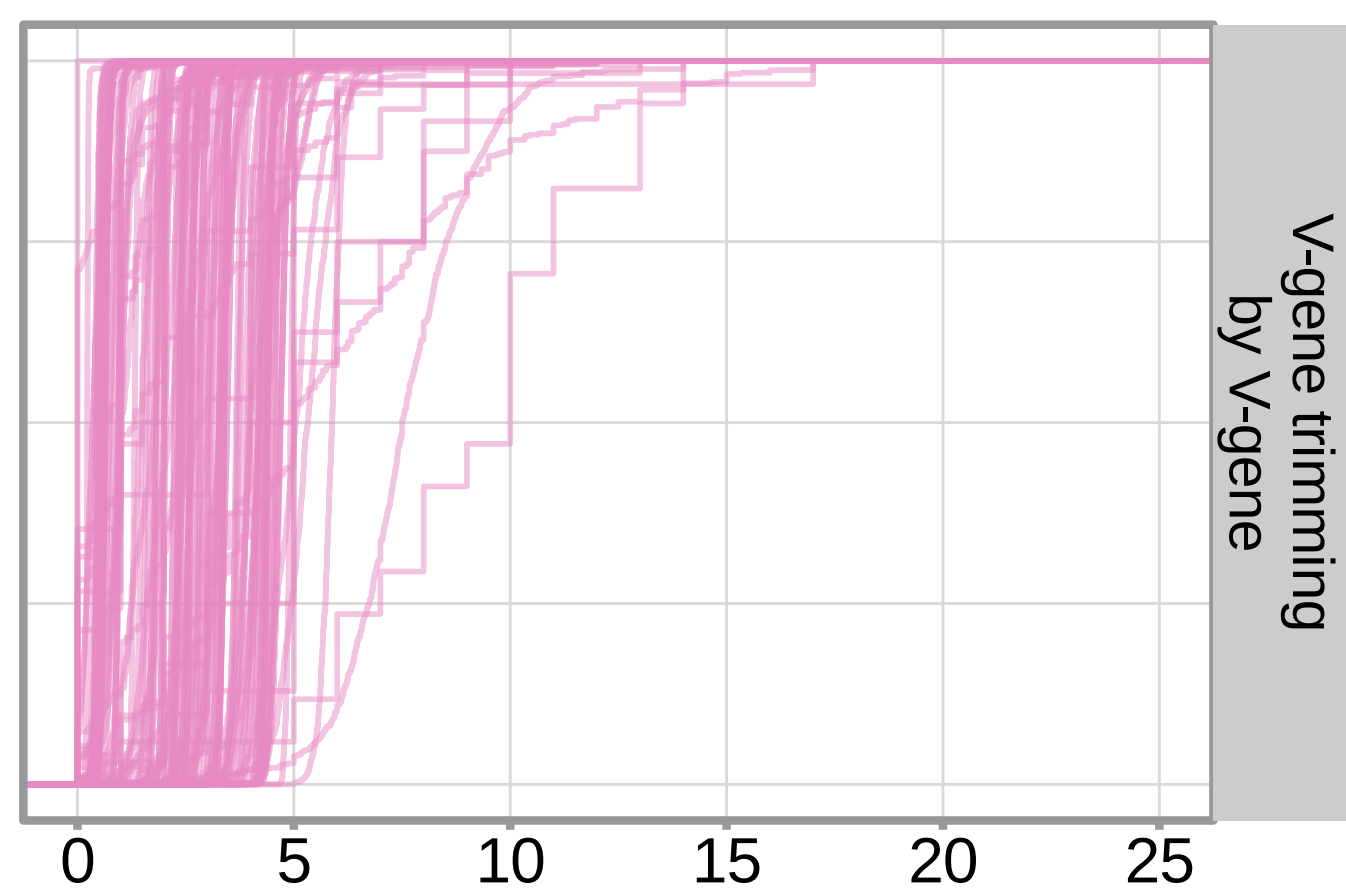
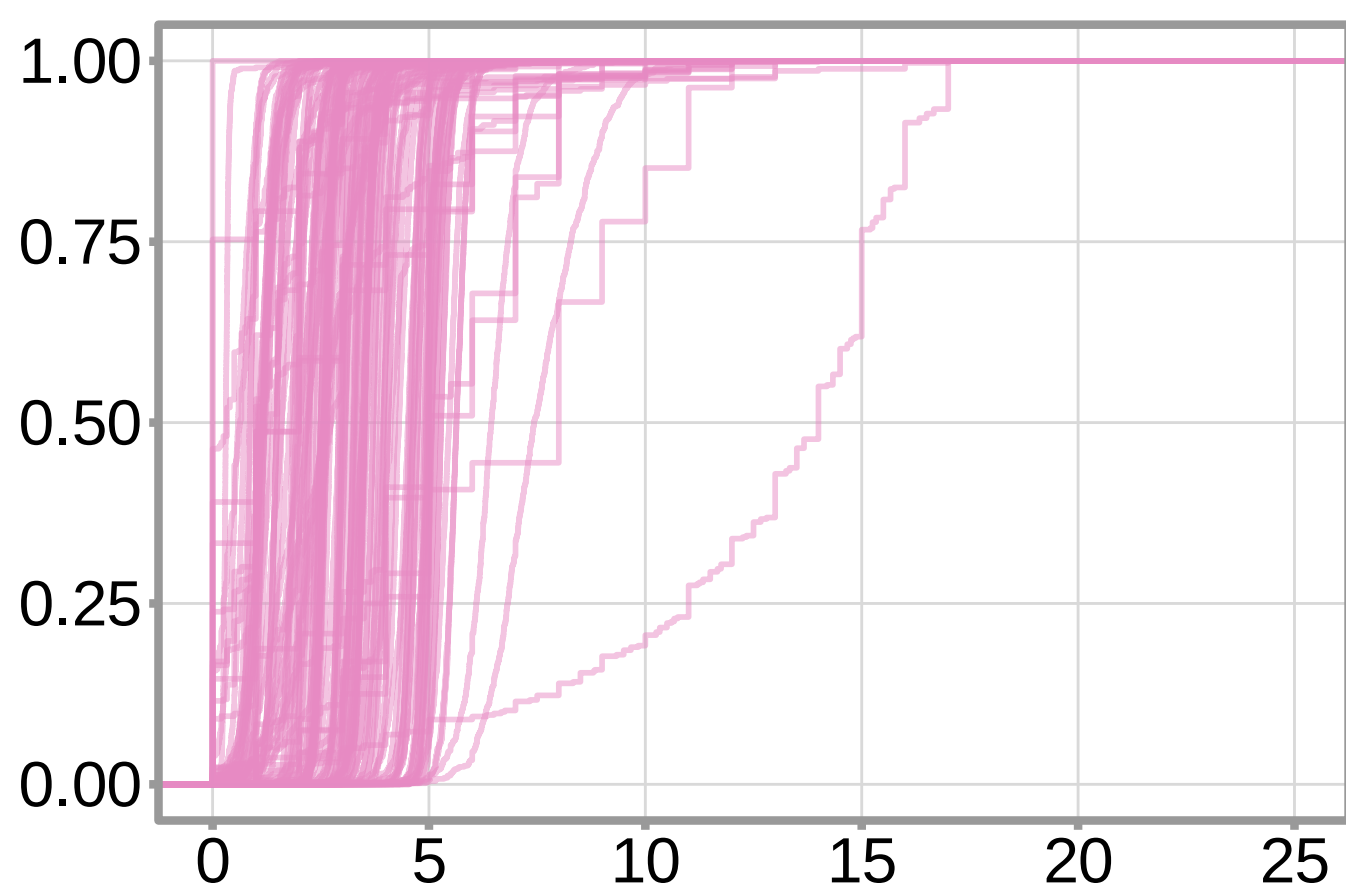
3'-end-D-gene trimming
by D-gene



5'-D-gene trimming
by D-gene



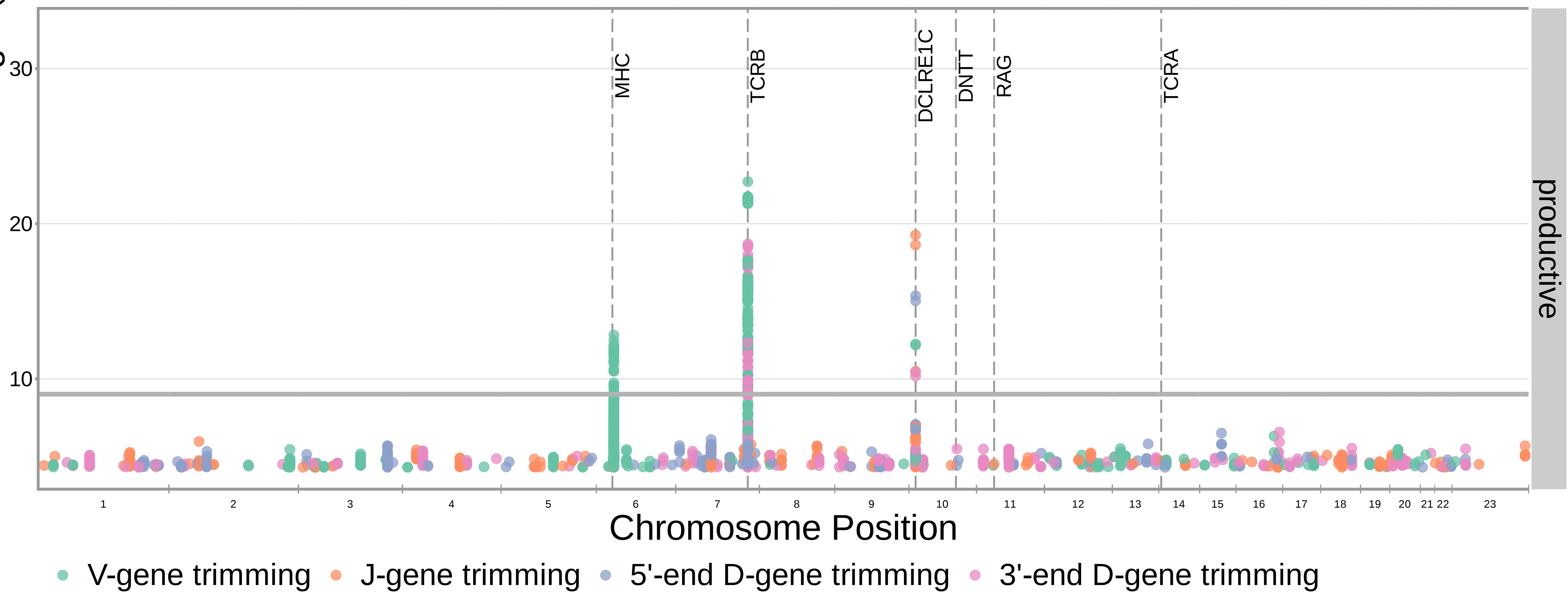
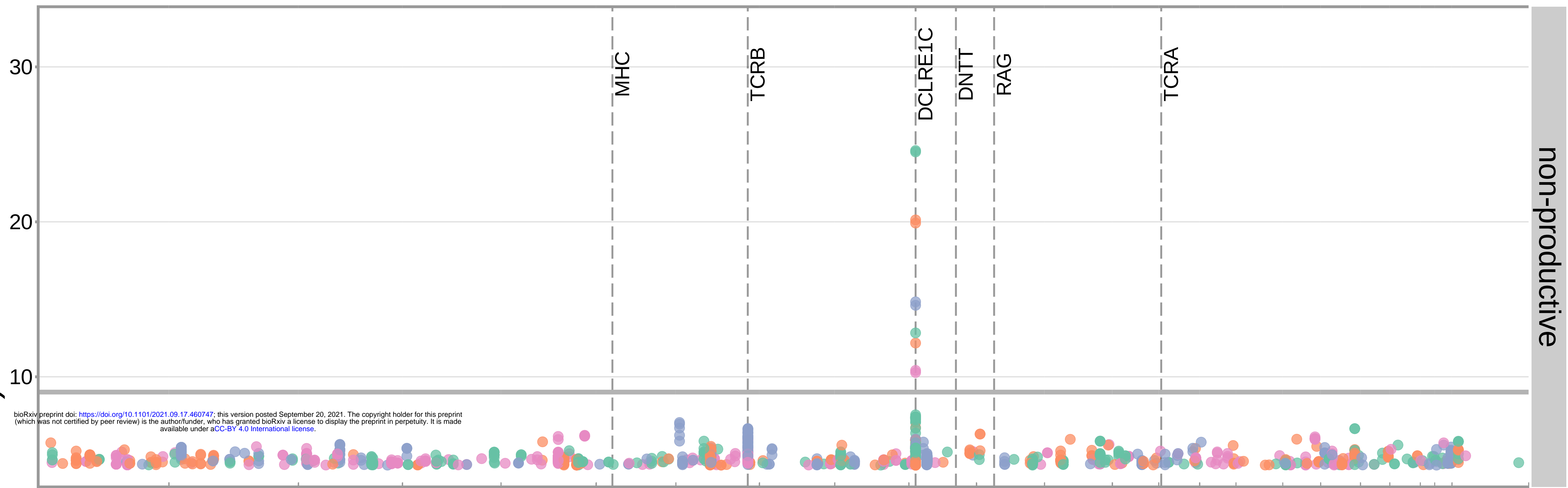
J-gene trimming
by J-gene

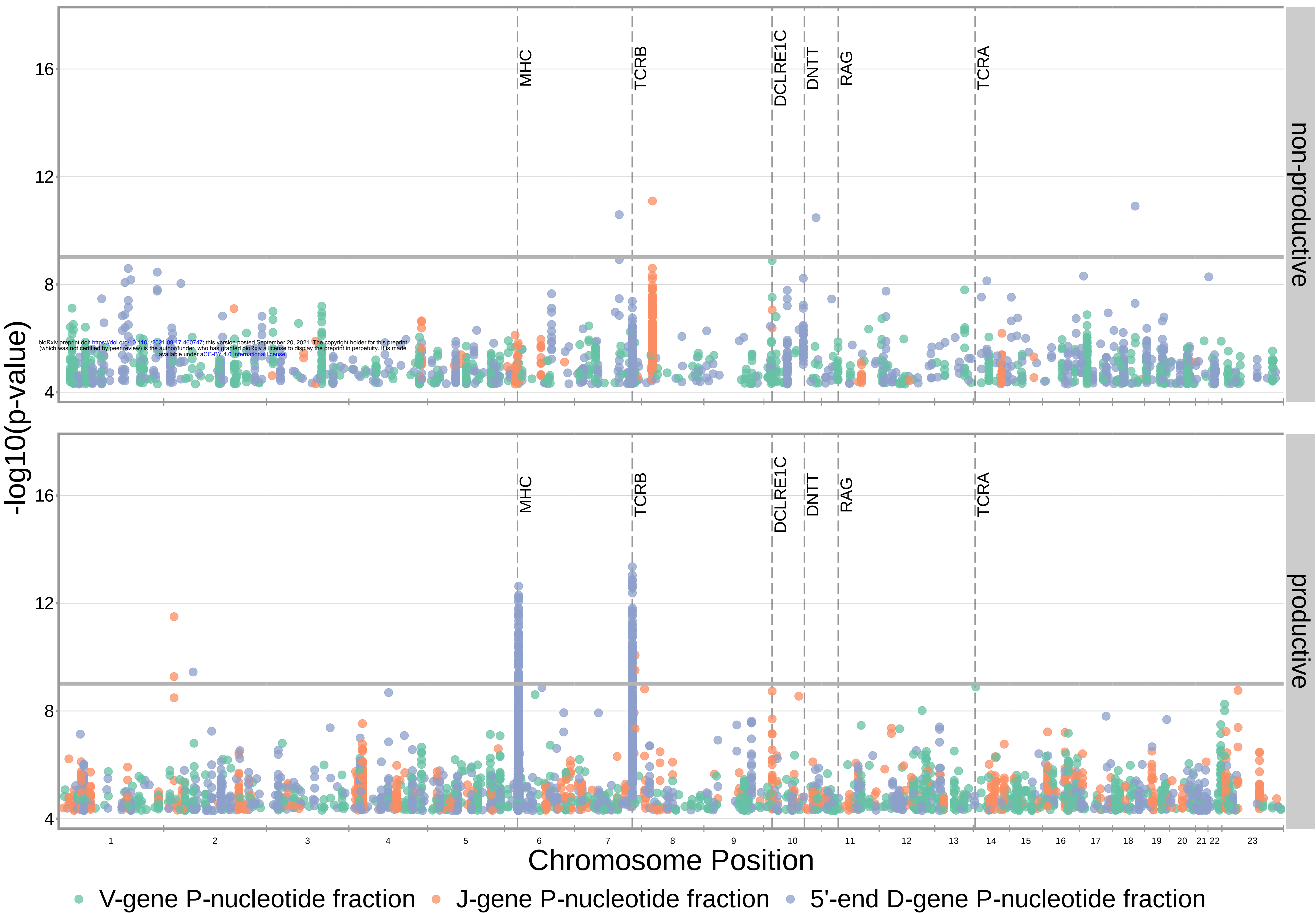


V-gene trimming
by V-gene

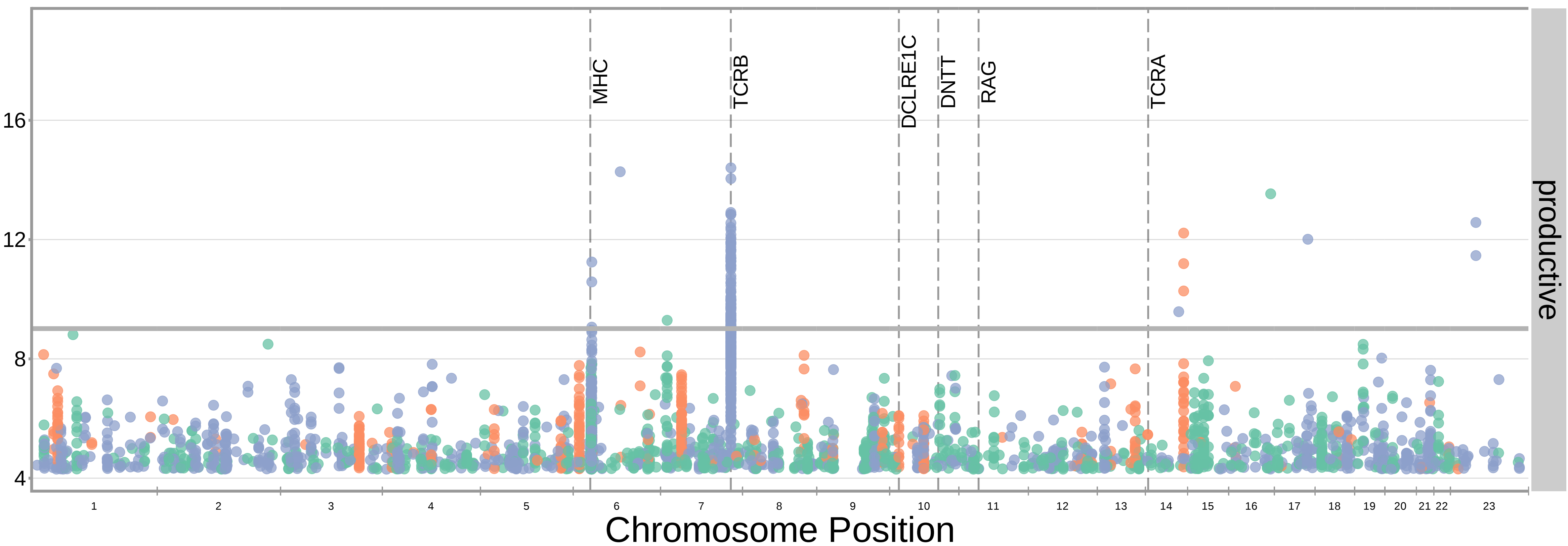
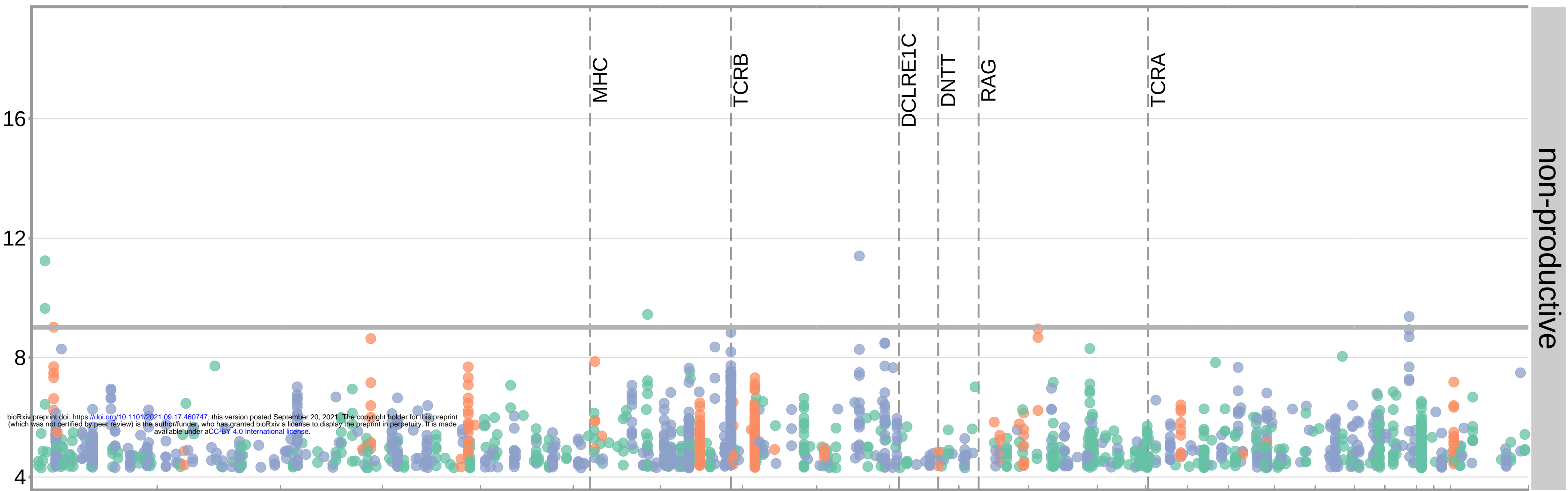
Number of trimmed nucleotides

$-\log_{10}(\text{p-value})$

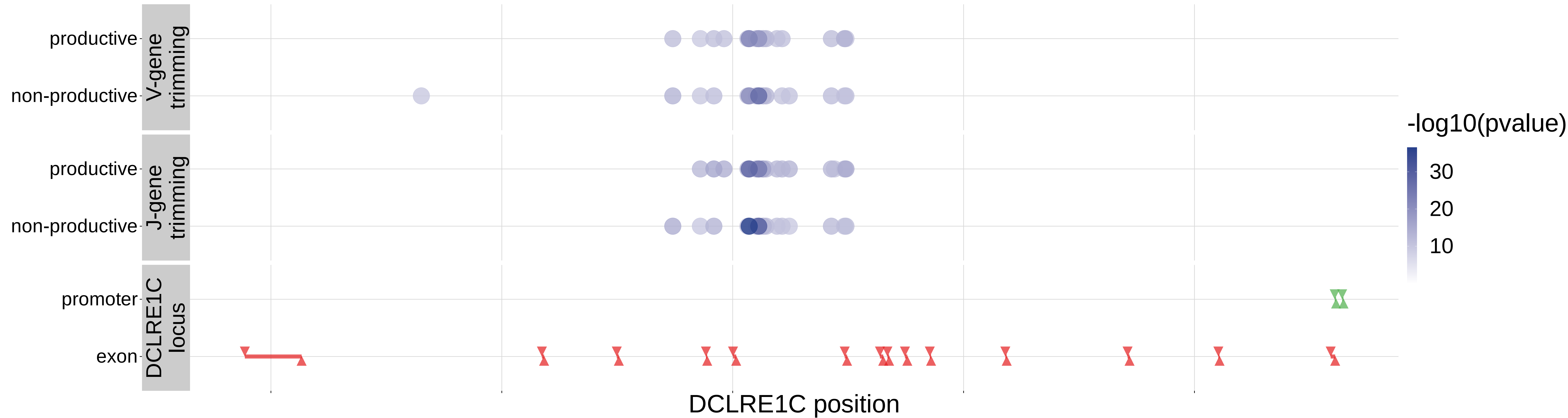




$-\log_{10}(\text{p-value})$



● V-gene P-nucleotides ● J-gene P-nucleotides ● 5'-end D-gene P-nucleotides



Number of J-gene nucleotides deleted

non-productive

productive

4.00
3.75
3.50

AA

CA

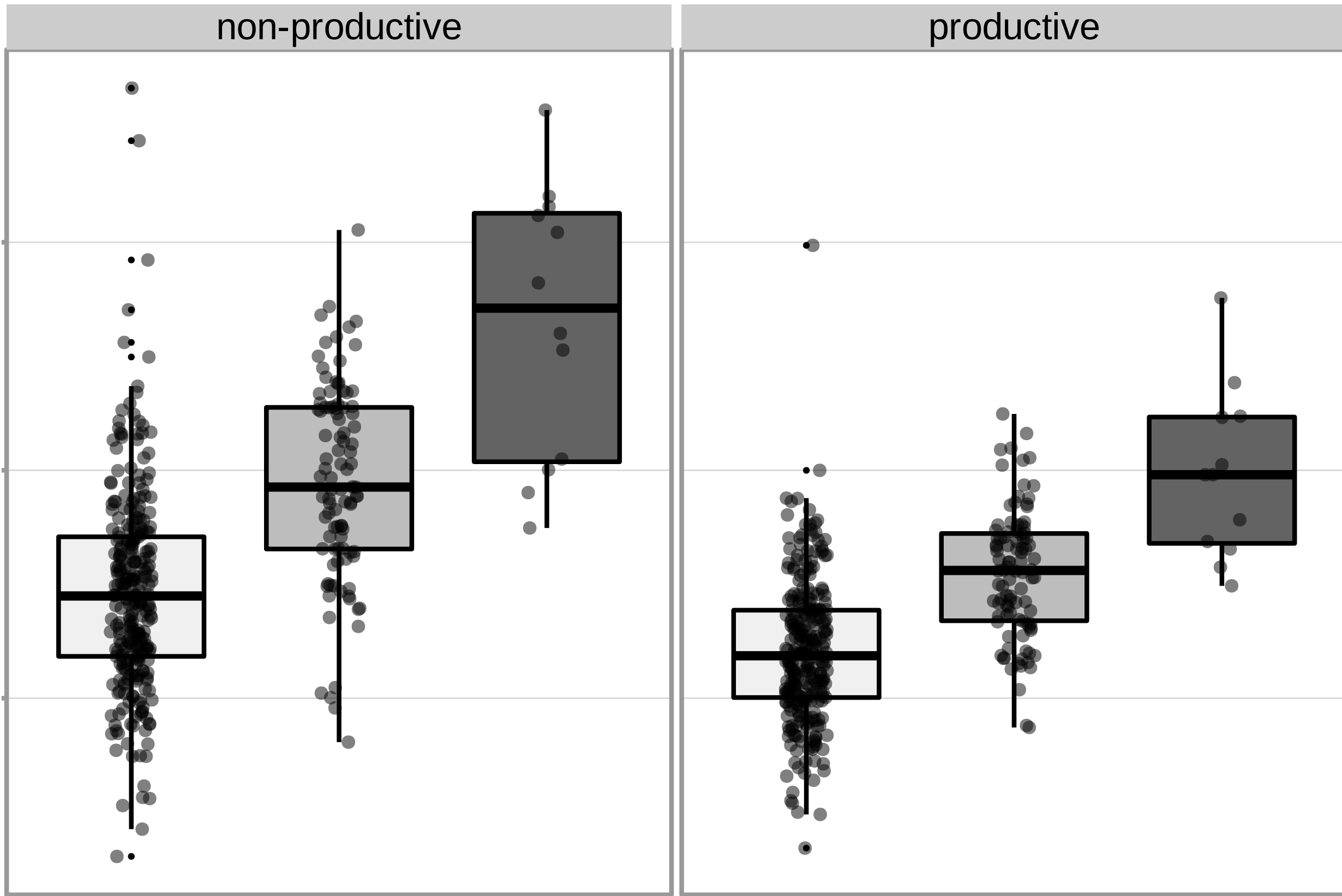
CC

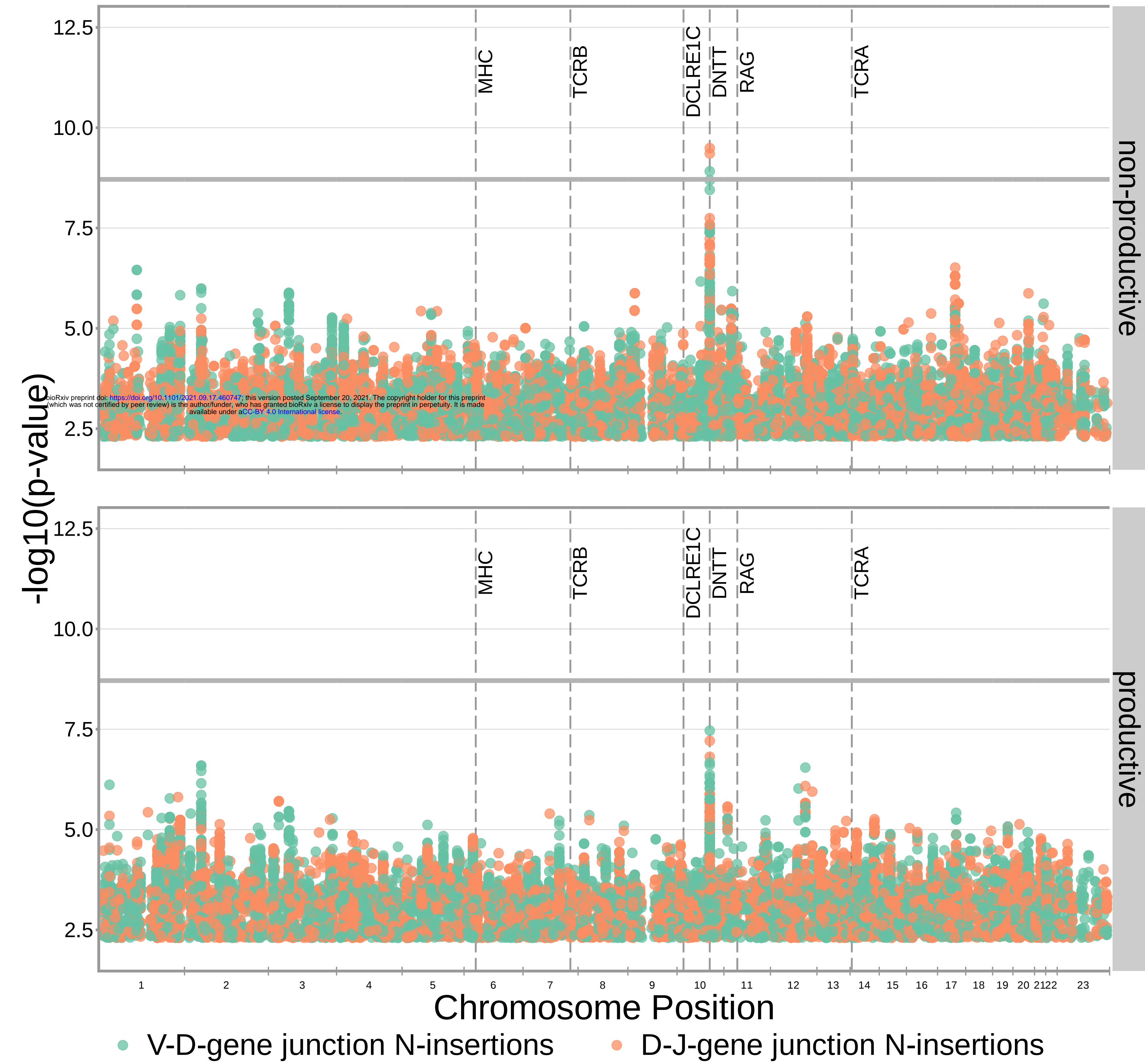
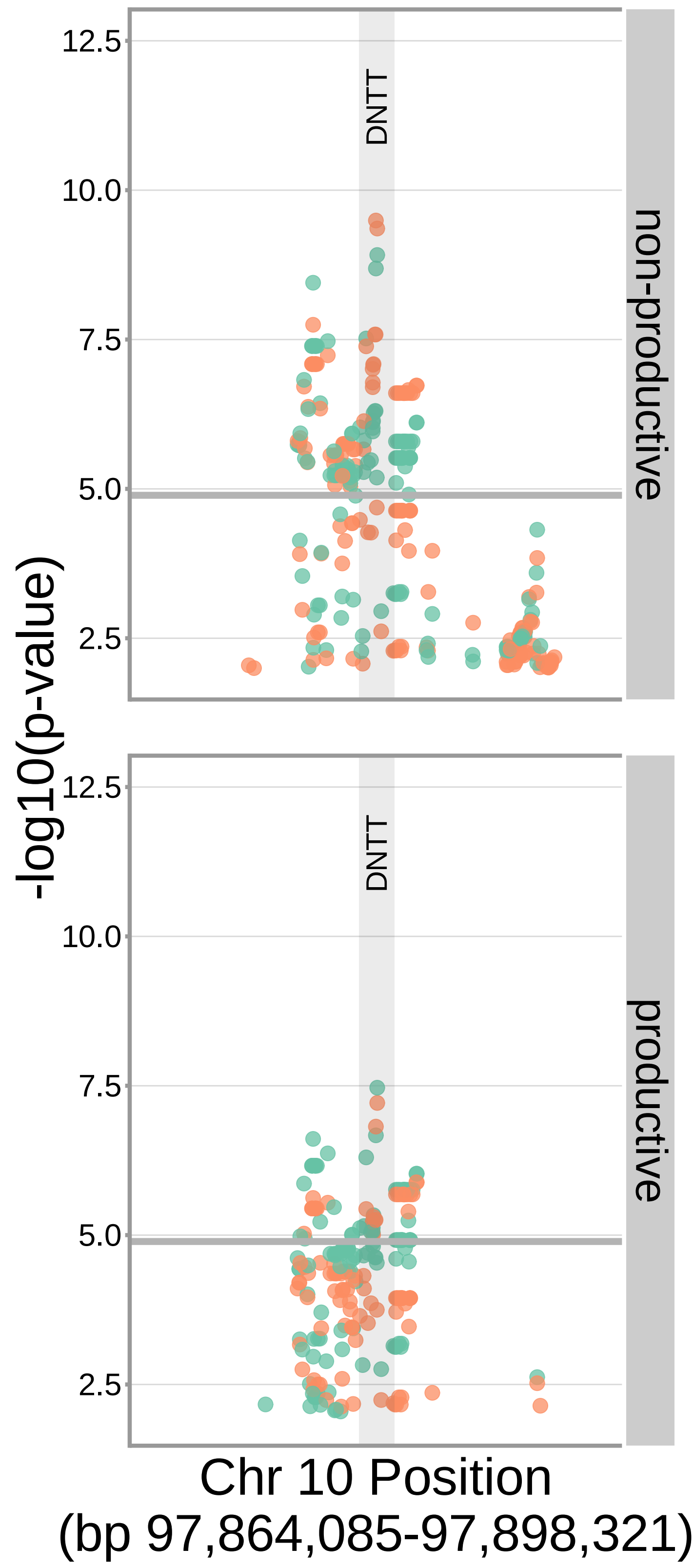
AA

CA

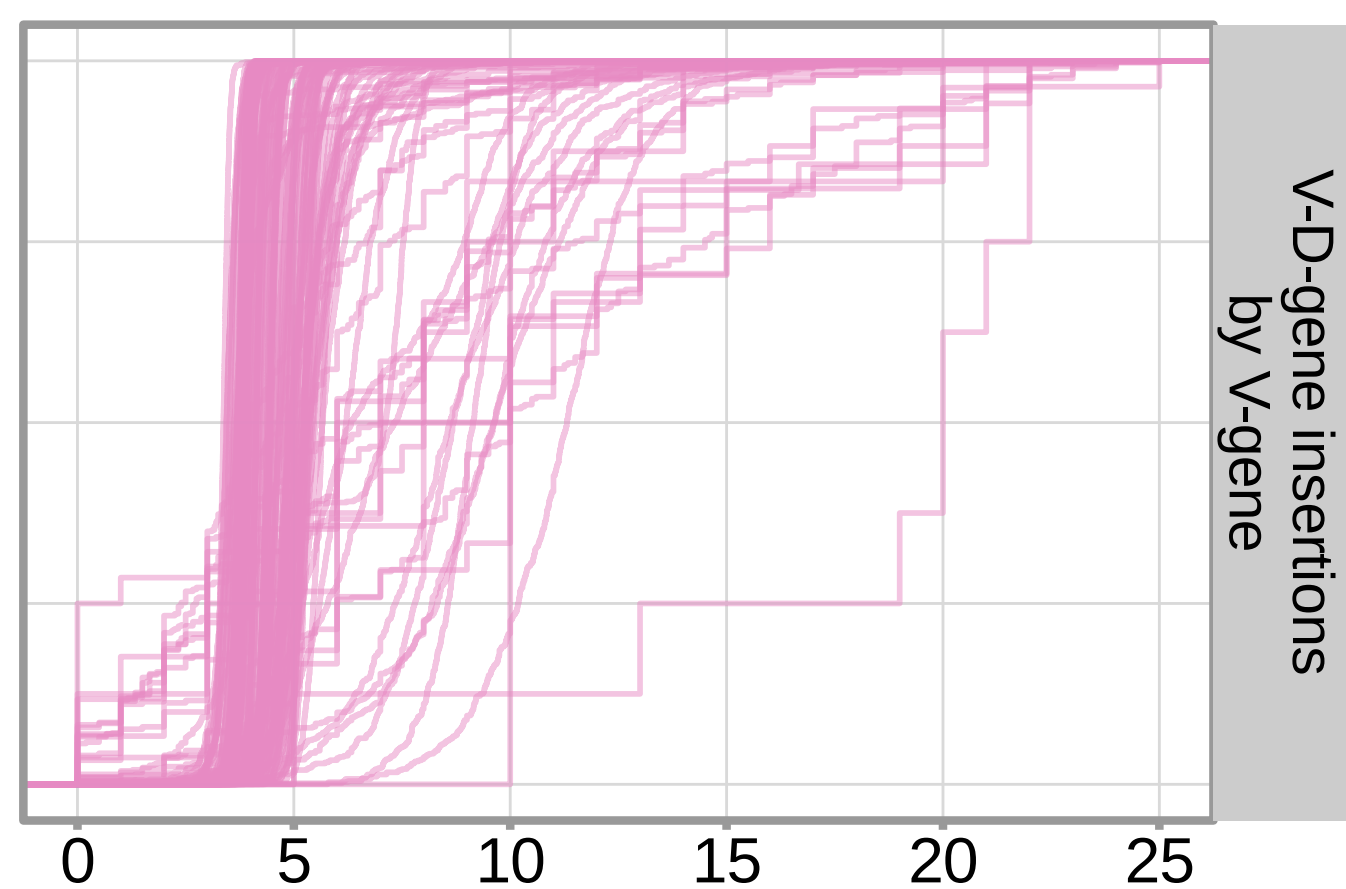
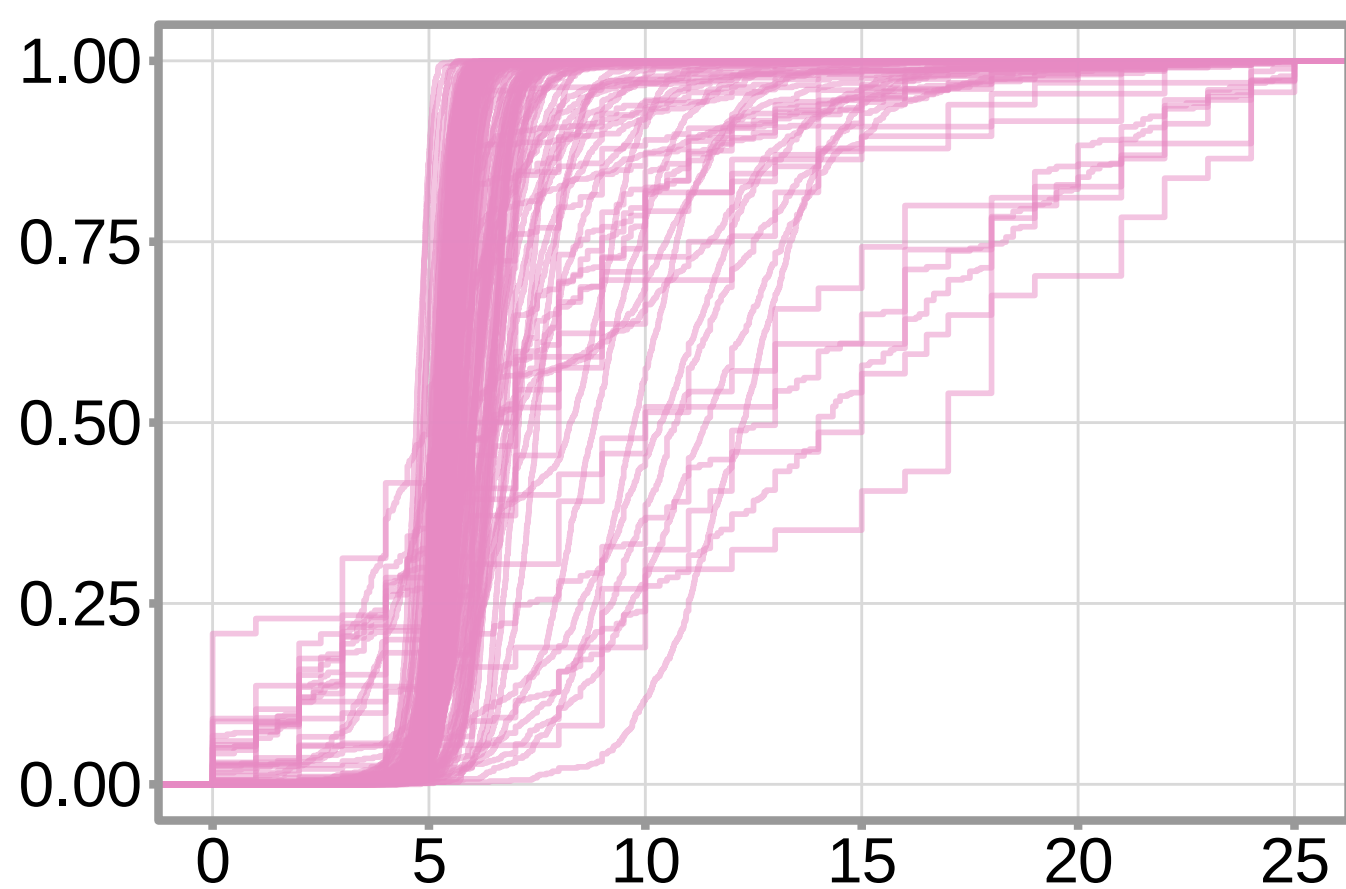
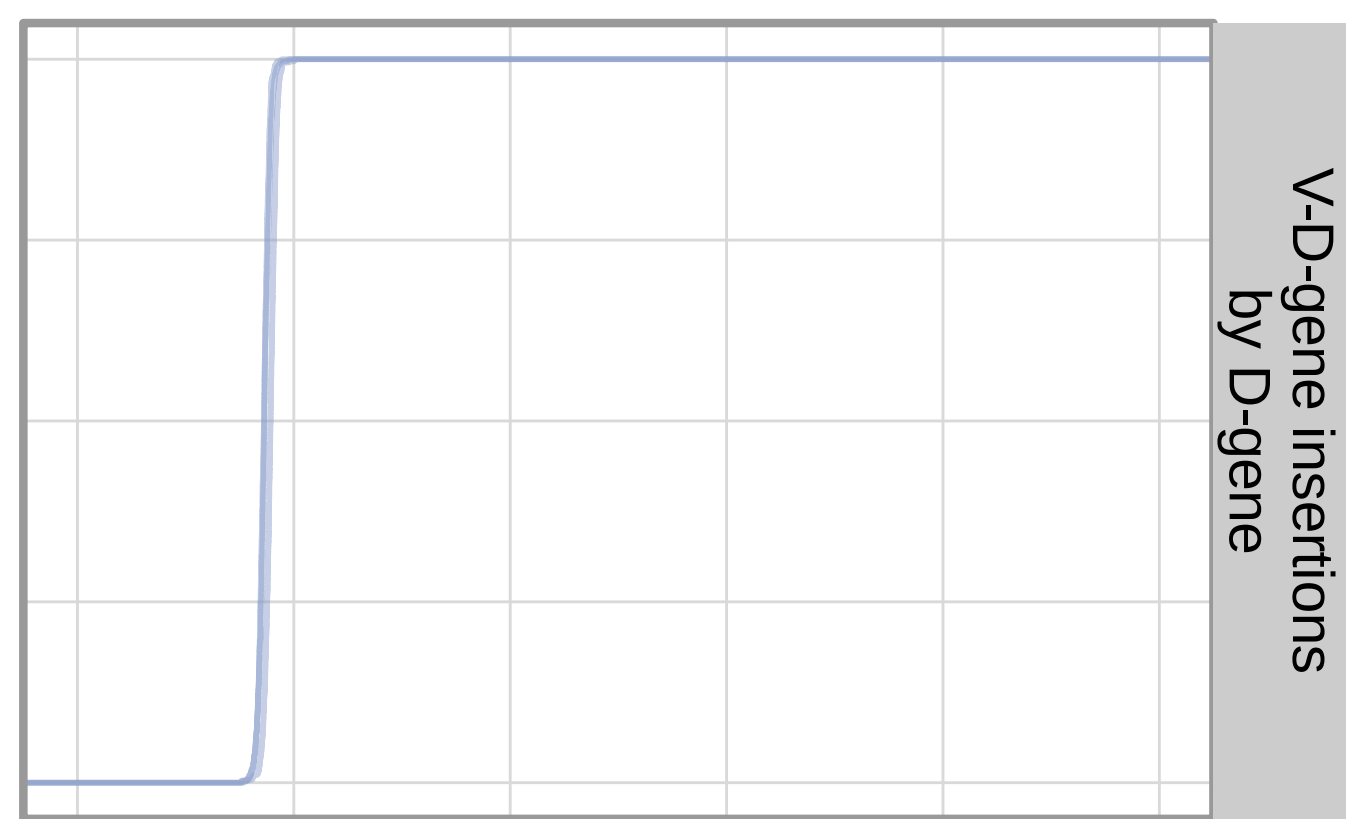
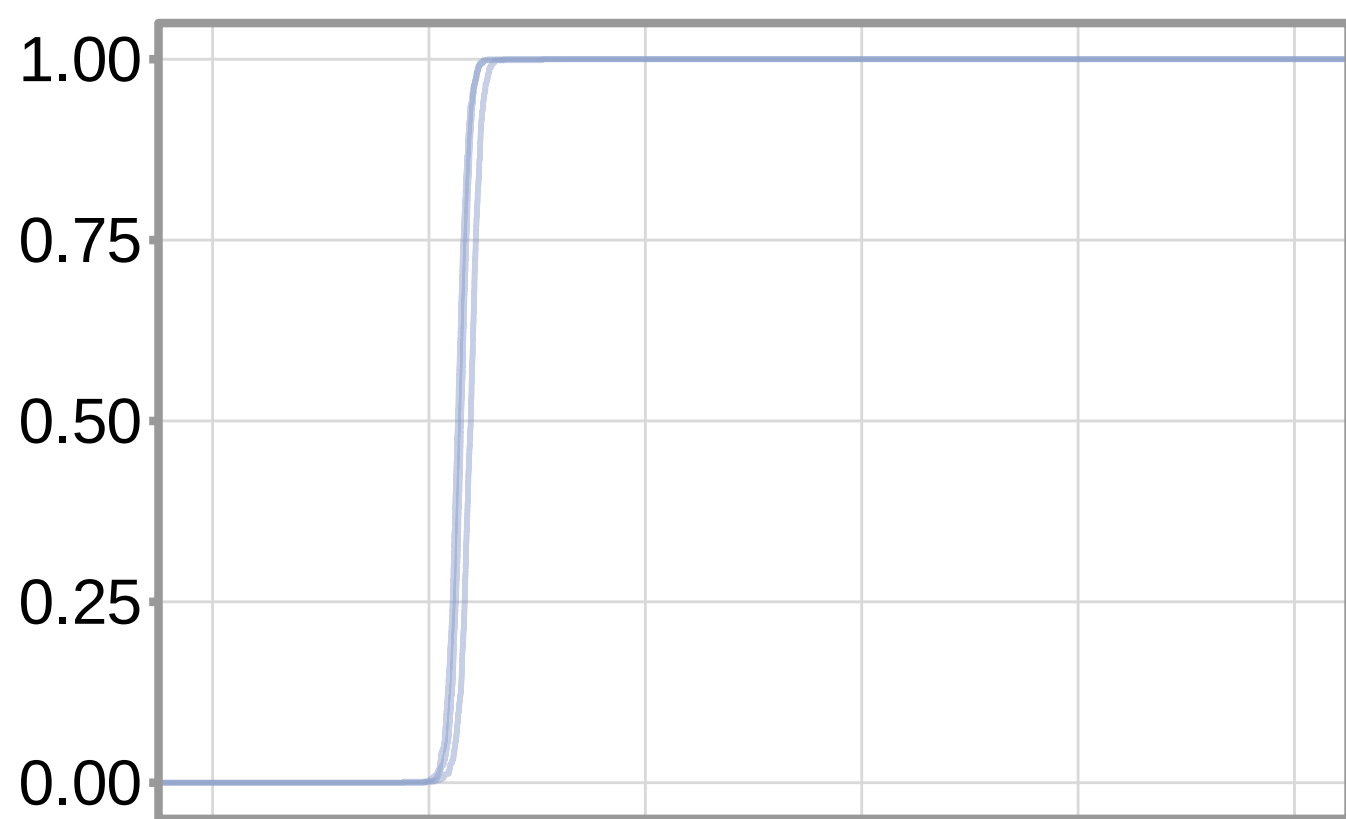
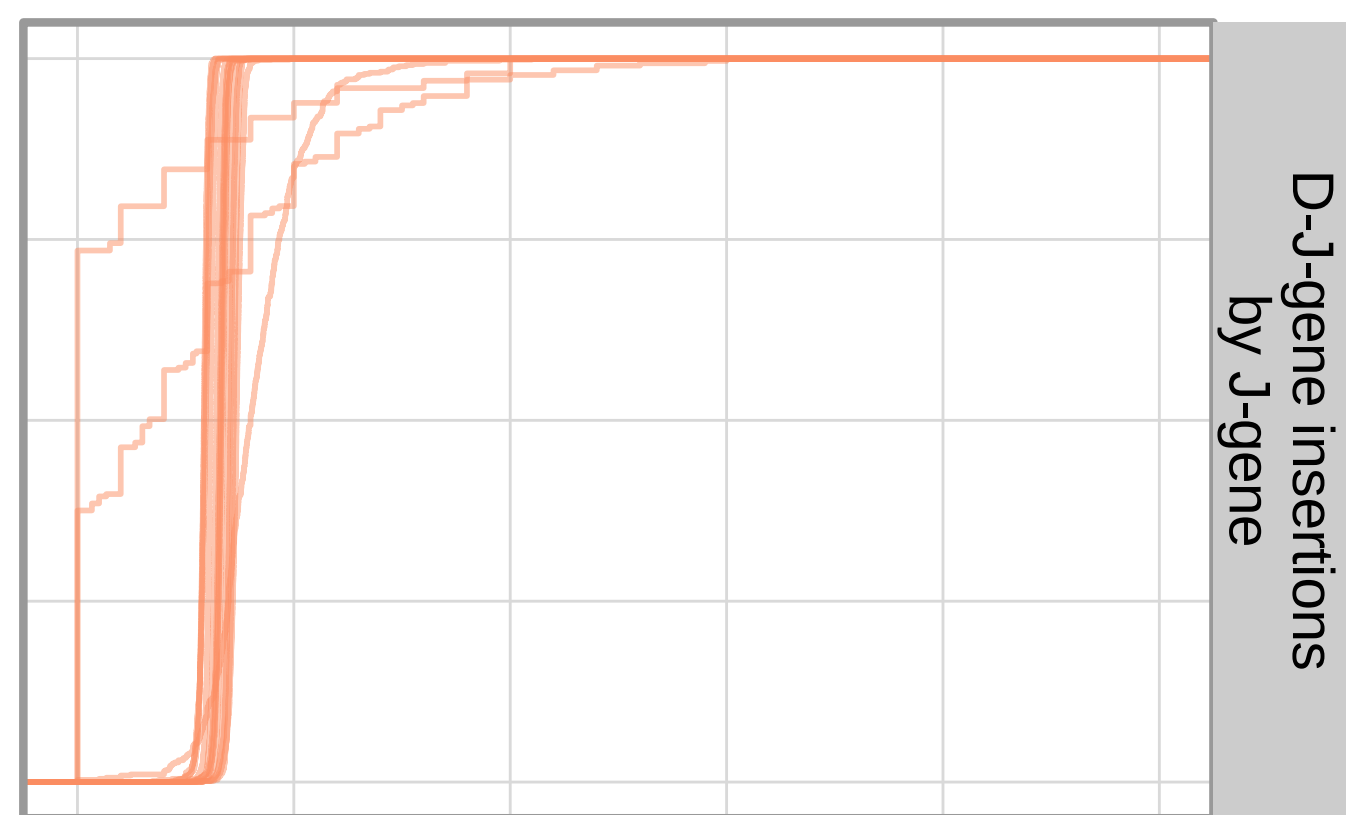
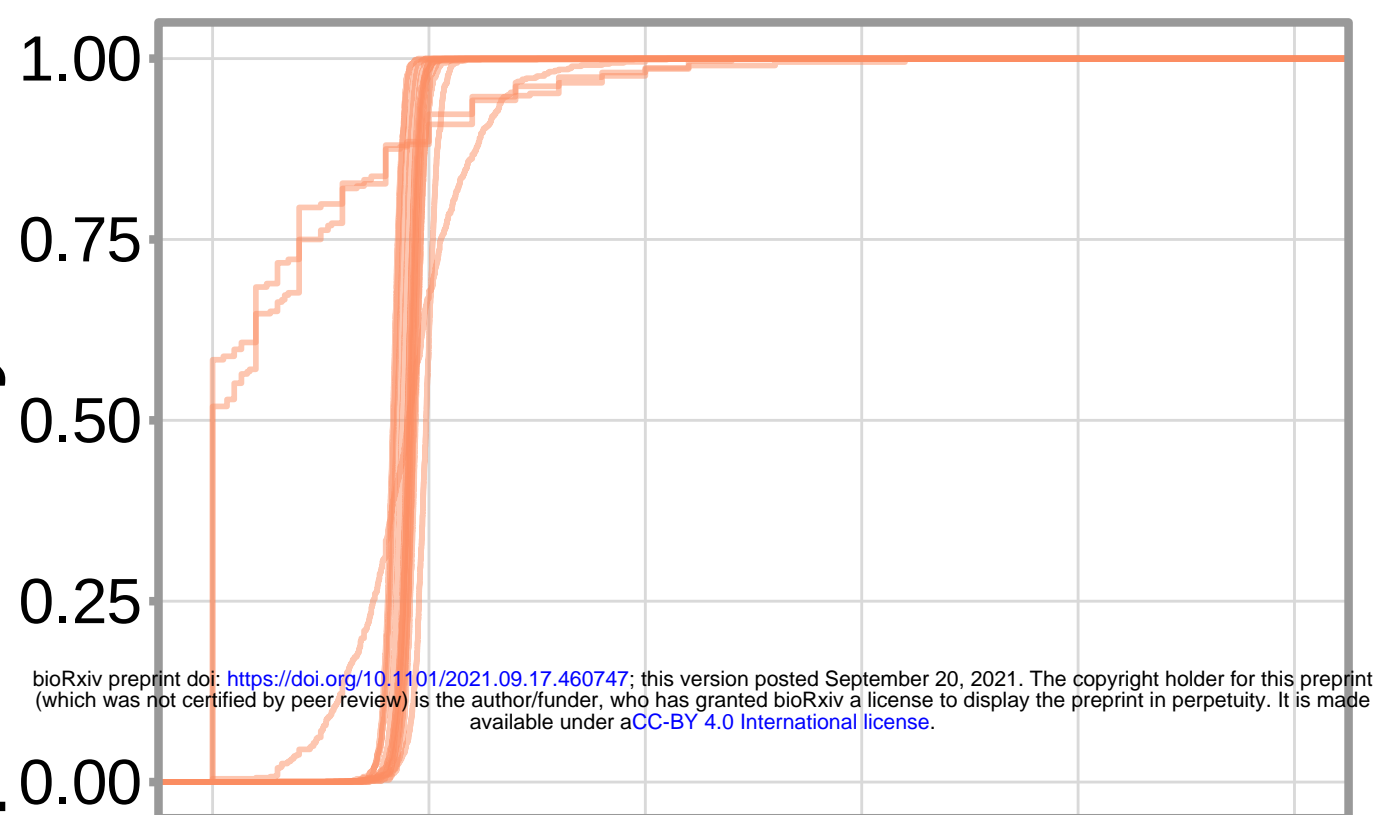
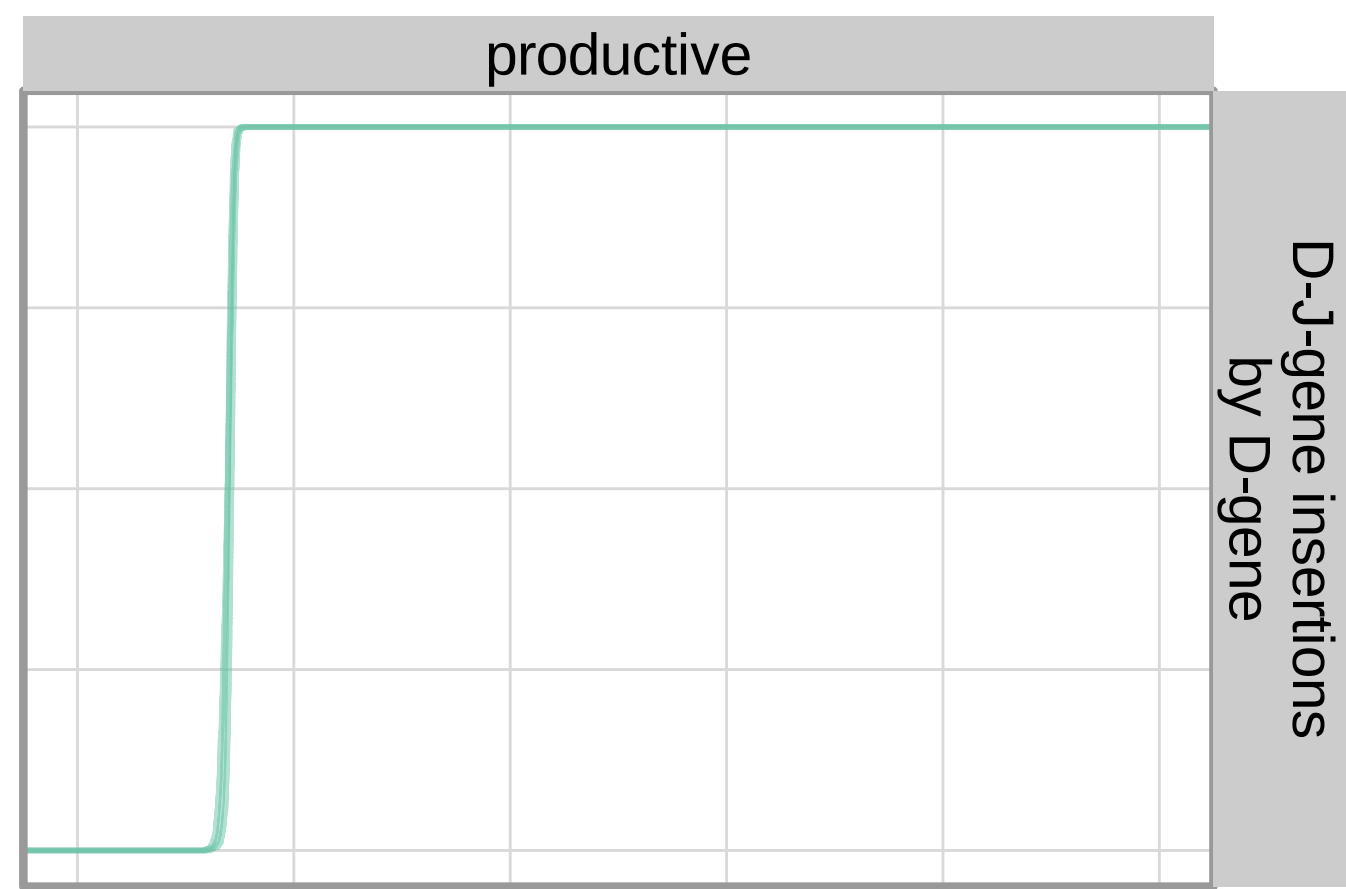
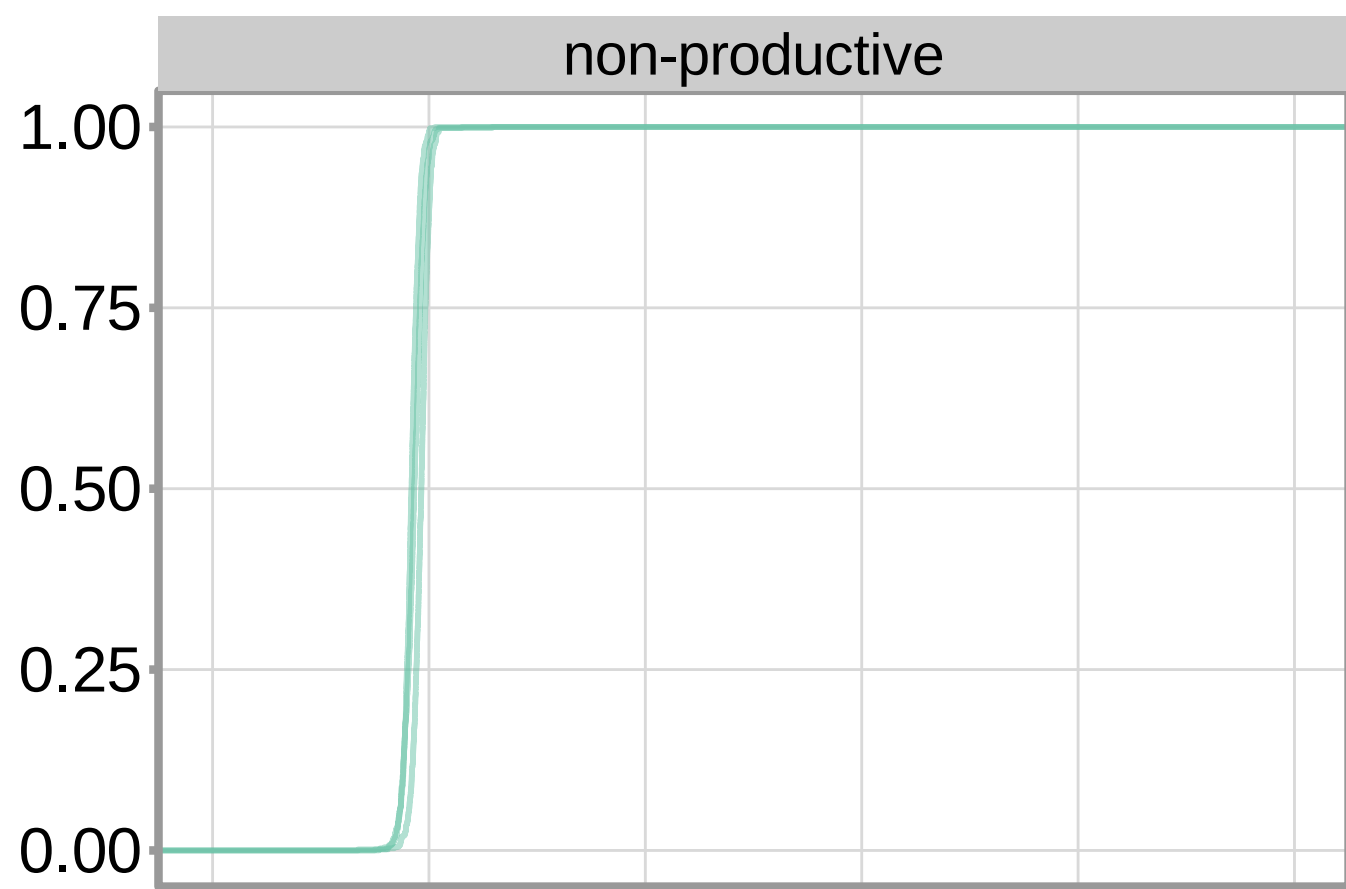
CC

rs41298872 SNP genotype



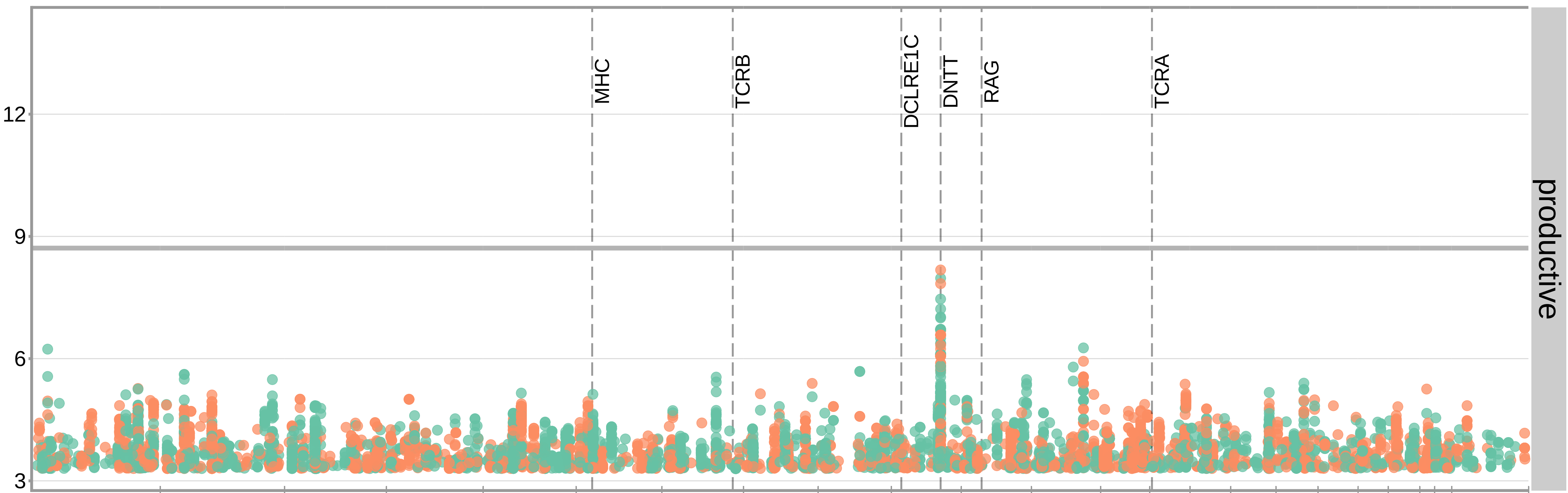
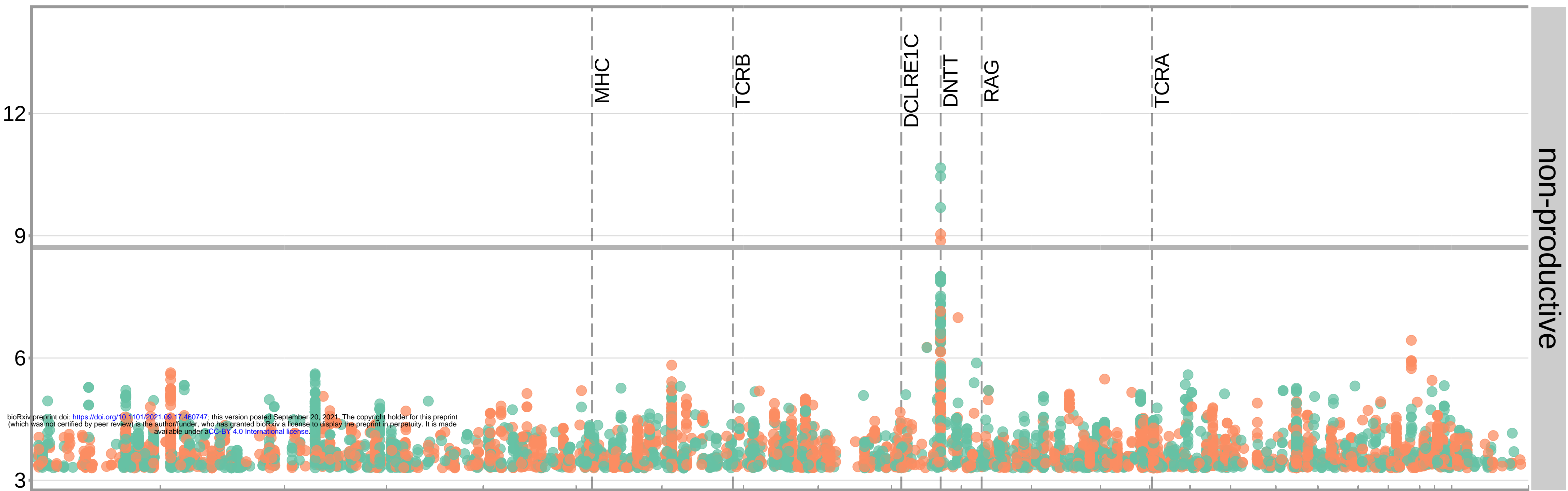
A**B**

Cumulative probability

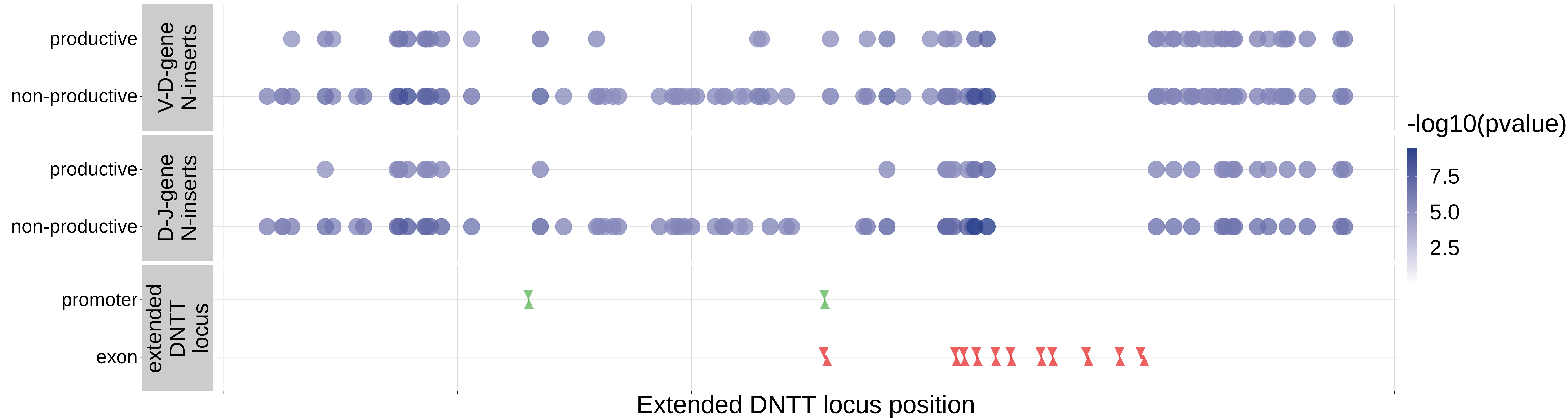


Number of N-insertions

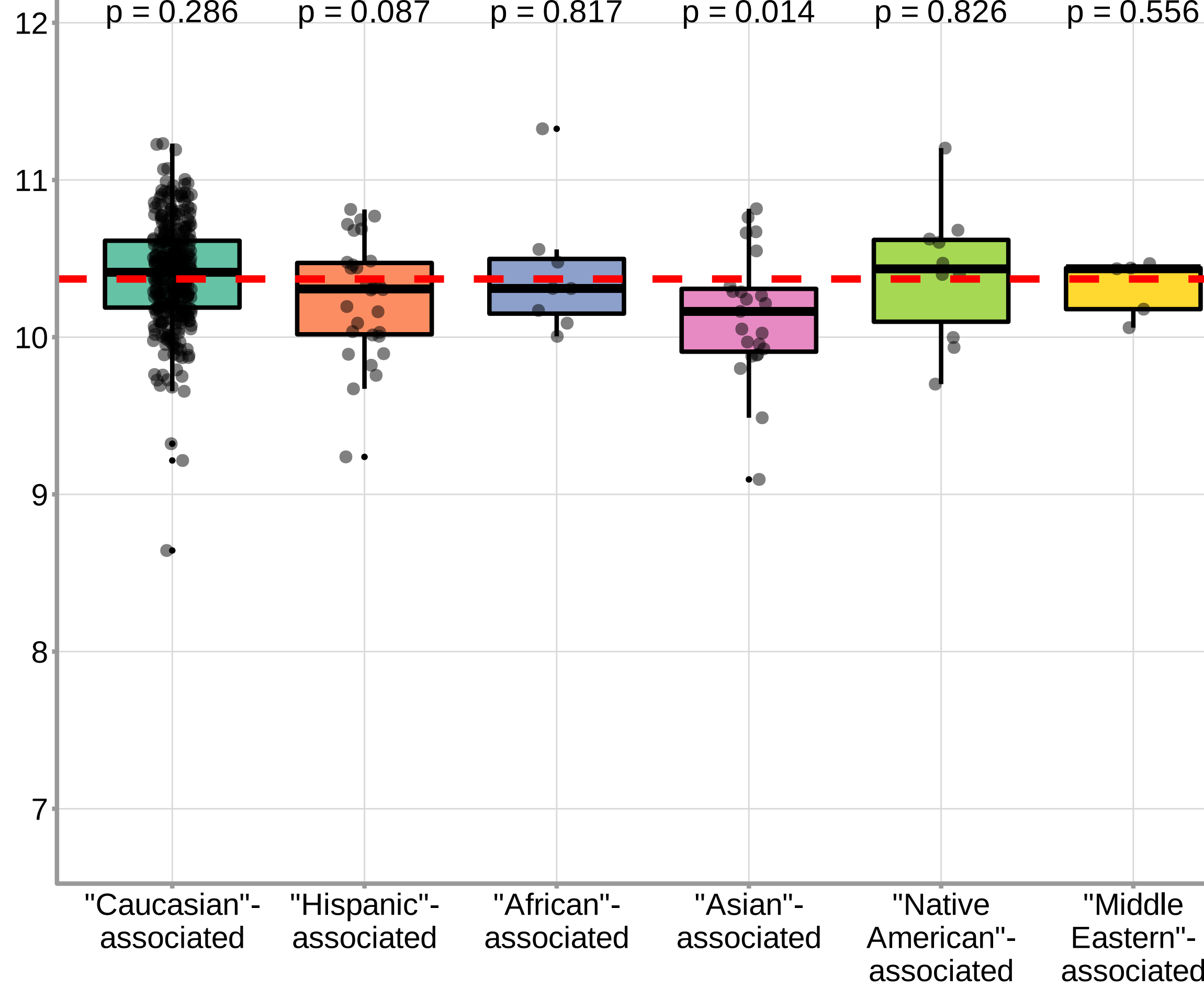
$-\log_{10}(\text{p-value})$



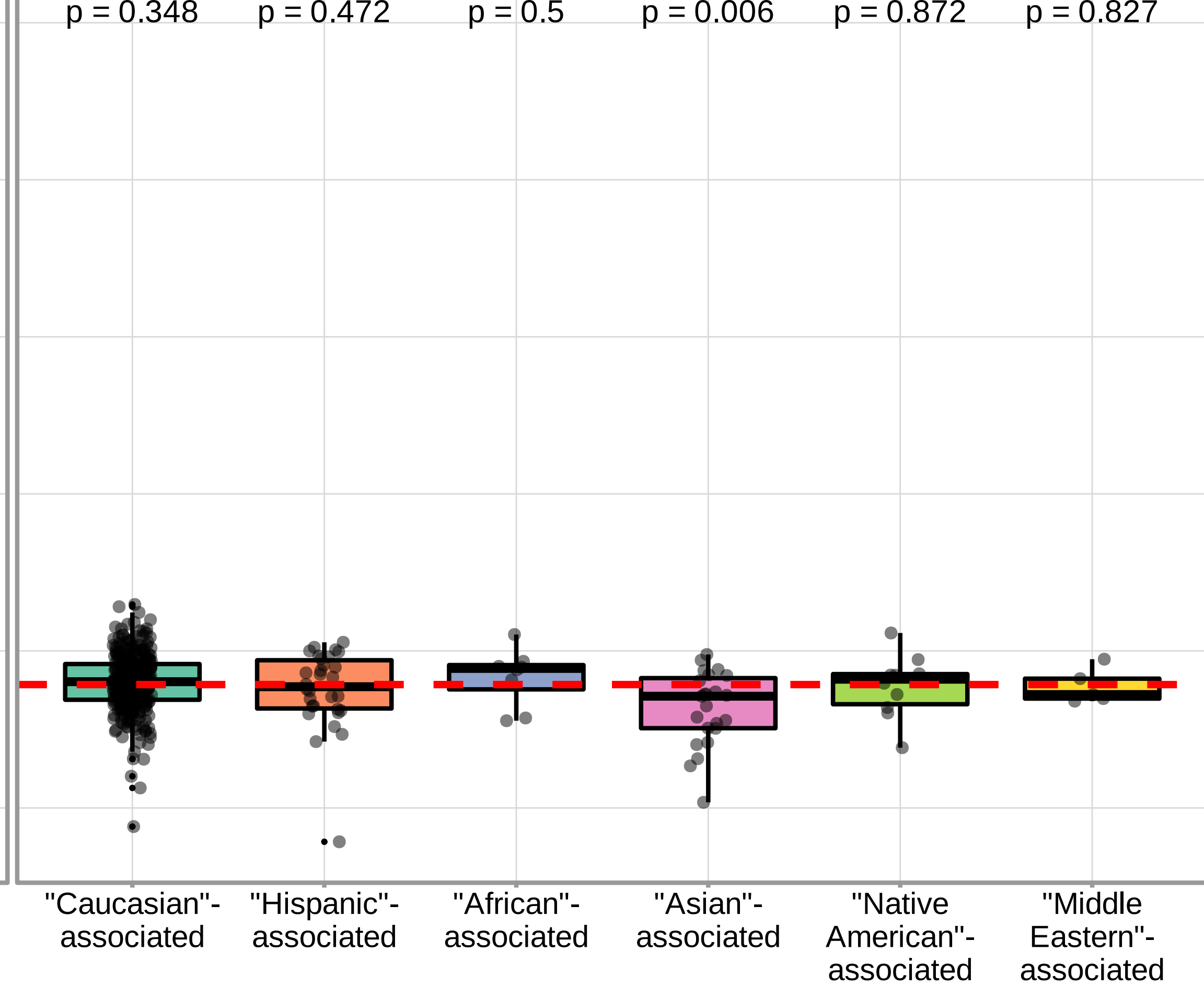
● V-D-gene junction N-insertions ● D-J-gene junction N-insertions



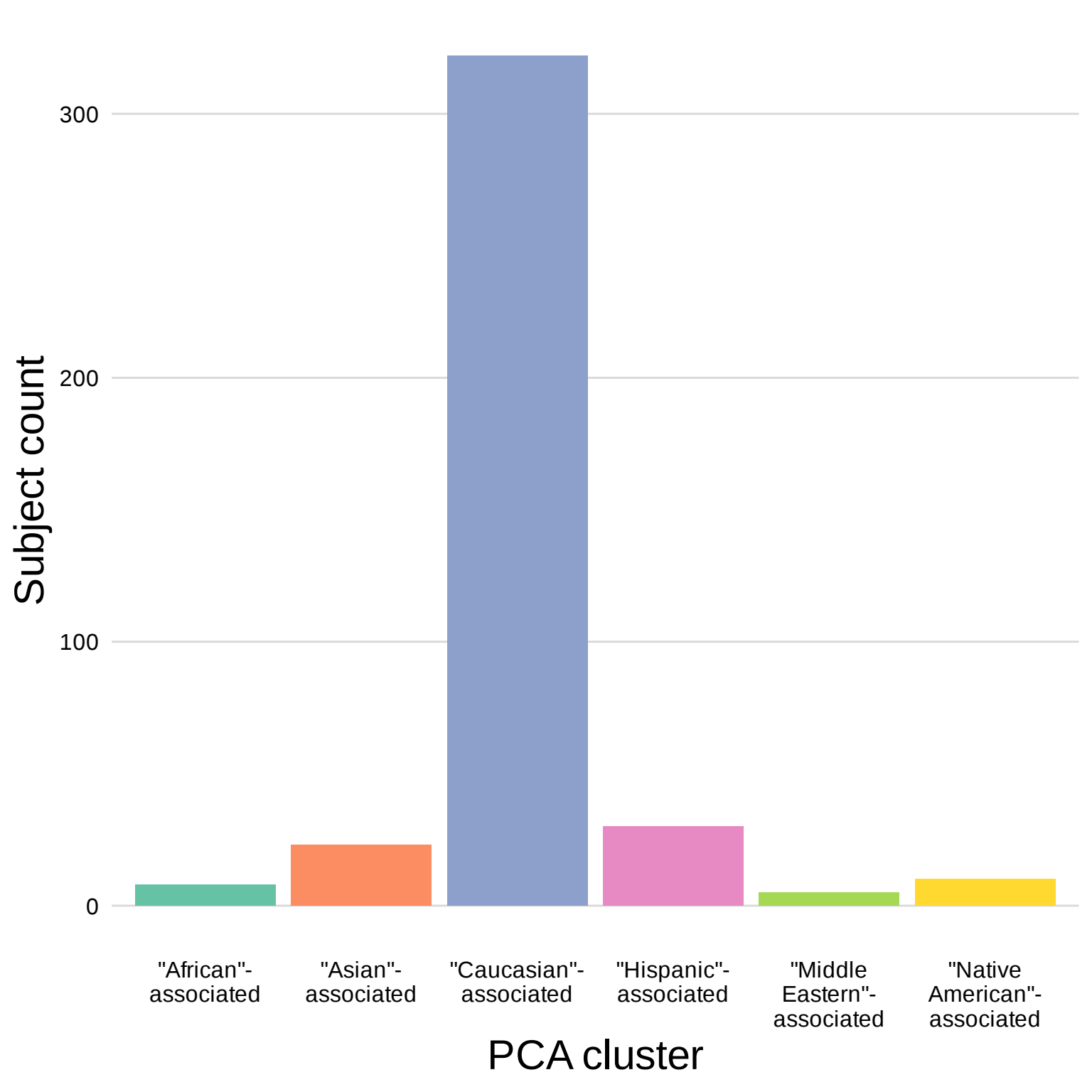
non-productive



productive



PCA cluster



Subject count

300
200
100
0

"African"-associated

"Asian"-associated

"Caucasian"-associated

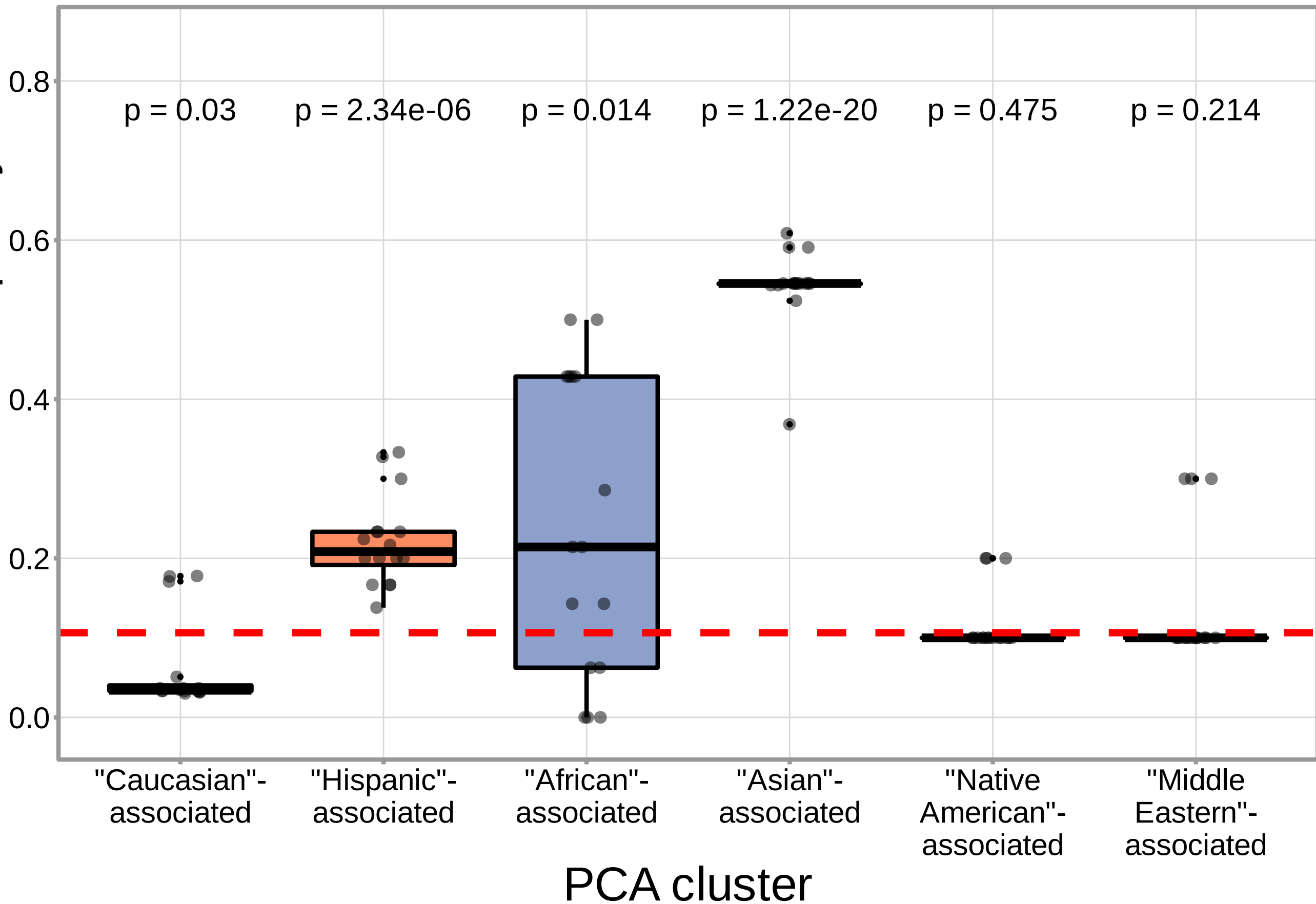
"Hispanic"-associated

"Middle Eastern"-associated

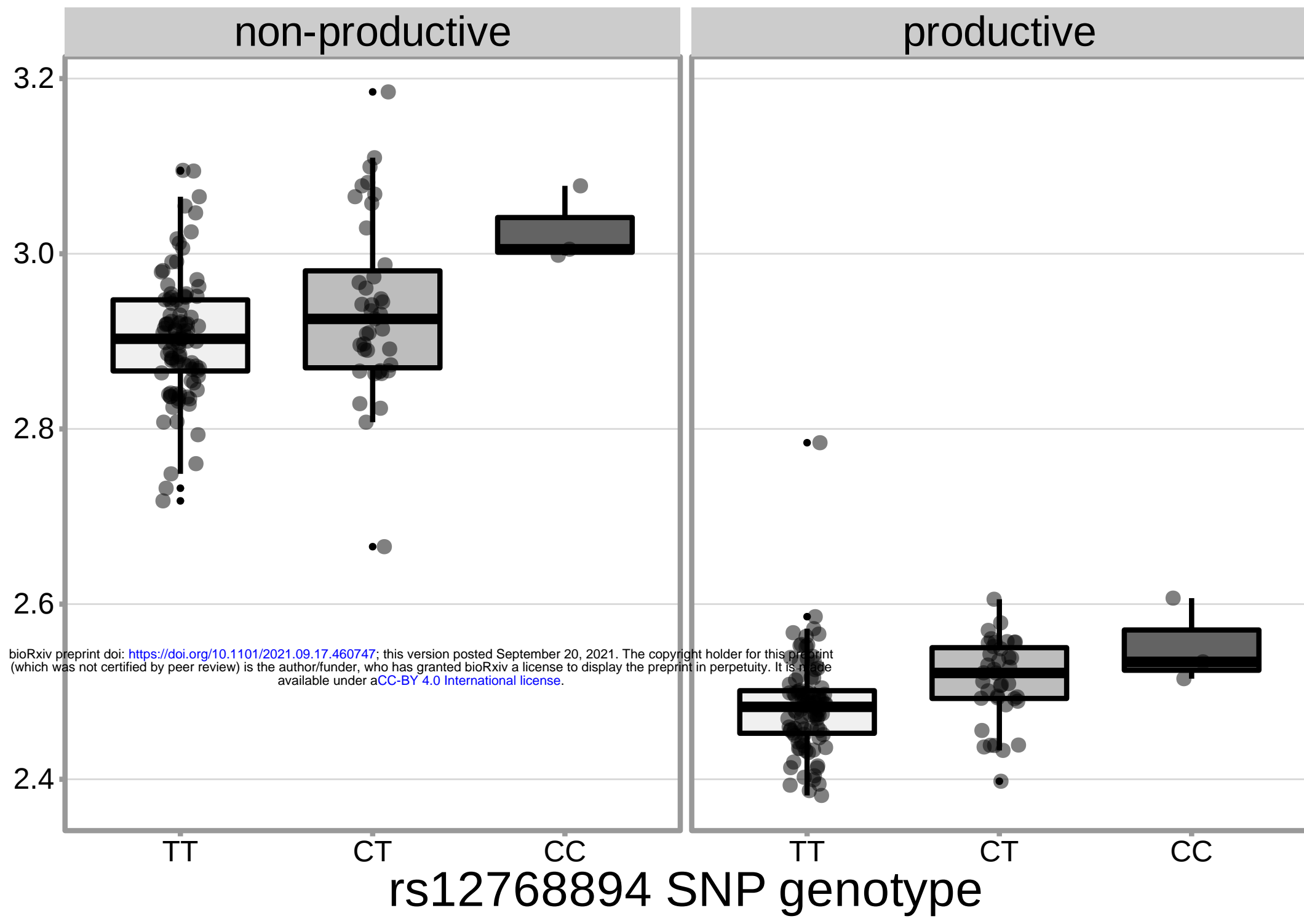
"Native American"-associated

PCA cluster

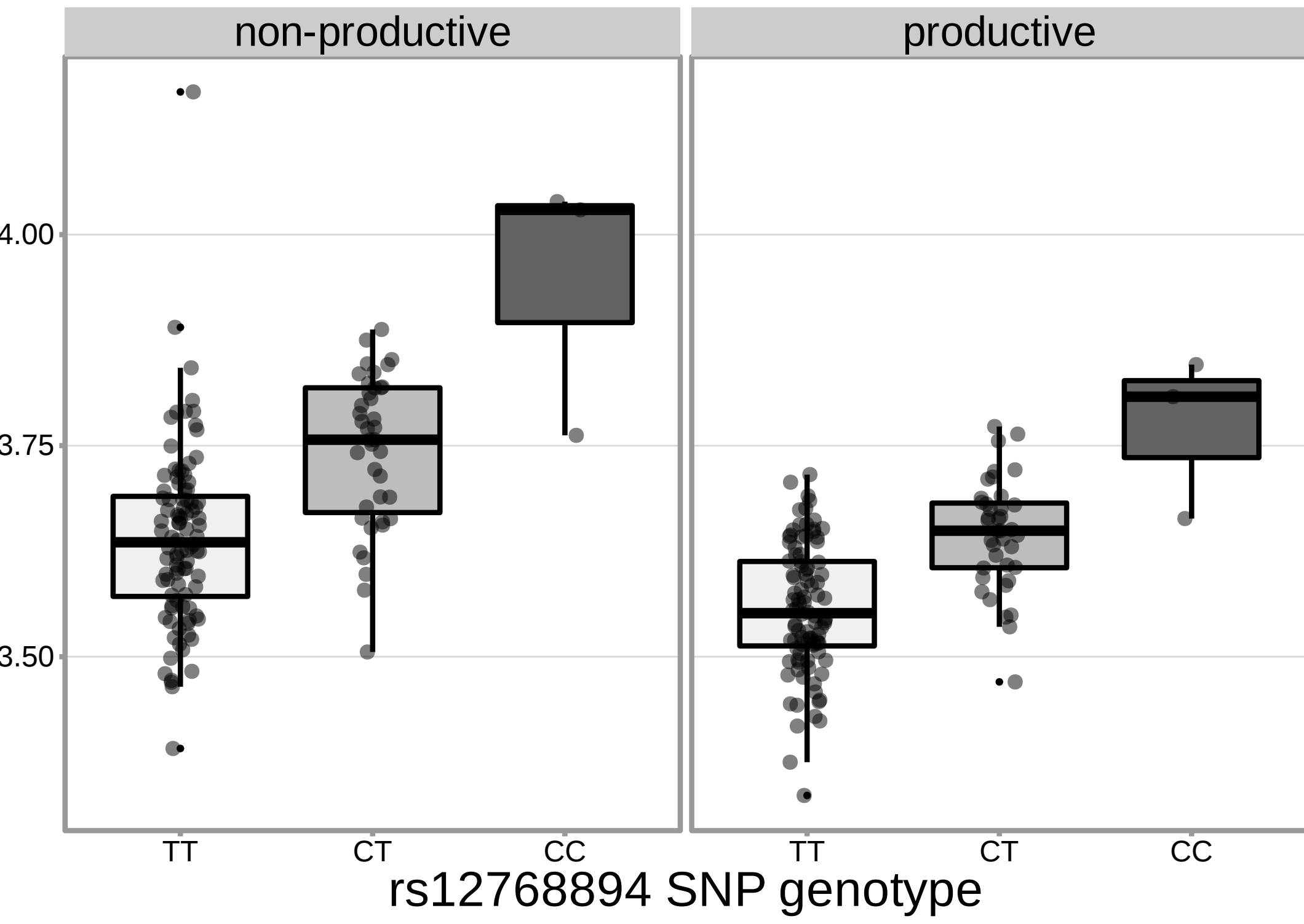
Minor allele frequency

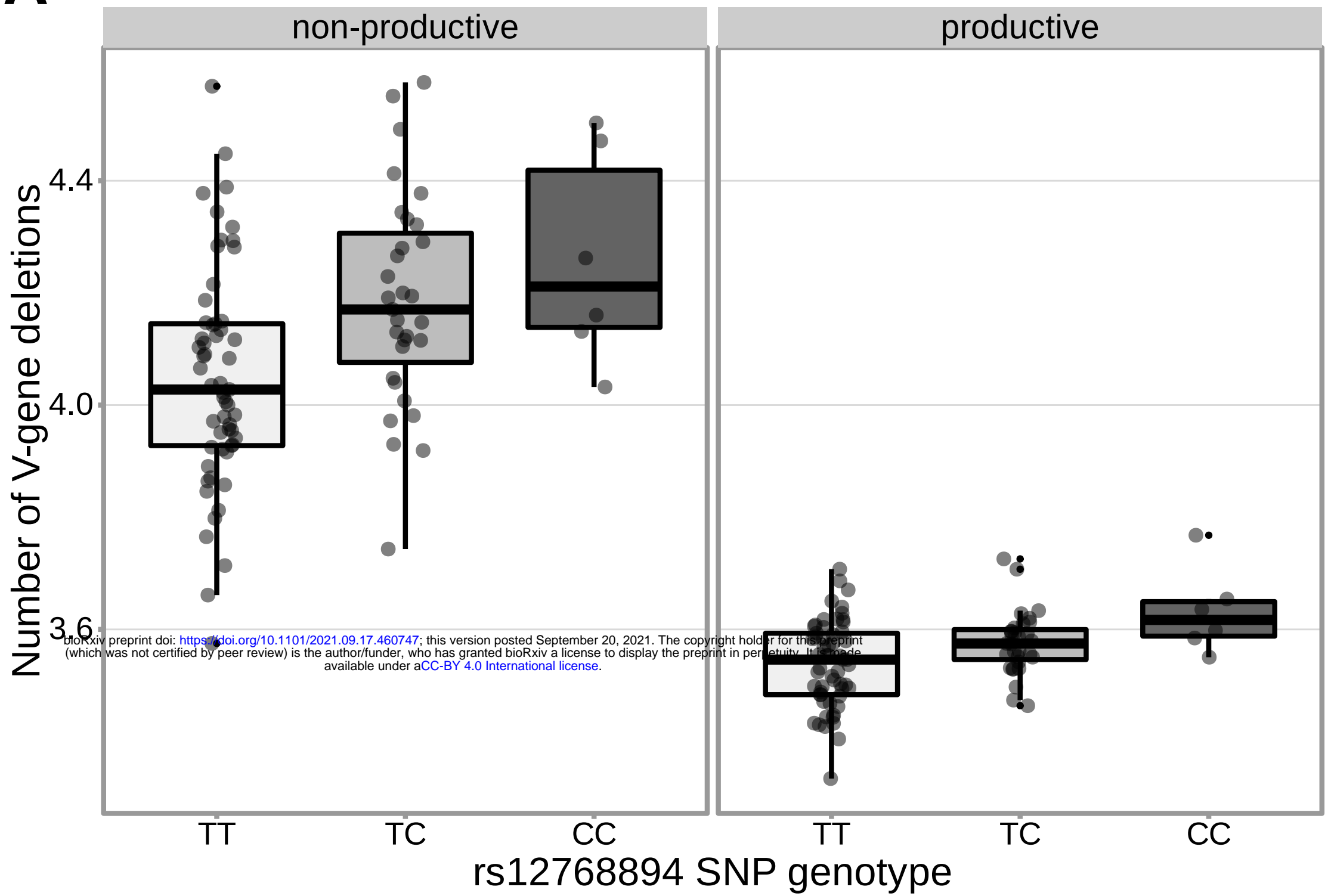
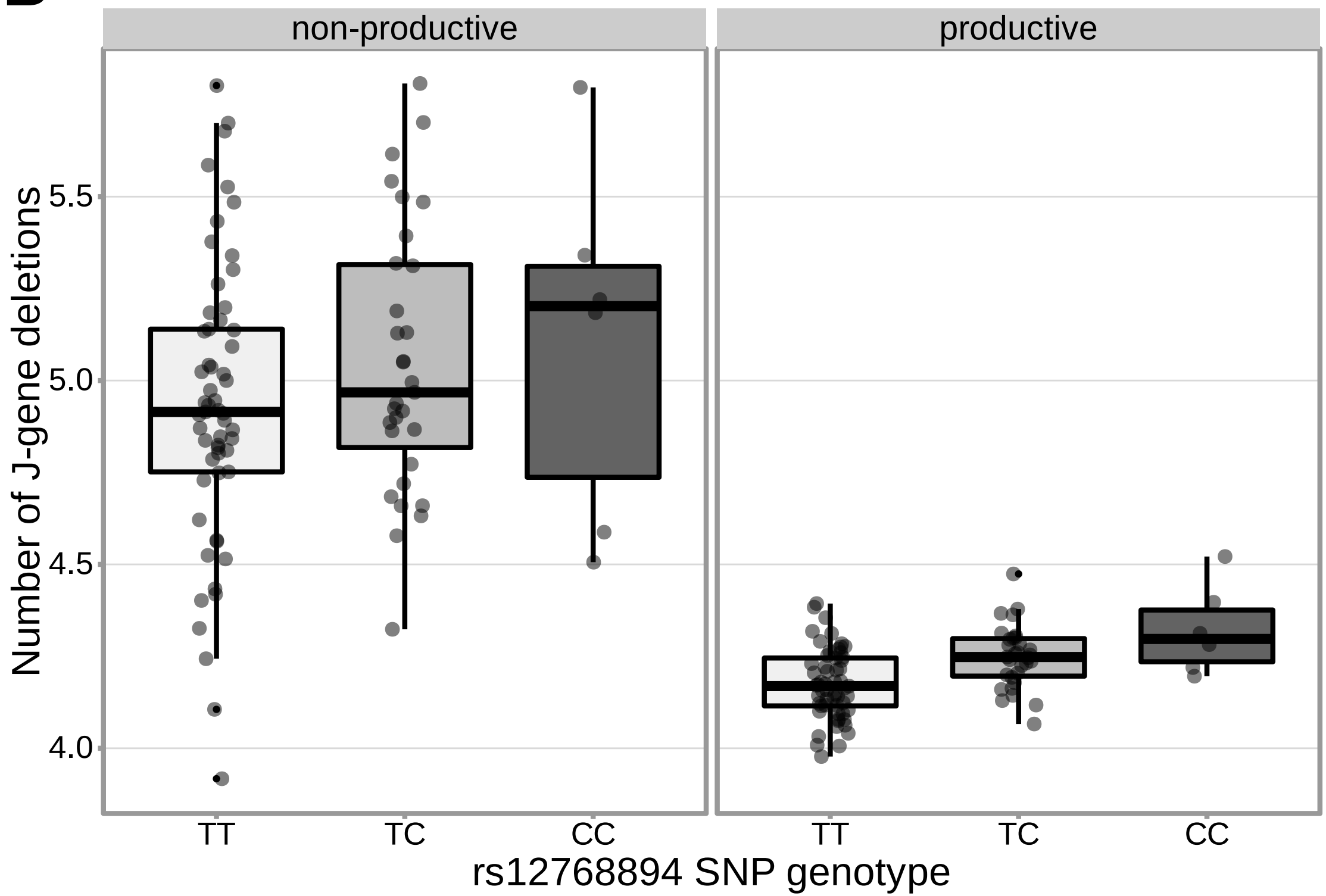


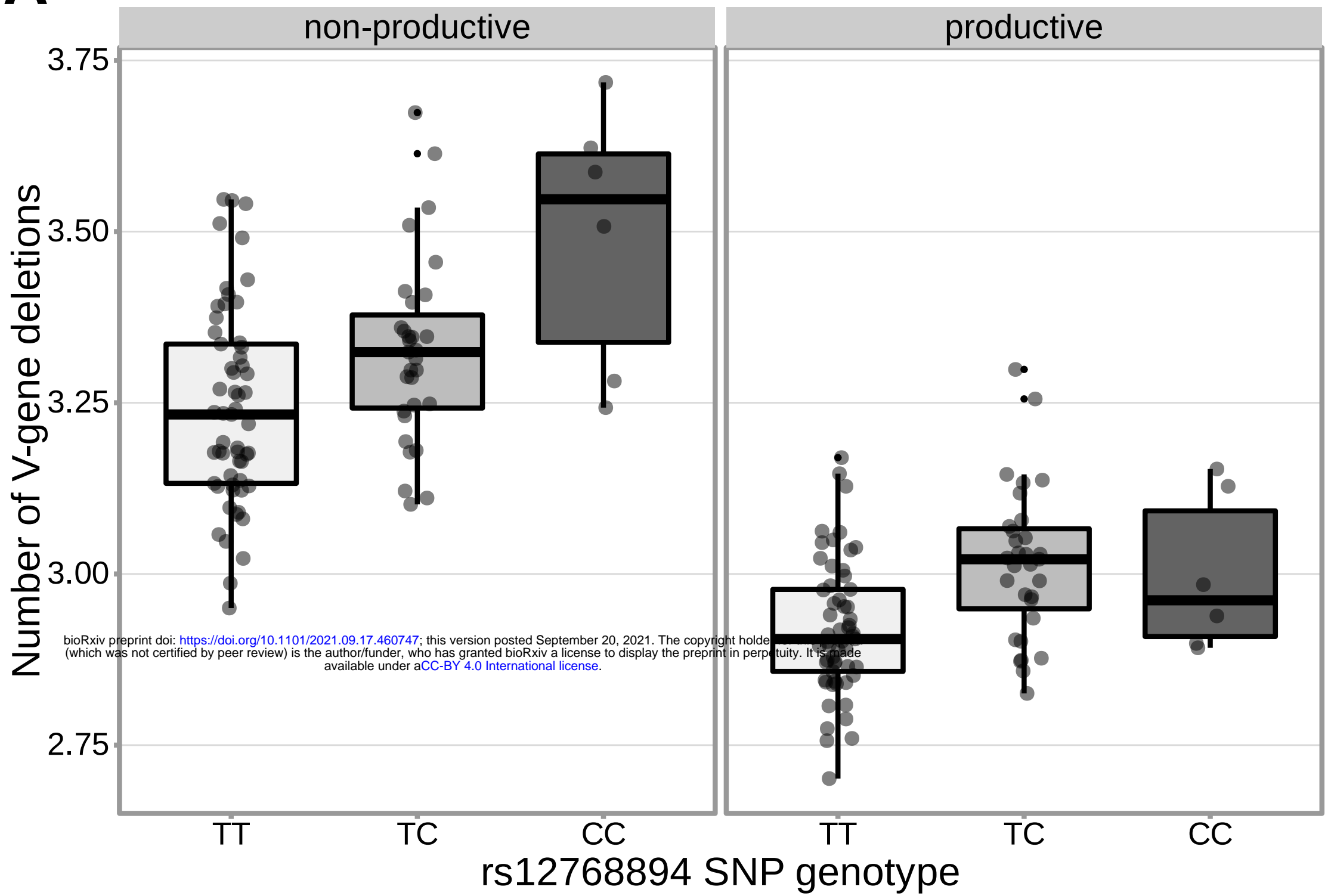
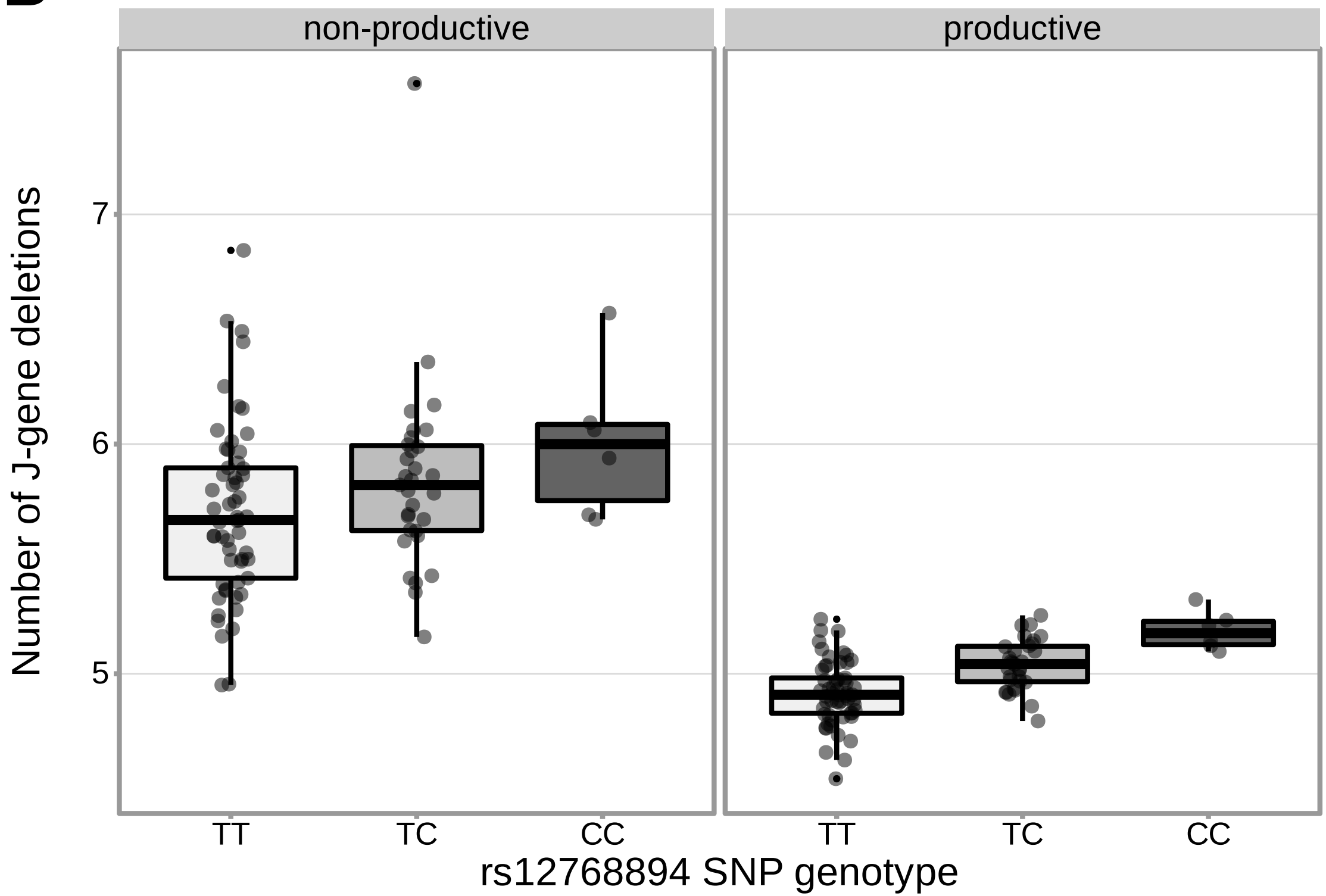
A Number of V-gene nucleotides deleted

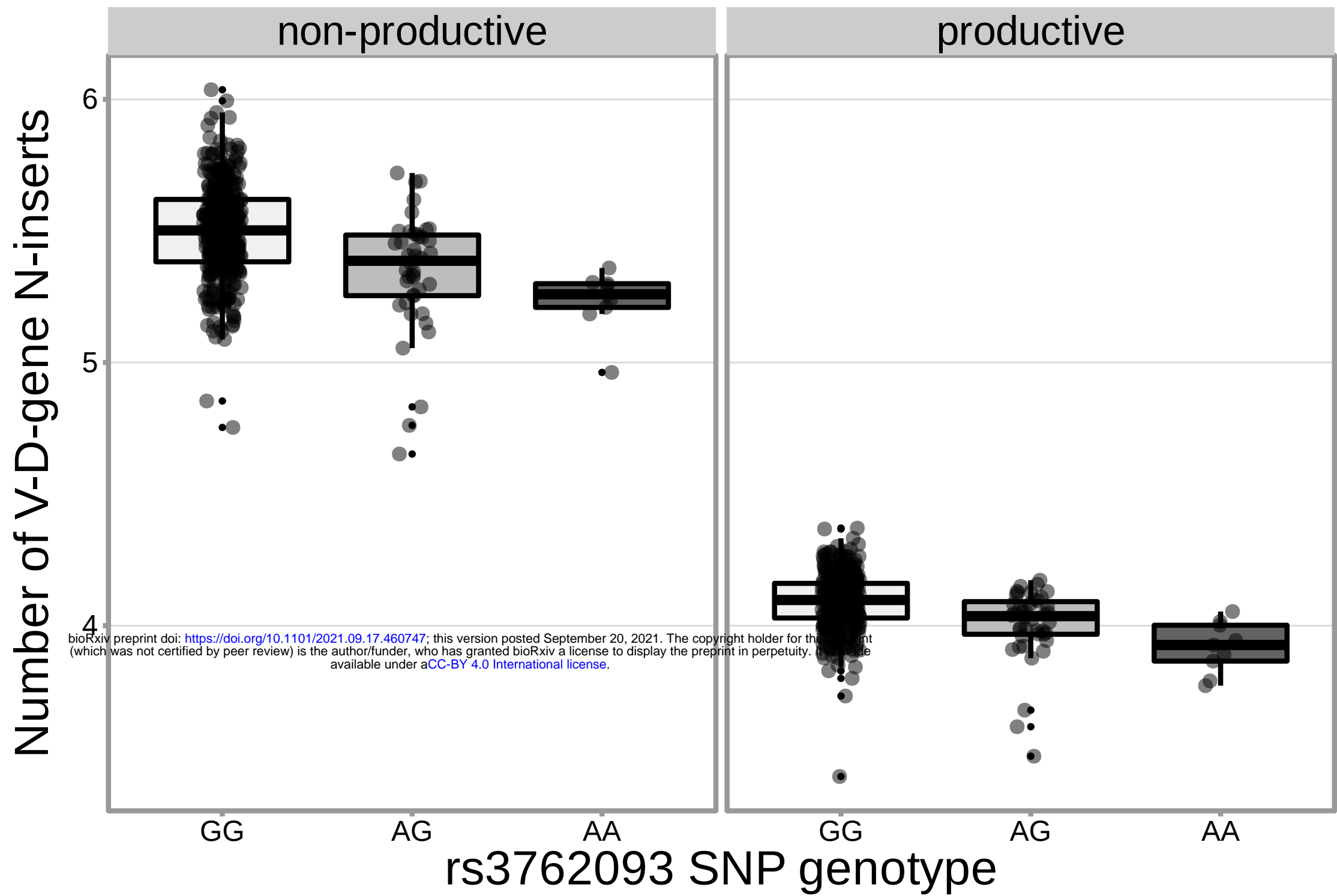
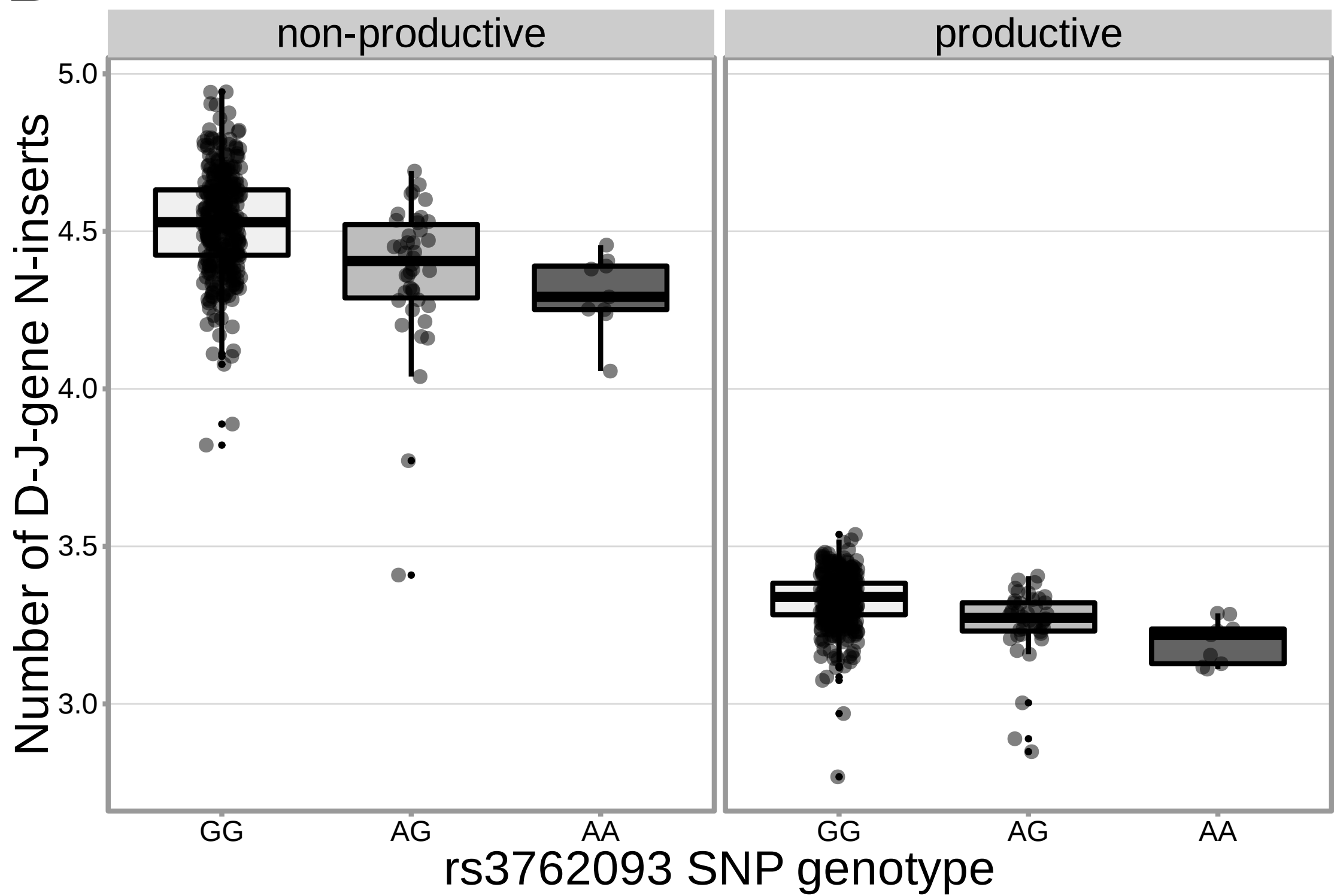


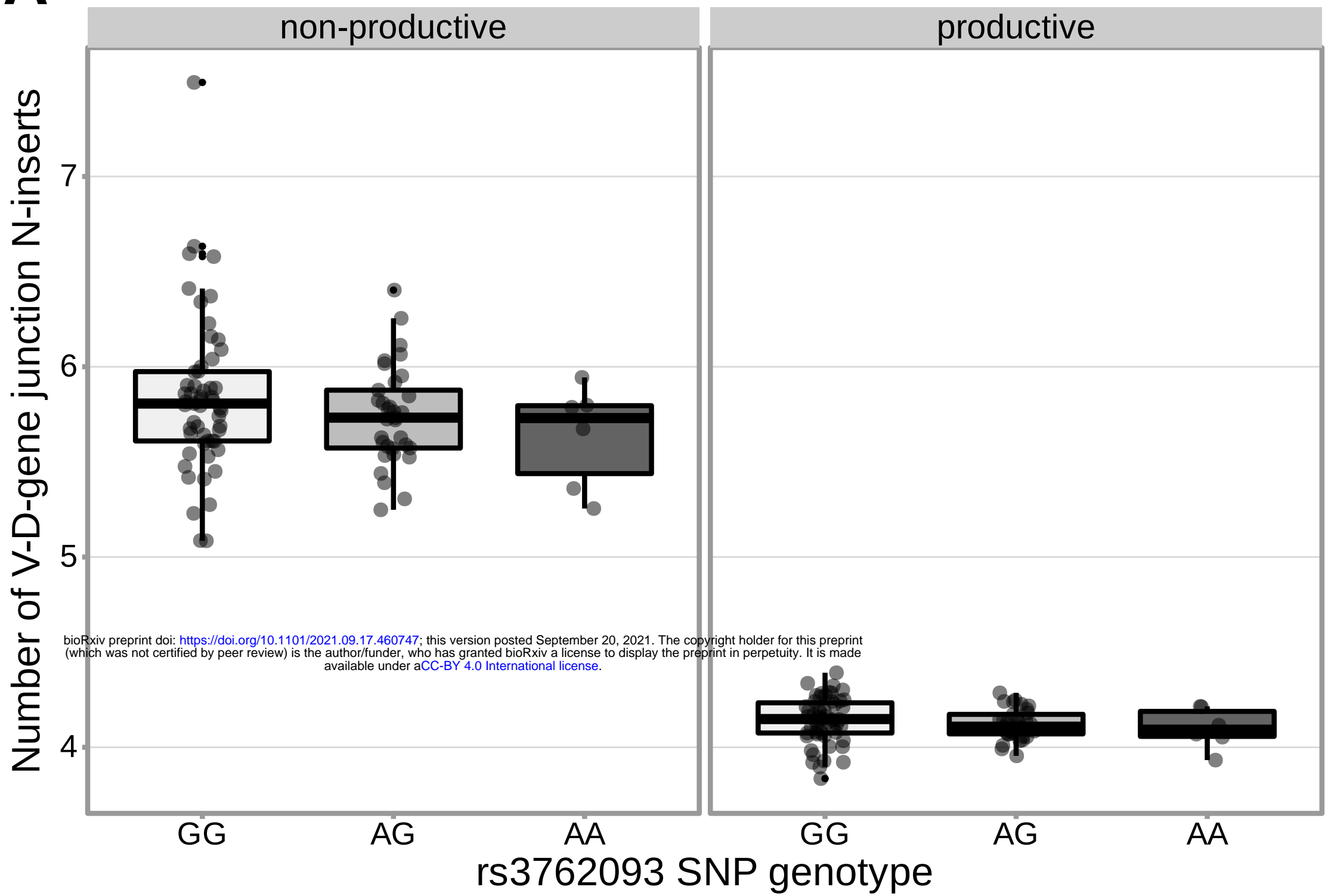
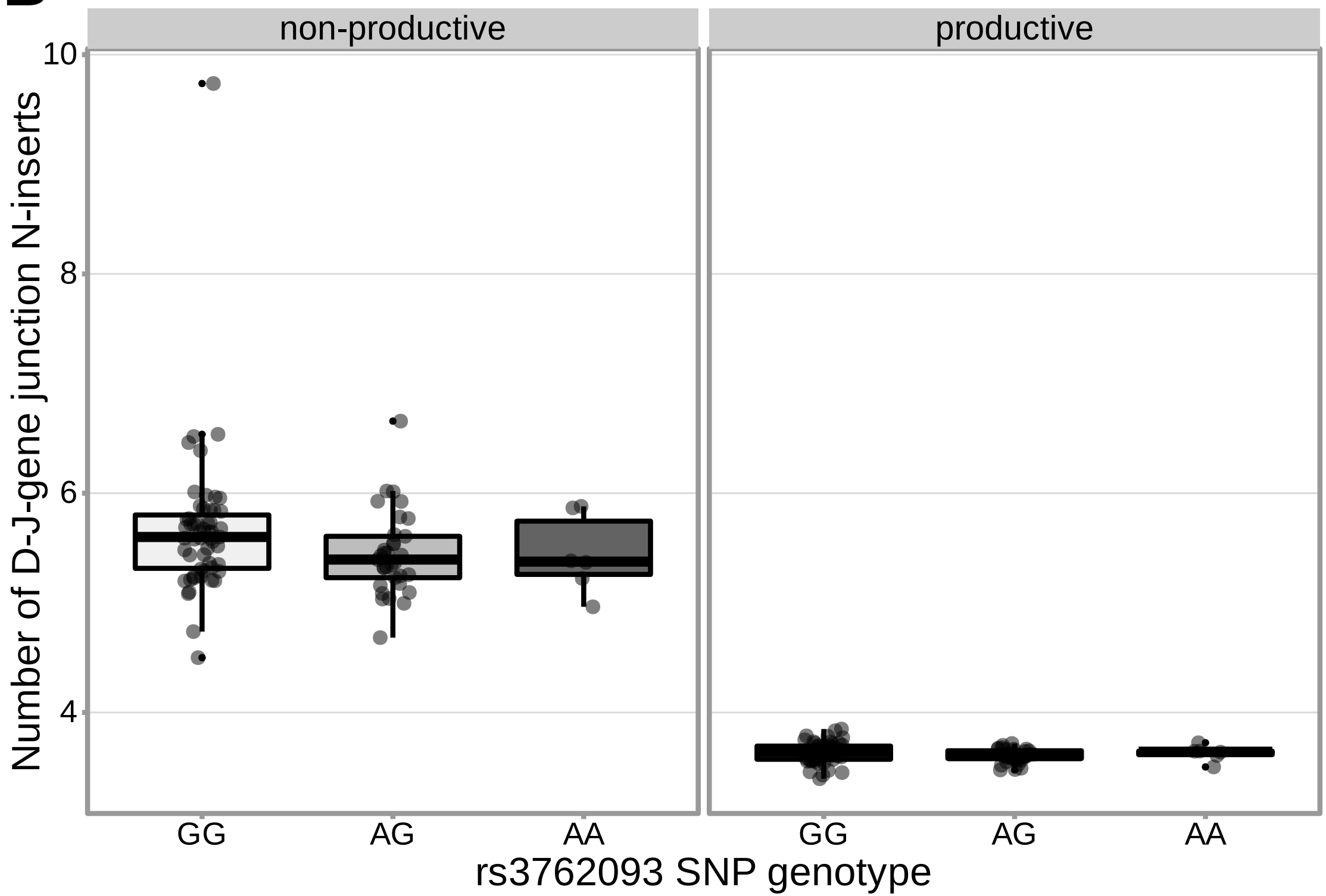
B Number of J-gene nucleotides deleted



A**B**

A**B**

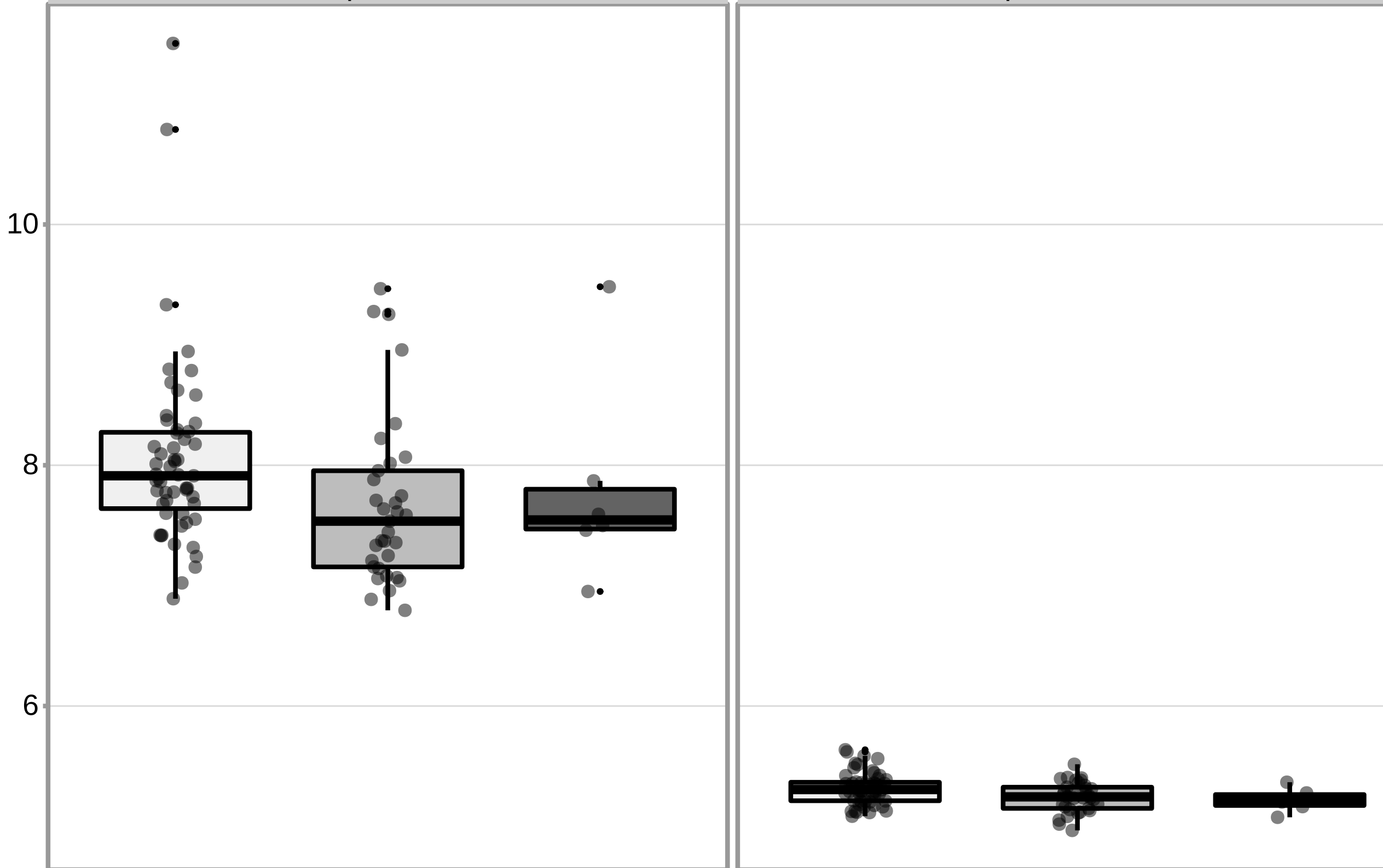
A**B**

A**B**

Number of V-J-gene junction N-inserts

non-productive

productive



GG

AG

AA

GG

AG

AA

rs3762093 SNP genotype

